Assessment of Molecular Weight and Drug Loading on Release From Hydrogel Therapeutics

BY

AMY ELIZABETH ROSS

B.A., DePaul University, 1998

THESIS

Submitted as partial fulfillment of the requirements
for the degree of Master of Science in Bioengineering
in the Graduate College of the
University of Illinois at Chicago, 2011

Chicago, IL

Defense Committee:
Richard A. Gemeinhart, Chair and Advisor
Michael Cho
Robert Chang, Ophthalmology and Visual Science

Acknowledgements

First and foremost, I would like to thank Dr. Richard Magin for his advice and encouragement to apply to the graduate Bioengineering program at UIC. Many others have helped me along the way:

Dr. Robert Capetta (College of DuPage)-for encouraging me to stick with Calc III when I felt doomed to fail right at the beginning.

My advisor, Dr. Richard A. Gemeinhart, and fellow committee members Dr. Michael Cho and Dr. Robert Chang.

My current labmates-Misuk Bae, Jason Buhrman, Melanie Köllmer, Jamie Rayahin, Mary Tang, and Yu Zhang. Special thanks to Mary and Yu for experimental assistance and valuable discussions. I would also like to thank previous members: Mohammed Rahman, Kristin Thomas, Ernie Gemeinhart, Dr. Milind Ghandi, Dr. Deepali Vartak, and Dr. Thomas Hauk. Other BPS members I would like to thank are Dr. William Beck for use of equipment and Yang Yang for advice and troubleshooting with HPLC issues.

Dr. Mohsen Makhsous (Northwestern University Medical School) for generous use of the tensile testing equipment, and Amelia Zellander for instruction and assistance with tensile testing.

A very special thanks to Sara Nowacki, my research assistant for the 2010-2011 school year, who did countless tedious and boring tasks without complaint.

Last but not least, I would like to thank my husband, Dave Ross, for his unfailing encouragement and support throughout my graduate career.

AER

TABLE OF CONTENTS

TABLE OF CONTENTS (CONTINUED)

LIST OF TABLES

TABLE PAGE

LIST OF FIGURES

FIGURE PAGE

LIST OF FIGURES (CONTINUED)

FIGURE PAGE

LIST OF FIGURES (CONTINUED)

FIGURE PAGE

LIST OF ABBREVIATIONS

ACN	acetonitrile
API	active pharmaceutical ingredient
APS	ammonium persulfate
BBB	blood brain barrier
BCNU	1,3-bis(2-chloroethyl) nitrosurea
$CaCl_2$-$2H_2O$	calcium chloride dihydrate
$CaCl_2$-$6H_2O$	calcium chloride hexahydrate
ConA	concanavalin A
DDIW	double deionized water
DMSO	dimethyl sulfoxide
DPBS	Dulbecco's phosphate buffered saline
ECM	extracellular matrix
EDTA	ethylenediamenetetraacetic acid
EMEM	Eagle's minimum essential medium
EPR	enhanced permeation and retention
GBM	glioblastoma multiforme
GFP	green fluorescent protein
HCl	hydrochloric acid
HPLC	high pressure liquid chromatography
MALDI-TOF	matrix assisted laser desorption/ionization time of flight
MMP	matrix metalloproteinase
mPEG	methoxy poly(ethylene glycol)
MS	mass spectrometry

MT-1 MMP	membrane type matrix metalloproteinase-1
m/z	mass charge ratio
NaCl	sodium chloride
PEG	poly(ethylene glycol)
PEGDA	poly(ethylene glycol) diacrylate
PEI	polyethyleneimine
pHEMA	poly (2-hydroxyl ethylmethacrylate)
RFU	relative fluorescence unit
SDS	sodium dodecyl sulfate
SF-EMEM	serum free Eagle's Minimum Essential Medium
TAMRA	tetramethyl rhodamine
TBS/Zn	tris-buffered saline with zinc
TCEP	tris-(2-carboxyethyl)phosphine
TEMED	N'-N'-N'-N'-tetramethylenediamene
TIMP	tissue inhibitors of matrix metalloproteinases
TMZ	temozolamide
w/v	weight to volume ratio
$ZnSO_4$-$7H_2O$	zinc sulfate septahydrate

SUMMARY

Hydrogels are hydrophilic crosslinked polymers that have been demonstrated to be useful in a variety of biomedical applications, including controlled drug delivery. This work pertains to an implantable polyethylene glycol diacrylate (PEGDA) hydrogel for controlled drug delivery triggered by the enzyme matrix metalloproteinase-2 (MMP-2). MMP-2 is one of a family of enzymes responsible for degrading and remodeling the extracellular matrix. MMP-2 is also overactivated in many forms of cancer. An active pharmaceutical ingredient (API), conjugated to the hydrogel matrix via an MMP-2 sensitive peptide, is released when MMP-2 cleaves the peptide. By attaching the API-peptide conjugate to the hydrogel backbone, drug release occurs in the presence of active MMP-2. This work explored optimization of this release and the ability of MMP-2 to enter the hydrogel.

Mesh sizes for different PEGDA molecular weights were measured by using swelling and tensile testing. PEGDA 3,400 had a mesh size smaller than the dimensions of MMP-2. PEGDA 10,000 and PEGDA 20,000 had a mesh size larger than MMP-2, with PEGDA 20,000 being larger than PEGDA 10,000.

Using the fluorescent molecule tetramethyl rhodamine (TAMRA) as a model drug, release studies with purified MMP-2 showed an increased ratio of release with MMP-2 compared to buffer for PEGDA 20,000 compared to PEGDA 3,400 at three different loading concentrations. PEGDA 10,000 had a higher ratio of release compared to PEGDA 3,400 at two of the three loading concentrations tested. No significant

difference was seen in percentage released among different loading concentrations at the same molecular weight. Cleavage was confirmed using HPLC. Alternate MMP sensitive peptide sequences TAMRA-PAGLLGC and TAMRA-IPVSLRSGC showed more consistent release than GPLGVRG as indicated by a smaller standard deviation in release amounts. TAMRA-IPVSLRSGC had a greater absolute amount released and a greater ratio of release than TAMRA-PAGLLGC, but not significantly different than TAMRA-GPLGVRGC. TAMRA-IPVSLRSGC had the greatest absolute amount of release among all three peptides.

U-87 MG cells embedded in collagen release peptide as confirmed by HPLC. GM6001, an MMP inhibitor, prevented release. MMP-2 secretion and activation was confirmed by gelatin zymography. Fractionated HPLC peaks were analyzed using mass spectrometry, and showed cleavage was occurring at TAMRA-GPLG, the expected site. There were also secondary cleavage sites, possibly by other proteases secreted by the cells.

The increase in ratio of release with PEGDA 10,000 and PEGDA 20,000 comapred to PEGDA 3,400 suggests MMP-2 enters the hydrogel. Optimization can be attained by using PEGDA 20,000 and the peptide sequence IPVSLRSG. Further optimization can be attained by further release studies with IPVSLRSG.

1. Introduction

1.1 Hydrogels

Hydrogels are three-dimensional cross-linked polymers that are capable of absorbing large amounts of water (Anseth, Bowman, & Brannon-Peppas, 1996) Hydrogels were first developed in the 1950s by Wichterlie and Lim, who developed the first soft contact lens using hydrogels composed of poly (2-hydroxyl ethylmethacrylate) (pHEMA) (Kopecek, 2009). Since then, hydrogels have been developed for a wide variety of industrial and biomedical applications.

Hydrogels are ideally suited to a number of biomedical applications, including tissue engineering and drug delivery. The high water content present in hydrogels while swollen and overall soft consistency makes them similar to natural soft tissue and highly biocompatible (Peppas, Bures, Leonbandung, & Ichikawa, 2000). The rubbery nature of hydrogels in their hydrated state has been shown to minimize mechanical irritation to surrounding tissue upon implantation. Hydrogels typically show little protein adsorption due to the low interfascial tension between the polymer matrix and surrounding aqueous solution. (Kim, Bae, & Okano, 1992). Additionally, the ability to maintain their shape when swollen makes them suitable for a variety of applications. The three-dimensional nature of hydrogel networks is especially useful in tissue engineering. The importance of a three-dimensional structure has been shown to be important in mesenchymal stem cell proliferation and differentiation (Guo, et al., 2010).

The properties of hydrogels largely depend on their physical and chemical characteristics. There are a wide variety of properties that can be chosen from that best meet the needs of a specific application. From a chemical standpoint, hydrogels can be composed of neutral or ionic polymers (Peppas, Huang, Torres-Lugo, Ward, & Zhang, 2000). Numerous synthetic polymers can be used to fabricate hydrogels, including poly(vinyl alcohol), poly(acrylic acid), poly(acrylamide), poly (n-vinyl pyrrolidone), and poly(ethylene glycol) (Peppas, Huang, Torres-Lugo, Ward, & Zhang, 2000). One of the advantages of using synthetic materials are that there is less variablility and more reproducibility of monomer characteristics, leading to greater control over the hydrogel properties (Randolph, Anseth, & Yaremchuk, 2003, Drury & Mooney, 2003). The properties of synthetic hydrogels can also be fine tuned to the application. For instance, a specific stiffness, mesh size, or the incorporation of specific moieties can be easily achieved (Salinas & Anseth, 2009). Natural materials can also be used, such as hyaluronan (Shu, et al., 2003), chitosan (Bhattarai, Gunn, & Zhang, 2010), collagen (Hesse, et al., 2009) alginate (Josef, Zilberman, & Bianco-Peled, 2010), dextran (Coviello, Matricardi, Marianecci, & Alhaique, 2007), methylcellulose (Klouda & Mikos, 2008), and gelatin (Ogawa, Akazawa, & Tabata, 2010). Hydrogels fabricated from natural materials are advantageous in that they more closely mimic the extracellular matrix and are biologically active (Hesse, et al., 2009). Natural hydrogel materials, in most cases, are inherently biodegradable. (Mann, 2003, Chao, Yodmuang, Wang, Sun, & Vunjak-Novakovic, 2010).

Hydrogels can be crosslinked either chemically or physically. Chemical crosslinking is consists of ionic or covalent bonds (Lin and Anseth 2009), while physical crosslinking can include entanglements, van der Waals interactions or hydrogen bonds (Peppas, Bures, Leonbandung, & Ichikawa, 2000; Peppas, Huang, Torres-Lugo, Ward, & Zhang, 2000). A hydrogel's physical structure can be nonporous, porous, or macroporous, with pores allowing for faster swelling of the dried polymer (Gupta & Shivakumar, 2009). Hydrogel size can range from the macroscopic scale to microparticles (Ogawa, Akazawa, & Tabata, 2010) and even nanoparticles (Hamidi, Azadi, & Rafiei, 2008) Hydrogels can either be static structures, or responsive to their environment. Stimulus-responsive hydrogels have been applied to a number of biomedical applications. Hydrogels sensitive to pH have been used for the delivery of insulin in a diabetic rats (Huynh, Im, Chae, Lee, & Lee, 2009). Temperature sensitive hydrogels, most often fabricated from N-isopropylacrylamide, have also been applied to cartilage tissue engineering and as an easily detachable cell culture substrate (Klouda & Mikos, 2008). Enzyme-sensitive hydrogels have been developed that undergo a sol to gel phase transition in the presence of the enzyme (Ulijn, 2006). Light sensitive, biomolecule sensitive, and pressure sensitive hydrogels have also been developed (Mamada, Tanaka, Kungwatchakun, & Irie, 1990, Lee, Cussler E.L., & McHugh, 1990, Miyata, Asami, & Uragami, 1999). Further modifications to and uses for hydrogels will undoubtedly be discovered in the future.

Hydrogels have long been recognized as an effective biomaterial for drug delivery applications due to its biocompatibility and high water content. The active

pharmaceutical ingredient (API) is encapsulated within or diffused into the polymeric matrix, and is subsequently released in a controlled manner. There are three potential release mechanisms: diffusion through the polymer matrix, degradation of the hydrogel, or a swelling-controlled mechanism. Mesh size, swelling kinetics, and permeability play a role in the rate of the release, depending on the release mechanism (Tauro, Lee, Lateef, & Gemeinhart, 2008, Gupta, Vermani, & Garg, 2002). Stimulus-responsive properties as those described previously can also be incorporated into hydrogel-based drug delivery systems, resulting in release under specific physiological or pathological conditions (Gupta, Vermani, & Garg, 2002). Hydrogel nanoparticles are also advantageous in that they can increase drug circulation time and prevent unintended enzymatic degradation (Lin & Metters, 2006).

1.2 Glioblastoma Multiforme

It is estimated there will be over 23,000 brain tumors diagnosed and 13,000 deaths in the United States in 2011 (Siegel, Ward, Brawley, & Jamal, 2011). Glioblastoma multiforme (GBM) is the most common primary brain tumor. Gliomas account for 81% of all malignant brain tumors, and glioblastomas account for one half of all gliomas (Central Brain Tumor Registry of the United States, 2007-2008). The current initial treatment for GBM consists of 1) surgical resection of the tumor when possible, 2) brain radiotherapy, and 3) concomitant or adjuvant chemotherapy with temozolamide (TMZ) (Bock, et al., 2010). Surgical resection may be accompanied by the insertion of the Gliadel wafer in the tumor bed, a biodegradable device made of

poly(carboxyphenoxy-pronpane sebacic acid) anhydride (Westphal, et al., 2003). The Gliadel wafer releases the antineoplastic agent 1,3-bis(2-chloroethyl) nitrosurea (BCNU) over a period of two weeks (Valtonen, et al., 1997). By providing local chemotherapy at the tumor site, use of the Gliadel wafer avoids systemic toxicity while increasing survival time (Bock, et al., 2010). Unfortunately, due to the invasiveness of the tumor, almost all GBMs recur. Further treatment options include stereotactic radiosurgery and further systemic chemotherapy (Wen & Kesari, 2008).

Systemic chemotherapy for GBM is impeded from reaching the tumor by the blood brain barrier (BBB). The BBB is a series of specialized endothelial cells, capillary basement membrane, pericytes, and astrocytoma sheathing. The extensive tight junctions between the endothelial cells selectively inhibit transport of many molecules across the BBB (Ballabh, Braun, & Nedergaard, 2004). This inhibits small molecule drugs, including antineoplastic agents, from reaching the brain and limits the effectiveness of systemic chemotherapy for brain malignancies. The membrane transporter p-glycoprotein prevents uptake and increases cellular efflux, preventing intracellular accumulation of potentially toxic agents including antineoplastic drugs (Demeule, et al., 2002)

GBM has a poor prognosis. One year survival is 29%. This figure drops to 3.4% after five years (Central Brain Tumor Registry of the United States, 2007-2008). Median survival time for GBM is 12-15 months (Wen & Kesari, 2008). Clearly, new treatments are necessary to improve survival in GBM patients.

1.3 Matrix Metalloproteinase-2

Matrix metalloproteinases (MMPs) are a family of over twenty zinc-dependent endopeptidases that are best known for degrading the extracellular matrix (ECM) (Vartak & Gemeinhart, 2007). The MMPs are divided into subgroups. MMP-2 is a member of the subgroup gelatinase, which consists of itself and MMP-9. MMP-2, also known as gelatinase A, is the most widely distributed MMP type throughout the body and is expressed by most cells (Fridman, 2003, Foda & Zucker, 2001). Both gelatinases have been shown to degrade gelatin and are believed to be responsible for late-stage collagen degradation (Fridman, 2003). MMP-2 has also been shown to degrade elastin, casein, type I, IV, V, VII, X Xi, and XIV collagen, fibronectin, laminin-1, lamin-5, and several other ECM proteins (Chakraborti, Mandal, Das, Mandal, & Charkraborti, 2003, Sawaya et. al. 1996).

All MMPs are expressed in a latent form and require activation in order to exhibit activity by the removal of the N-terminal propetide domain (Haas & Madri, 1999). Inactivity of the latent form (also known as the proMMP form) is maintained by a “cysteine switch”. The highly conserved propeptide domain sequence PRCGXPD prevents proenzyme activity by interactions between the cysteine and zinc (Brinckerhoff & Martrisian, 2002). MMP-2 is expressed in a 74 kDa form, which is activated by a tri-molecular complex of membrane-type 1 MMP- (MT1-MMP), and tissue inhibitor of matrix metalloproteinase-2 (TIMP-2) to its 64 kDa intermediate form (Foda & Zucker,

2001). It is then further cleaved by an already active MMP-2 molecule to its 62kDa active form (Butler, et al., 1998).

Normal MMP function includes participation in growth, would healing, embryogenesis (Brinckerhoff & Martrisian, 2002) ovulation, and menstruation (McCawley & Matrisian, 2000). MMPs have also been shown to be involved in cell signaling by altering active sites on ECM molecules for cell-ECM interactions. MMPs may also release growth factors or other biomolecules during ECM degradation, thereby playing a further role in cell signaling. (McCawley & Matrisian, 2000). MMPs are regulated by a number of factors at the transcriptional and physiologic level. These include cytokines, hormones, the general protease inhibitor α-2 macroglobulin, and the tissue inhibitors of matrix metalloproteinases (TIMPs) (Nelson, Fingleton, Rothenberg, & Martrisian, 2000). This regulation normally ensures a normal balance and function of the ECM, but can be imbalanced in numerous diseases. For instance, an MMP-TIMP imbalance has been seen in many diseases such as arthritis, atherosclerosis, and cancer (Bode & Maskos, 2003).

MMP levels have been demonstrated to be elevated in many forms of cancer. Many members of the MMP family have been shown to be involved in various functions related to cancer such as tumor growth, cell migration, and tumor angiogenesis. (Lu, et al., 2010). It has been shown that elevated levels of MMP-3 and MMP-7 were associated with enhanced breast tumorigenesis in a mouse model (McCawley & Matrisian, 2000).

MMP-2 has been shown to play a role in the degradation and remodeling of the ECM during angiogenesis, allowing tumors to increase their blood supply (McCawley & Matrisian, 2000). MMPs have been found to not to be distributed throughout solid tumors, but localized at the invasive portions, supporting the role of MMPs in tumor invasion (Deryugina & Quigley, 2006). MMPs have also been implicated in degrading peritumoral ECM and having anti-apoptotic affects on migrating cells, leading to tumor metastasis (Deryugina & Quigley, 2006).

However, the role of MMPs in cancer is more complex than overactivation resulting in tumor progression. MMPs can also exhibit protective effects against tumors. For instance, MMP-2 has been shown to generate angiostatin, an angiogenesis inhibitor, from plasminogen (O'Reilly, Wiederschain, Stetler-Stevenson, Folkman, & Moses, 1999). MMP-8 has been identified as a tumor growth suppressor, and MMP-12 inhibits tumor growth when expressed in tumor-associated macrophages. MMP-9 has been shown to have a protective effect against metastasis in some cases (Martin & Matrisian, 2007).

It was originally thought MMPs were produced by the cancer cells, but further research indicated MMPs are produced by connective tissue and inflammatory cells in the tumor environment. MMP-2 has been shown to be produced by the stromal (connective tissue) cells and tumor epithelium in breast, colorectal, and prostate cancer (Nelson, Fingleton, Rothenberg, & Martrisian, 2000). Additionally, MMPs can be stored

by neutrophils and macrophages for later release (Zucker, Pei, Cao, & Lopez-Otin, 2003).

1.4 MMP Cleavable Peptides in Drug/Gene Delivery

Since MMPs play a role in both the proliferation and suppression of tumors, targeting MMPs using inhibitory drugs has not been shown to be effective in humans (Mannello, Tonti, & Papa, 2005). However, the elevation of MMPs in disease states such as cancer can be used as an activator for a drug delivery system. In such a system, the API is connected to an implantable or injectable biomaterial via an MMP-cleavable peptide. The MMP cleaves the peptide, releasing the API in the presence of MMP, but releasing little or no API in the presence of healthy tissue.

Several drug delivery systems have been developed using MMP activation (Vartak & Gemeinhart, 2007). As seen in Table 1, most systems involve conjugating the API to a particle via an MMP cleavable peptide. The particle used prevents cellular uptake of the API and decreases clearance, allowing the drug-particle complex to stay in systemic circulation longer than the API alone. Kratz et. al developed such a system where doxorubicin was conjugated to albumin via an MMP cleavable peptide. This system exploited the tendency of serum proteins to accumulate in the leaky tumor vasculature, known as the enhanced permeation and retention (EPR) effect. Structural and lymphatic drainage abnormalities in tumor neovasculature allow molecules of a specific size range attainable by nanoparticles, including liposomes and micelles

TABLE 1: SUMMARY OF PUBLISHED MMP-CLEAVABLE PEPTIDE DRUG DELIVERY SYSTEMS

Authors	Material	Delivery vehicle	API	Efficacy testing
Albright et. al.	None	Peptide-drug conjugation	Doxorubicin	HT-1080 cells, HT-1080 xenografted mice
Bae et. al.	PEG methyl ether	Micelle	Doxorubicin	Lewis lung carncinoma (LLC) xenografted mice
Chau, Tan, and Langer	Dextran	Polymer-peptide-drug conjugate	Methotrexate	MMP-2 and MMP-9, HT-1080 cells
Garripelli et. al.	Pluronic	Thermogel	Paclitaxel	HT-1080 cells
Kim et. al	Amphiphillic peptide	Nanofiber	Cisplatin	MMP-2
Kratz et. al.	Albumin	Polymer-peptide-drug conjugate	Doxorubicin	RENCA (renal carcinoma) cells, A375 melanoma cells, A375 xenografted mice
Lee et. al.	PEGylated peptide	Micelle	Doxorubicin	MMP-2, LLCs, LLC xenografted mice
Lim et. al	MPEG	Polymer-peptide-drug conjugate	Adriamycin	U-87 MG cells
Tauro et. al.	PEGDA	Hydrogel	Platinum	MMP-2 and MMP-9, U-87 MG cells
Terada et. al.	PEG-peptide dioleoylphosphatidylethano-lamine	Liposome	NOAC	MMP-2, HepG2 cells

(Matsumura & Maeda, 1986). This system was able to successfully increase the therapeutic index of doxorubicin in studies with nude mice (Kratz, et al., 2001, Mansour, et al., 2003). Other such peptide-drug-molecule conjugates include dextran-peptide-methotrexate and methoxy poly(ethylene) glycol-peptide adriamycin, the latter of which was intended to treat gliomas (Chau, Tan, & Langer, 2004, Lim, et al., 2010). Albright et. al. developed a system consisting solely of API-peptide conjugation, allowing the drugs to be activated after MMP peptide cleavage (Albright, et al., 2005). Enclosing the API in a delivery vehicle such as a liposome or micelle takes advantage of the EPR effect. Micelles were used by Bae et. al. (PEG methyl ether) and Lee et. al (PEGylated peptide) for the treatment of lung cancer (Bae, et al., 2003, Lee, Park, Kim, & Byun, 2007). A PEG-peptide dioleoylphosphatidylethano-lamine liposome was used by Terada et. al. intended for the treatment of liver cancer (Terada, Iwai, Kawakami, Yamashita, & Hashita, 2006). Delivery methods using gelation include MMP-2 degradable temperature sensitive thermogels and self-assembling nanofiber gels, and implantable hydrogels (Garripelli, Kim, Son, Kim, Repka, & Jo, 2011, Kim & Yoo, 2010, Tauro & Gemeinhart, 2005).

MMP cleavable peptides have also been successfully utilized in gene delivery. Kim and Yoo used polyethyleneimine (PEI) electrospun nanofibers for DNA delivery for the treatment of diabetic ulcers. They were able to demonstrate DNA release in the presene of MMP-2. Animal studies using mice showed that the DNA green fluorescent protein (GFP) was able to transfect cells, resulting in GFP expression. (Kim & Yoo, 2010). Hatakeyama et. al. developed a system in which a PEG conjugated peptide was

bonded to a lipid envelope containing plasmid DNA. Designed for delivery to tumors, they were able to achieve high transfection levels in HT-1080 cells. They also demonstrated increased circulation time for the PEG-peptide-lipid envelope system compared to the lipid envelope alone (Hatakeyama, et al., 2007).

1.5 Controlled Drug Delivery Using a MMP-2 Triggered Implantable Hydrogel

A hydrogel-based, implantable chemotherapy system for the treatment of GBM has been developed in which the API is conjugated throughout the hydrogel matrix by an MMP cleavable peptide. Unlike the Gliadel wafer, which provided a nonspecific release of a chemotherapeutic agent, this system would release the API in the presence of MMP-2 producing tumor cells (Figure 1.1).

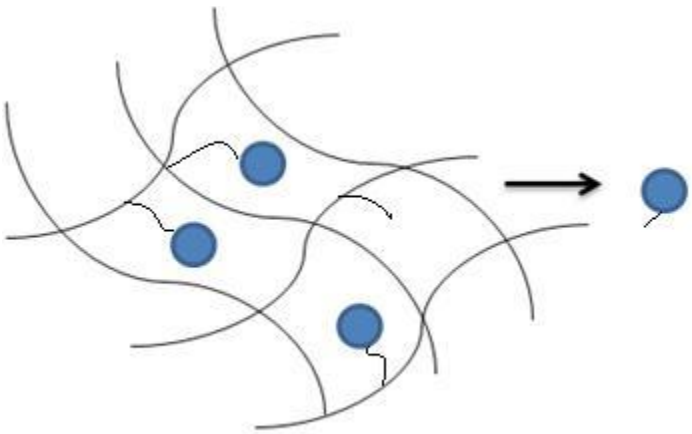

Figure 1.1 Schematic of MMP triggered drug delivery system.

The hydrogel is made of poly(ethylene glycol) diacrylate (PEGDA) (Figure 1.2). PEGDA is a biocompatible, FDA approvable material which has been used in many applications, including tissue engineering and wound repair. The fabrication of PEGDA hydrogels is a chain growth type polymerization that can be accomplished either chemically or by using ultraviolet light. A potential approach in both drug delivery and tissue engineering is to perform *in situ* polymerization, allowing the hydrogel shape to conform to the area of use. This will also allow a less invasive approach to therapy, as the hydrogel solution can be injected rather than surgically implanted. The molecular structure can be modified without serious difficulty, thus allowing the attachment of MMP cleavable peptides (Lin and Anseth 2009). The repeating unit, poly(ethylene glycol) (PEG), has been shown to be biocompatible in brain tissue. A recent study involving implanting PEG hydrogels in mouse brains showed less inflammatory response when compared to needle penetration, as measured by the levels of microglia (neural macrophages) present in brain tissue surrounding the hydrogel implant (Bjugstad, Lampe, Kern, & Mahoney, 2010). PEGDA has demonstrated little adsorption of proteins that could block the mesh and interfere with drug release. PEG is as known as a “stealth” polymer in that its implantation does not result in an immunogenic response (Kim, Hefferan, & Lu, 2000) (Peppas, Bures, Leonbandung, & Ichikawa, 2000). By using a synthetic polymer, greater control over the characteristics can be achieved. There will be greater control over the dosage and timing of delivery than if a natural polymer was used.

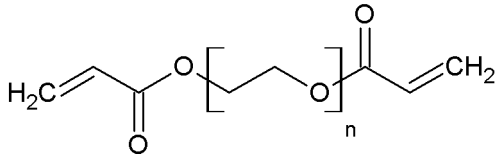

Figure 1.2-Structure of poly(ethylene glycol) diacrylate (PEGDA) macromer

In this system, the drug is attached to the N-terminus of the MMP cleavable peptide. The peptide is attached to the hydrogel by conjugating the peptide to one of the acrylate groups prior to polymerization. For this study, the peptide was conjugated by adding a cysteine residue to the C-terminus of the peptide, and conjugating the sulfylhydryl group on the cysteine to an acrylate group via Michael addition. In place of an API, the fluorescent molecule tetrmethyl rhodamine (TAMRA) was used as a model drug (Figure 1.3). The use of a fluorophore simplifies the measurement of release compared to using a small molecule API. Fluorescence intensity-and therefore release-can be quantified quickly and easily by using a flurorimeter, and these measurements can be further verified by using high-pressure liquid chromatography (HPLC). However, there are several disadvantages to using a fluorophore as a model drug. Any potential interactions between the hydrogel matrix and an actual API would not be elucidated. Fluorophores are sensitive to environment. Fluorescence intensity can change based on pH, solvent, and hydrophilicity. In addition, the excitation and emission wavelengths may vary depending on the composition of the conjugated peptide. For these studies, it was assumed the excitation and emission wavelengths did not change when the

peptide was cleaved. Using TAMRA also elimintated photopolymerization as a possibility, as the UV would have degraded the fluorescent signal. Therefore, chemical initiators were used to introduce the radical species necessary for chain growth polymerization.

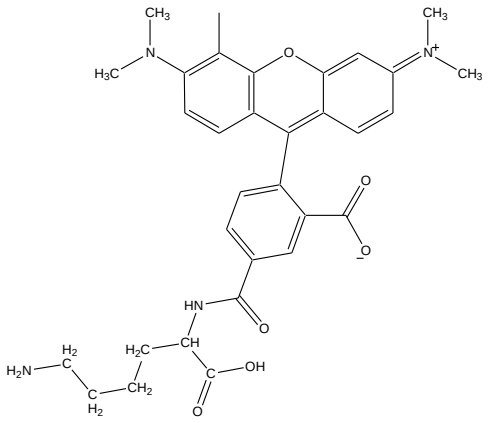

Figure 1.5-Structure of tetramethyl rhodamine (TAMRA)

There are several potential advantages to using this MMP-triggered drug delivery system for brain tumors. Since the initial treatment for brain tumors is surgical resection, the introduction of a catheter for injections would require no additional procedure on a patient. The localized drug delivery would reduce systemic side effects of chemotherapy. Finally, implantation would bypass the blood-brain barrier that inhibits the effects of systemically administered medications. Using a hydrogel-based implantable system, due to its biocompatibility, would result in little to inflammatory reaction from the body and would not adversely affect normal brain tissue.

MMP-2 is useful as a drug delivery activator for two reasons. MMP-2 has high levels of expression in glioblastoma multiforme, but much less in normal brain tissue. (Sawaya, et al., 1996). A cleavable peptide sequence can be designed that is highly specific to MMP-2, yet is short enough to be conjugated to the hydrogel matrix without blocking the mesh and preventing API diffusion.

Previous work with this system showed release of platinum, the model drug, in the presence of MMP-2 and MMP-9 when platinum was conjugated to the hydrogels with an MMP-cleavable peptide. When compared to hydrogels loaded with platinum not conjugated to the hydrogel matrix and incubated with MMP-9, the release with conjugation was more controlled-than when the platinum was merely encapsulated in the hydrogel, and greater release for the conjugated platinum in the absence of MMP-2 (Tauro & Gemeinhart, 2005). MMP-9, also called gelatinase B, shares many overlapping substrates with MMP-2 and is also present in GBM (Tauro, 2006, Rao et. al. 1996). However, this work has not demonstrated that either MMP-2 or MMP-9 enters the hydrogel structure. Previous work by Rahman used bovine serum albumin, a protein roughly the same size as active MMP-2, to study diffusion through PEGDA hydrogels. These studies showed diffusion only occurred when the molecular weight of the PEGDA macromer was increased to 20,000 (Rahman, 2010). Larger molecular weights increase the mesh size, as there is more polymer backbone between crosslinks.

1.6 Study Aims

The ability for MMP-2 to enter the hydrogel, rather than cleaving peptide on the surface, is essential for the maximum efficacy of this drug delivery system. This study answered this question by examining the effects of macromer molecular weight and model drug loading on release. PEGDA macromer molecular weights were assessed with a mesh size both larger and smaller than the dimensions of MMP-2. Therefore, it was hypothesized that hydrogels with larger macromer molecular weights larger than the dimensions of MMP-2 would show a greater MMP-2 mediated release compared to a hydrogel with macromer molecular weight smaller than the dimensions of MMP-2. Optimization of the drug delivery system was also a goal of this study. It was expected that an ideal combination of molecular weight and loading can be found that will maximize the MMP-2 mediated release of the API while minimizing nonspecific release. This assessment included testing the drug delivery system with glioblastoma cells as the ensuing progression to clinical use. Finally, the peptide cleavage and its specific site will were confirmed through multiple analytical methods. These studies were done to refine the MMP triggered drug delivery system and progress this system towards a clinical application.

2. Swelling and Mesh Size

2.1 Background

Hydrogels are viscoelastic polymer systems that are known for their ability to swell to many times their dry weight in the presence of water. The ability to intake water is what allows diffusion of API from the polymer matrix and the ability of the hydrogel to favorably interact in a physiological environment. The degree of swelling and the mesh sizes of hydrogels are of great interest because they determine the rate of diffusion and the mechanical strength of the hydrogel. Hydrogel pores, mentioned in Chapter 1, differ from mesh in that pores are a space in which polymer is continuously absent. Mesh describes the space borderd by polymer chains and crosslinks at a given instant of time. The hydrogel used in the MMP-triggered drug delivery system is nonporous; thus mesh is the primary focus in characterization.

The characteristics of a hydrogel change dramatically upon contact with aqueous solvents. In the dried state, the xerogel's physical properties are glassy-the material is brittle and stiff. Upon solvent penetration between the polymer chains, the material experiences a stress that results in an increase in radius of gyration and the end-to-end length of the polymer chains, which is observed as swelling (Gupta, Vermani, & Garg, 2002). The hydrogel transitions to a rubbery state; upon adding solvent, the glass transition temperature drops. As the hydrogel swells, the retractive force of the elongating polymer chains counters the thermodynamic force of dilution of polymer in

solvent. When these two forces are equal to each other, the hydrogel reaches equilibrium swelling (Peppas N. A., 1986).

Hydrogel swelling can be expressed as weight swelling ratio (q):

$$q=\frac{m_s}{m_d} \qquad (2.1)$$

m_s is the mass of the hydrogel as equilibrium swelling, and m_d is the mass of the xerogel.

Swelling can also be computed as a volumetric swelling ratio (Q) :

$$Q=\frac{v_s}{v_d} \qquad (2.2)$$

where v_s is the volume of the hydrogel at equilibrium swelling, and v_d is the volume of the xerogel.

Another component to determining hydrogel mesh size is the average molecular weight between crosslinks (M_c). The Flory-Rehner model of molecular weight between crosslinks is derived from the change in free energy from mixing and elasticity. The model assumes a Gaussian distribution of polymer chain lengths prior to crosslinking, the chemical structure is neutral in charge, and that all crosslinks are tetrafunctional. This equation applies to polymers crosslinked in the absence of a solvent (Flory & Rehner, 1943) :

$$\frac{1}{M_C} = \frac{2}{M_n} - \frac{\frac{v}{V_1}[\ln(1-\upsilon_{2,s}) + \upsilon_{2,s} + \chi_1 \upsilon_{2,s}^2]}{[(\upsilon_{2,s})^{\frac{1}{3}} - \frac{\upsilon_{2,s}}{2}]} \qquad (2.3)$$

In this equation, M_n is the number average molecular weight, v is the specific volume of the polymer, V_1 is the molar volume of solvent, $\upsilon_{2,s}$ is the polymer volume fraction ($\upsilon_{2,s} = Q^{-1}$), and χ_1 is the Flory solvent interaction parameter.

Peppas and Merrill modified this equation for use with crosslinked networks polymerized in the presence of solvent:

$$\frac{1}{M_C} = \frac{2}{M_n} - \frac{\frac{v}{V_1}[\ln(1-\nu_{2,s}) + \nu_{2,s} + \chi_1 \nu_{2,s}^2]}{\nu_{2,r}[(\frac{\upsilon_{2,s}}{\upsilon_{2,r}})^{\frac{1}{3}} - \frac{\upsilon_{2,s}}{2\upsilon_{2,r}}]} \qquad (2.4)$$

Where $\nu_{2,r}$ is the polymer volume fraction in the relaxed state, when the hydrogel is first polymerized but prior to swelling.

.

Once M_c is determined, the correlation length and average mesh size can be calculated. The correlation length is:

$$\xi = \alpha(r_0^2)^{\frac{1}{2}} \qquad (2.5)$$

where α is the elongation factor of the polymer chains, and r_0 is the root-mean-square distance of the unperturbed polymer chains. In an isotropic hydrogel (a hydrogel that swells equally in all dimensions):

$$\alpha = \nu_{2,s}^{-\frac{1}{3}} \qquad (2.6)$$

To find $(r_0^2)^{\frac{1}{2}}$, between crosslinks, the molecular weight between crosslinks (M_c) and the length of the repeating unit (M_r) are used, along with the length of a single carbon-carbon bond (l)

$$(r_0^2)^{\frac{1}{2}} = \left(l\frac{2M_c}{M_r}\right)^{\frac{1}{2}} \qquad (2.7)$$

Putting these equations together gives the equation for average mesh size (Peppas, Bures, Leonbandung, & Ichikawa, 2000):

$$\xi = \nu_{2,s}^{-\frac{1}{3}} \left[l\frac{2M_c}{M_r}\right]^{\frac{1}{2}} \quad (2.8)$$

There are two methods to determine M_c. Swelling studies can be used to determine $\nu_{2,r}$ and $\nu_{2,s}$. Immediately after polymerization but prior to swelling, the hydrogel is suspended in a nonsolvent. The hydrogel volume is found by employing Archimedes' principle-the apparent weight is equal to the weight of liquid displaced.

The hydrogel is then swollen in water and reweighed until it reaches equilibrium swelling, typically defined as <5% change in weight. It is then reweighed suspended in butanol. The hydrogel is then dried, and the volume determined by weighing in air and dividing by the density of the polymer. Equations 2.9 and 2.10 calculate polymer volume fraction:

$$\nu_{2,s} = \frac{\frac{m_{s,b}}{\rho_b}}{\frac{m_{d,a}}{\rho_p}} \quad (2.9) \qquad \nu_{2,r} = \frac{\frac{m_{r,b}}{\rho_b}}{\frac{m_{d,a}}{\rho_p}} \quad (2.10)$$

where $m_{d,a}$ is the mass of the xerogel in air, ρ_p is the density of the polymer, $m_{r,s}$ is the mass of the hydrogel in the relaxed state suspended in nonsolvent, $m_{s,b}$ is the mass of the hydrogel at equilibrium swelling suspended in nonsolvent, and ρ_s is the density of the solvent. This method requires no special equipment and produces reliable results.

The other method for finding M_c is tensile testing of the hydrogel. Tensile testing is a measurement typically employed to find the strength and stiffness of materials. Rubber elasticity theory describes how polymers are able to enlongate up to several times in original length under stress, yet return to their original dimensions upon the removal of stress. Normally, a polymeric material is composed of many chains, which are coiled and entangled with each other. The coiled length dimensions are much shorter than the end-to-end distance of the chain, largely because the polymer chain is able to lengthen in three dimensions and steric interactions between the functional groups within the chain. When a polymer experiences strain, the polymer chains, normally coiled, uncoil and elongate. This elongation, while allowing for a large deformation in the material, results in a decrease in entropy. Upon removal of stress, the polymer chains revert back to initial coiled state (Flory P. J., 1953). The length of the individual polymer chains affects the ability of the polymers to undergo deformation without failure, as longer chains will undergo greater elongation.

In tensile testing, the material is stretched while clamped, and the force applied to stretch the material a given length is measured. The stress, σ, is calculated by dividing the force by the cross-sectional area, and is measured in pressure units

(typically pascals). Stress is plotted against the strain, ε (percentage change in the length), which is dimensionless.

From the tensile testing information, elastic modulus is calculated :

$$E=\frac{\sigma}{\varepsilon} \quad (2.11)$$

While E is typically in the gigapascal range for metals, hydrogels have a much lower elastic modulus and are typically in the kilopascal range (Callister, 2007).

M_c is calculated using Equation 2.12

$$\frac{1}{M_c}=\frac{2}{M_n}+\frac{\sigma}{RT\rho\left(\alpha-\frac{1}{\alpha^2}\right)} \quad (2.12)$$

where R is the gas constant, T is temperature, ρ is the polymer density, and α is the elongation factor. α can be related to the strain by the equation: α=1+ε. An advantage to M_c determination by tensile testing are that it is more accurate than finding mesh size by weighing, as there are fewer parameters to measure and therefore fewer possibilities for error. Another is that other critical information can be obtained by using this method. Material stiffness and ultimate tensile strength (the largest amount a stress a material can withstand prior to rupture) are useful properties to determine in a number of biomedical applications, though they are not essential for drug delivery. The disadvantage is that tensile testing requires specialized, expensive equipment and proper training on such equipment for accurate results.

For the MMP-2 triggered drug delivery system, the mesh size is important for two reasons. One, the rate of diffusion of cleaved drug from the hydrogel will be determined by the size of the mesh. Two, the mesh size must be large enough for active MMP-2 molecules to enter. The size of the proMMP-2 protein, measured by X-ray crystallography is approximately 9.65 nm in length and 6.76 nm is breadth. The active form is believed to be slightly smaller in breadth (Morgunova, et al., 1999). Determining and controlling the mesh size will be essential to the efficacy and success of the drug delivery system. The hydrogel must have a large enough mesh for MMP-2 entry, but must also be durable enough to withstand the physiological environment.

2.2 Materials and Methods

2.2.1 Determining Mesh Size Through Swelling

Hydrogel creation. Poly(ethylene glycol) diacrylate (PEGDA) (Laysan Bio, Arab, AL) of varying amounts (Table 2.1) was dissolved in 920 μL DDIW. Three different molecular weights of PEGDA were investigated using this procedure: PEGDA 3,400, PEGDA 10,000, and PEGDA 20,000. A stock solution of ammonium persulfate (APS) (Sigma-Aldrich, St. Louis, MO) was prepared by dissolving 500 mg APS in 2.5 mL DDIW (20% weight/volume). A stock solution N'-N'-N'-N'-tetramethylenediamene (TEMED, Sigma-Aldrich, St. Louis, MO) was prepared by dissolving 500 mg TEMED in 2.5 mL DDIW (20% w/v). Hydrogels were polymerized by adding 35 μL APS and 45 μL TEMED to the PEGDA solution. Using a 21 gauge needle, the solution was aspirated and injected into

a mold consisting of two glass slides on either side of a 1/16” silicone rubber spacer (McMaster Carr, Elmhurst, IL), held together with binder clips (Figure 2.1) The mold was incubated for 30 minutes at 37°C.

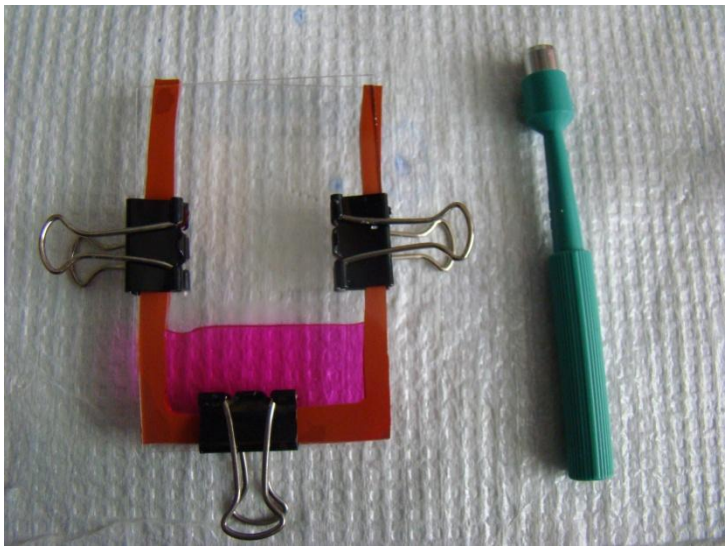

Figure 2.1-Polymerization setup and materials. The hydrogel is sheet cast between the glass slides. Once swollen, the hydrogel sheet is cut into discs using the biopsy punch. PEGDA normally polymerizes as a clear material, but the addition of TAMRA gives the hydrogel its pink color.

TABLE 2.1 MACROMER COMPOSITIONS FOR PEGDA USED IN MESH SIZE EXPERIMENTS.

PEGDA w/v (%)	PEGDA (mg)
10	100
15	150
20	200

Swelling hydrogels. Immediately after incubation, hydrogel sheets were cut into 8 mm discs using a biopsy punch. Three discs were weighed while suspended in 1-butanol. The hydrogels were swollen in DDIW. The hydrogels were re-weighed the next day in air. The hydrogels were weighed again in air at an interval of at least three hours until equilibrium swelling was reached, as defined by a <5% change in mass from the previous weighing. At that point, the hydrogels were weighed again in butanol using the same procedure. The hydrogels were then freeze-dried using a Labonco lyophilizer (Kansas City, MO) for a minimum of eight hours. The xerogels were weighed in air.

Equations 2.9 and 2.10 were used to calculate polymer volume fraction, equation 2.4 was used to calculate molecular weight between crosslinks, and equation 2.8 was used to calculate mesh size. Additional values used were polymer specific density (v) of 0.89 mL/cm^3, molar volume of water (V_1) of 18.1 cm^3/mol, Flory solvent interaction parameter (χ_1) of 0.426, density of butanol of 0.81 g/cm^3, length of the repeating unit (M_r) of 44 g/mol, and the carbon-carbon bond length of 0.154 nm.

2.2.2 Determining Mesh Size Through Tensile Testing

Creation of hydrogels without peptide. Hydrogels were polymerized with APS and TEMED, sheet casted, and incubated. After removing from incubation, hydrogel sheets were swollen in DDIW at and stored at room temperature until further use.

Creation of hydrogels with peptide. The TAMRA conjugated peptide sequence GPLGVRGC (UIC Protein Research Laboratory) was dissolved in DDIW at twice the

intended concentration. PEGDA macromer (150 mg) was dissolved in 500 μL of the peptide solution and 420 μL DDIW. The solution was stirred overnight. The hydrogels were polymerized using APS and TEMED, sheet casted, and incubated. After removing from incubation, hydrogel sheets were swollen in DDIW and stored at room temperature until further use.

Tensile testing. Rectangular hydrogel sheets were measured in three dimensions using electronic calipers. The hydrogel was clamped into a tensile testing load cell (Test Resources, Minneapolis, MN). The hydrogel was preconditioned by stretching at 5%, 10%, or 30% of the length between clamps for PEGDA 3,400, PEGDA 10,000, and PEGDA 20,000 respectively. Preconditioning was performed at different percentages to ensure the maximum amount of stretching without rupture. The preconditioning was performed at 0.1 Hz for thirty cycles. Due to the length of the testing process, hydrogels were periodically sprayed with DDIW to prevent drying. The hydrogel was then extended until rupture. The hydrogel pieces were weighed suspended in butanol and freeze dried to determine $\nu_{2,s}$

From the data output and the measurements of cross-sectional area, stress (σ), strain (ε) and elongation factor (α) were calculated. Elastic modulus was calculated by plotting stress against strain and taking the slope of the trendline. Molecular weight between crosslinks was calculated by plotting stress versus the term α-($1/\alpha^2$), and substituting the slope of the trendlne into Equation 2.12 to find M_c. Temperature was 295 K, ρ was 1.2 g/cm^3, R was 8.31 $\frac{MPa \cdot cm^3}{K \cdot mol}$. Equation 2.10 was used to determine

polymer volume fraction, and equation 2.8 was used to calculate mesh size. The other values in the mesh size equation were M_r of 44 g/mol and l of 0.154 nm.

2.2.3 Statistics

Swelling experiments were performed in triplicate for verification. To determine significant differences, one way Analysis of Variance (ANOVA) was used. Post-hoc Student t-test was used to find statistically significant differences between groups. P-values less than 0.05 were considered to be statistically significant. Tensile testing was performed once, as will be further discussed in 2.3.2.

2.3 Results and Discussion

2.3.1 Determining Mesh Size Through Swelling. It was expected that as molecular weight increased, the hydrogel mesh size would also increase. This is due to two factors. One, by increasing the molecular weight of the PEGDA macromer, the number of repeating units is increased, resulting in greater PEG chain lengths between crosslinks. Root-mean-square end to end distance of solvated PEGDA macromer is approximated by Equation 2.13:

$$<\mathrm{r}>=(3X_n)^{\frac{1}{2}}\mathrm{l}\mathrm{C}_\mathrm{n}\alpha \quad (2.13)$$

where X_n is the degree of polymerization (number of repeating units), l is bond length, C_n is the characteristic ratio, and α is the elongation factor. The characteristic ratio is a factor unique to each material that accounts for restricted chain rotation and fixed angles within the polymer chain (Fried, 2008)Values for <r> were calculated using l of 0.147 nm (the average of the carbon-carbon and carbon-oxygen bonds), C_n of 4.1, and α of 1 (Table 2.2).

TABLE 2.2 END TO END CHAIN LENGTHS FOR PEGDA MACROMERS

PEGDA Molecular Weight (g/mol)	**X_n**	**<r> (nm)**
3,400	76	9.1
10,000	227	15.7
20,000	454	22.2

The second factor as molecular weight increases, the amount of acrylate groups decreases, provided the composition is held constant (Table 2.3). It was also expected that as the composition (w/v%) increased, the mesh size would decrease. This is also due to the presence of increased acrylate groups available for crosslinking.

TABLE 2.3 ACRYLATE GROUP CONCENTRATION IN PEGDA HYDROGEL COMPOSITIONS.

PEGDA Molecular Weight (g/mol)	Acrylate Group Concentration (mM)		
Composition	10%	15%	20%
3,400	59	88	118
10,000	20	30	40
20,000	10	15	20

The swelling and mesh size measurements followed expected patterns in that larger molecular weight resulted in larger mesh size, and increased w/v% decreased mesh size . Large differences in mesh size were seen between the different PEGDA macromers of the same composition (Table 2.4) (Figure 2.2).

TABLE 2.4 VOLUMETRIC SWELLING RATIO AND MESH SIZE OF HYDROGELS MEASURED BY SWELLING.

Composition (w/v %)	Q	ξ (nm)
PEGDA 3,400		
10	14.79±1.99	4.73±0.22
15	9.86±0.04	4.19±0.01
20	7.90±0.40	3.98±0.09
PEGDA 10,000		
10	31.16±2.44	10.43±0.25
15	19.08±2.10	9.11±0.25
20	16.87±0.87	9.20±0.12
PEGDA 20,000		
10	64.76±7.40	18.46±0.18
15	43.26±2.89	16.71±0.30
20	39.75±16.24	17.03±1.07

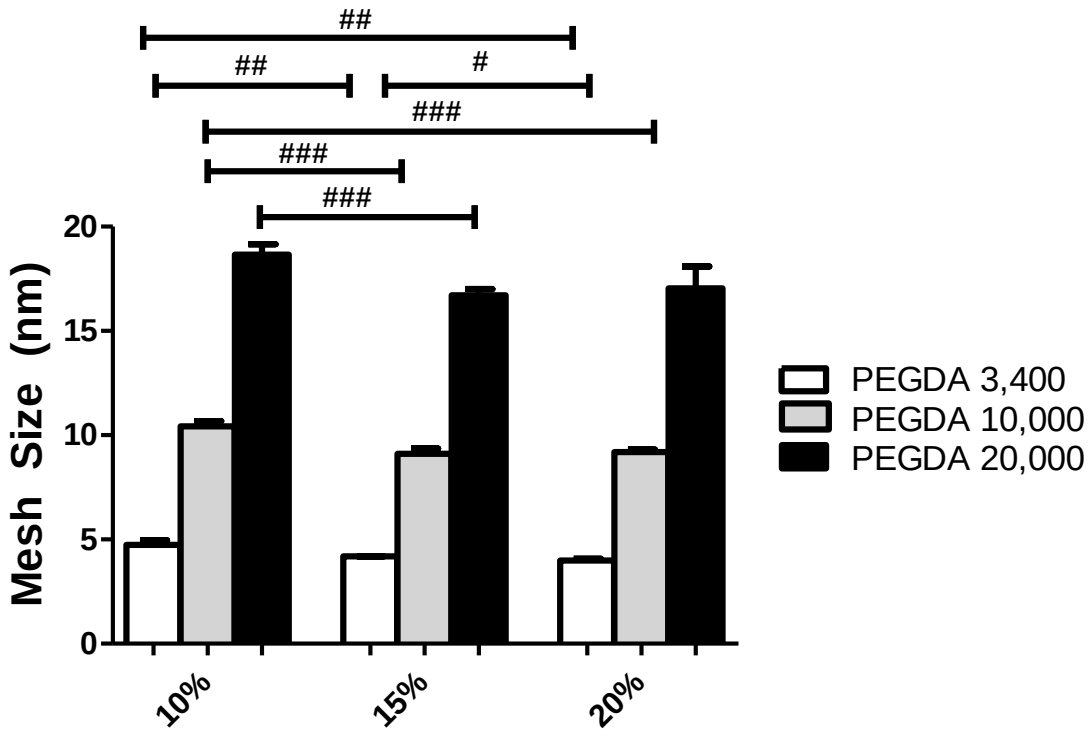

Figure 2.2 Mesh sizes as measured by swelling. Mesh size increased with increasing PEGDA macromer molecular weight and with decreased PEGDA macromer content in the precursor solution. White is PEGDA 3,400, grey is PEGDA 10,000, black is PEGDA 20,000. *p<0.05, ** p<0.01, *** p<0.005. Mean ± SD, n=3

The swelling difference between the different molecular weights of PEGDA macromer was grossly visible (Figure 2.3).

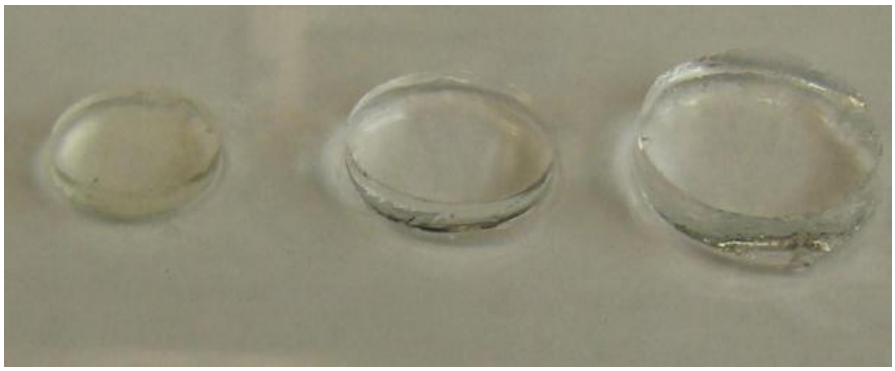

Figure 2.3 Hydrogels at equilibrium swelling. From left to right: PEGDA 3,400, PEGDA 10,000 and PEGDA 20,000. All hydrogels are at 15% w/v initial macromer composition and were originally 8 mm in diameter.

Although changing the composition had less of an effect on mesh size than altering macromer molecular weight, significant differences were still present between the different compositions for the same PEGDA macromer molecular weight. There was a statistically significant difference between the 10% and 15% compositions for all three macromer molecular weights. There was also a statistically significant difference between the 10% and 20% compositions for PEGDA 3,400 and PEGDA 10,000. Significant differences were not seen between the 15% and the 20% for PEGDA 10,000 and PEGDA 20,000. The reason for this is likely due to the terms of the mesh size equation, as will be further discussed in section 2.3.4. Another potential reason is that as the hydrogel polymerizes, the polymer solution becomes more viscous. Although there are may be additional acrylate groups, they cannot form additional crosslinks due to the inability to physically move through the solution. This is a phenomenon observed in other chain growth polymerizations known as gel effect (Cowie & Arrighi, 2008).

Although the 10% w/v composition resulted in the largest mesh size, there were limitations to using this composition. As the weight/volume percentage decreased, the strength of the hydrogel also decreased, as there are fewer polymer chains present to maintain the hydrogel shape. Durability and handling difficulties were observed with the PEGDA 20,000 hydrogels when the 10% w/v composition was used. The ability of the hydrogel to be handled is essential for use in further drug release experiments and eventual clinical applications. The 15% w/v composition allowed for suitable durability at all macromer molecular weights used, and was selected for future release studies.

Based on these results, the PEGDA 20,000 and the PEGDA 10,000 have a mesh size larger than the size of the active MMP-2 protein at a 15% w/v composition. The PEGDA 3,400 has a smaller mesh size than active MMP-2. If mesh size is a factor in MMP-2 entry in the hydrogel, the percent release should be smaller in the PEGDA 3,400 than the PEGDA 10,000 and the PEGDA 20,000. Some peptide cleavage and drug release would occur on the surface of the hydrogel, but the inability of the MMP-2 to penetrate the hydrogel would limit the amount of drug release. The large mesh size difference between PEGDA 10,000 and PEGDA 20,000 may also influence the rate of release.

There are several limitations to the calculations of molecular weight between cross-links and mesh sizes. Although hydrogels have a defined structure, there are irregularities and variations within the structure. There may also be multiple types of crosslinks: both physical and chemical crosslinks may occur in the same hydrogel. Also,

the Flory solvent interaction parameter, χ_1, while normally expressed as a constant, is variable with changes in M_n. The Flory parameter is a measure of the interchange energy between the polymer and solvent. The parameter can be measured by several techniques including light scattering, vapor osmometry, and inverse gas chromotagraphy (Peppas N. A., 1986). However, as M_n decreases, the actual χ_1 decreases from the theoretical value (Cowie & Arrighi, 2008). Another assumption made by equation 2.8 is that all polymer chains are perfectly crosslinked, i.e., there are no non-crosslinked acrylate groups. In reality, pendant polymer chains, polymer chains with a noncrosslinked end, are present in hydrogels. Other variations exist in the hydrogel such that any equation used to determine M_c is only an estimate. However, a more pertinent factor in the measurement is that these measurements were made without the incorporation of the MMP cleavable peptide, GPLGVRGC. The peptide is conjugated to the PEGDA macromer via one of its acrylate groups. By conjugating the peptide, the number of available acrylate groups for crosslinking decreases, which as previously discussed is a factor in increasing mesh size. The measurement is complicated by the fact that the incorporation of the peptide also introduces a zwitterionic component. The model drug, TAMRA, has two carboxyl groups which are deprotonated at physiological pH. The peptide itself has an arginine residue which is positively charged at physiological pH. The previously mentioned equation for determining M_c is valid solely for neutral hydrogels. No equation in the literature exists for finding M_c for zwitterionic hydrogels. Nonetheless, since the negatively charged groups outnumbered the positively charged groups, it was attempted to find M_c using the equation for anionic

hydrogels by Peppas et. al (Peppas, Huang, Torres-Lugo, Ward, & Zhang, 2000), and using this information to determine mesh size.

Mesh size was measured for several of the compositions of PEGDA 3,400 and PEGDA 20,000 with 0.5 mM TAMRA-GPLGVRGC by measuring swelling as previously described. Despite values for $\nu_{2,r}$ and $\nu_{2,s}$ that were comparable to those in hydrogels without peptide, the M_c equation for anionic hydrogels did not produce a reasonable answer. The M_c values obtained for PEGDA 3,400 were 0.00007-0.00011 g/mol, six orders of magnitude smaller than M_r (44 g/mol). The resulting mesh size was from 0.004 to 0.005 nm. A thorough search of the literature reveals several slightly different versions of this equation by Peppas, Bures et. al (Peppas, Bures, Leonbandung, & Ichikawa, 2000), and by Brannon-Peppas and Peppas (Brannon-Peppas & Peppas, 1990) but the alternate versions did not provide a realistic answer either. Dimensional analysis of all of the equations reveals a mismatch in the units. Therefore, tensile testing was employed to find M_c in the hydrogels with conjugated peptide.

2.3.2 Determining Mesh Size Through Tensile Testing. Due to time and accessibility constraints, only one sample of each molecular weight for both conditions (with and without peptide) were subjected to tensile testing. No temperature control was performed for the testing conditions. Temperature can affect tensile testing measurements, as polymer chain movement increases with increasing temperature. The ambient temperature was consistent throughout testing sessions and far above the glass transition temperature for a PEGDA hydrogel in the swollen state. The glass

transition temperature has a sigmoidal curve with a steep transition at T_g. Entanglements are closely packed and movement is limited in the glassy state, therefore modulus is high. In the rubbery state, the polymer chains are able to move more freely, and modulus decreases (Fried, 2008). Therefore, it was decided to forgo strict temperature controls for tensile testing. Although three different peptide loading amounts were used in the release study, only one amount-0.5 mM-was used in tensile tests. Also, only hydrogels with in the 15% PEGDA composition were tested. This was also due to accessibility constraints, and that the presence or absence of peptide would have a greater impact than differences in loading amounts. These factors are limitations in the interpretation of the results, but a reasonable estimate of the elastic moduli and resulting mesh size can be obtained.

Elastic moduli in all groups were within expected values and followed expected trends (Table 2.5). PEGDA 3,400 had the highest elastic modulus, and PEGDA 20,000 had the lowest. Elastic moduli were lower for the hydrogels with peptide compared to hydrogels without peptide at the same molecular weight. The PEGDA 20,000 was the most severely affected by the incorporation of peptide, with the modulus dropping from 16.1 kPa to 4.7 kPa. It was expected that the strength of PEGDA 20,000 would be the most severely affected, as the PEGDA 20,000 has the fewest acrylate groups.

TABLE 2.5 ELASTIC MODULUS OF PEGDA HYDROGELS

MW	E without peptide (kPa)	E with peptide (kPa)
3,400	58.0	44.6
10,000	Not measured	39.9
20,000	16.1	4.7

Mesh sizes measured by tensile testing were slightly smaller than measured with swelling alone, but not small enough to affect the entry or lack of entry of MMP-2 (Table 2.6). Between the hydrogels with peptide and the hydrogels without peptide, the PEGDA 3,400 showed a larger mesh size with peptide than without peptide. Surprisingly, PEGDA 20,000 with peptide showed a smaller mesh size (9.75 nm) compared to the same molecular weight hydrogel without peptide. A model was created to explain this finding as discussed below.

TABLE 2.6 MESH SIZE COMPARISON OF PEGDA HYDROGELS

MW	Mesh Size by Swelling, no peptide (nm)	Mesh Size by Tensile Testing, no peptide (nm)	Mesh Size by Tensile Testing, Peptide (nm)
3,400	4.19±0.01	3.81	4.03
10,000	9.11±0.25	Not measured	9.13
20,000	16.71±0.30	13.65	9.75*

2.3.3 Mesh Size Model. It was observed that the swollen polymer volume fraction ($\nu_{2,s}$) for the tensile tested hydrogel was 0.11, larger than the values obtained with other PEGDA 20,000 hydrogels measured at the 15% w/v composition. The mean $\nu_{2,s}$ for the hydrogels whose mesh size was measured by swelling was 0.023. Equation 2.8 was used to model the relationship between mesh size and swollen polymer volume fraction. Molecular weight between crosslinks was estimated as half macromer molecular weight ($M_c=M_n/2$). Substituting carbon bond length and mass of the repeating unit into the equation gives:

$$\xi = \nu_{2,s}^{-\frac{1}{3}} * 8.37 \quad (2.14)$$

The equation was normalized by dividing all mesh size values by the mesh size obtained for $v_{2,s}=0.023$. The actual mesh size data for all PEGDA 20,000 hydrogels was normalized by dividing by all values by the mean mesh size at 15% w/v. Values for $v_{2,s}$ were graphed against $\xi/\xi_{0.023}$.

The mesh size data obtained from both swelling of the hydrogels and tensile testing fits the model well (Figure 2.4). The effect of $\nu_{2,s}$ on mesh size decreases with increasing polymer volume fraction. The 9.75 nm mesh size obtained for the hydrogel tensile tested with peptide is roughly 58% of the value seen at the mesh size of 0.23, which is close to the model's prediction. The measurement of molecular weight between crosslinks and swollen polymer volume fraction are independent of each other. From this it can be ascertained that the unexpected mesh size measurement with this hydrogel is not due to an error or irregularity in the tensile testing, but from the unexpectedly high measurement for $\nu_{2,s.}$

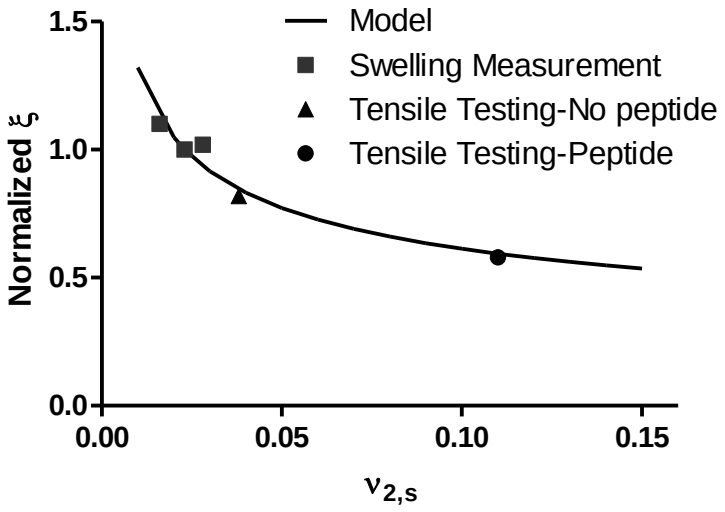

Figure 2.4 Model and actual data of mesh sizes in PEGDA 20,000 hydrogels. Squares are measurements by swelling at all three compositions, triangle is tensile testing without peptide, and circle is tensile testing with peptide.

The reason for the hydrogel with peptide having a higher $\nu_{2,s}$ than its counterparts without peptide cannot be determined from this study. The total amount of peptide added to the hydrogel was less than 1 mg. The 8 mm disc xerogel measurements were 6-12 mg, and the xerogel measurement for the tensile tested sample was 39.02 mg. It is unlikely that the presence of peptide skewed the mass and volume measurements. It is possible that the measurement made was an aberrant sample. Replication of tensile testing with the peptide-conjugated PEGDA 20,000 will determine if this is the case. Despite the substantial decrease, the mesh size measured for this hydrogel was large enough for MMP-2 entry and larger than the PEGDA 3,400.

2.4 Conclusions

The mesh sizes of PEGDA hydrogels were measured by swelling and by tensile testing. Swelling revealed measurements revealed mesh sizes varied slightly but significantly by changing compositon from 10 to 15% w/v PEGDA. Measurements varied substantially among different macromer molecular weights. PEGDA 3,400 was found to have a mesh size smaller than the dimensions of MMP-2, while PEGDA 10,000 and PEGDA 20,000 had mesh sizes larger than active MMP-2. These results indicate that PEGDA hydrogel mesh size can be finely tuned to the application as necessary for maximum clinical efficacy.

Preliminary tensile testing results showed hydrogel mesh sizes close in value to the measurements made by swelling. Elastic moduli were consistent with expected values for hydrogels and followed the expected pattern of lower modulus for larger macromer molecular weight. It was expected that hydrogels with peptide would have a

lower elastic modulus and greater mesh size than hydrogels without peptide. This pattern was not observed with the PEGDA 20,000 hydrogels due to the larger than expected swollen polymer volume fraction. How the mesh size affects release will be explored in the next chapter.

3. Release Studies Varying Molecular Weight and Drug Loading

3.1 Background

The ultimate test of a drug delivery system is its ability to release its API. The delivery amount and timing of release are crucial to the success of the drug delivery system in a clinical setting. In the MMP-triggered hydrogel system, once the MMP-2 has cleaved the MMP-sensitive peptide the API and the cleaved peptide fragment are released from the hydrogel via diffusion. It must be determined that drug is released in the presence of active MMP-2 in a greater amount than seen in the absence of MMP-2. The entry of MMP-2 to the hydrogel is a critical factor to the appropriate functioning and efficiency of this drug delivery system.

One of the variables examined was the effect of molecular weight on release. Previous work on this system by Tauro demonstrated greater release of platinum from PEGDA hydrogels of molecular weight 4,000 compared to PEGDA hydrogels of molecular weight 574 (Tauro & Gemeinhart, 2005). This indicates molecular weight is a factor in the release of the API. As seen in Chapter 2, the mesh sizes greatly increase with increases in molecular weight, and the PEGDA 3,400 hydrogels had a smaller mesh size than the dimensions of MMP-2. It was hypothesized the release in the presence of MMP-2 would be significantly less than PEGDA 10,000 or PEGDA 20,000 because the MMP-2 could not enter the hydrogel. It is also that greater release will be seen in the PEGDA 20,000 compared to the PEGDA 10,000 due to the larger mesh of PEGDA 20,000.

Another variable examined was the initial peptide concentration in the hydrogels. The amount of drug loading affects the amount released both specifically by the MMP-2, and the amount released in its absence (nonspecific release). The absolute amount of conjugated peptide across hydrogels of different molecular weight also varies. Absolute peptide content decreases as molecular weight increases. This happens for two reasons. Because the peptide is conjugated to the PEGDA via its acrylate groups, the amount conjugated will depend on the concentration of acrylate groups. PEGDA 3,400, having the greatest number of acrylate groups available, would be expected to have the greatest amount of conjugated peptide. The other reason why peptide loading varies with molecular weight is the amount of swelling. As the hydrogel imbibes water, the hydrogel volume increases. This happens to a greater extent with the PEGDA 10,000 and the PEGDA 20,000 than with the PEGDA 3,400. For these studies, all hydrogels were swollen prior to cutting into discs for the release study in order to keep sample volume similar among all three molecular weights. Thus, the amount of peptide present in the samples decreased with increased molecular weight. It was hypothesized that the peptide concentration would affect the amount of drug release not only in absolute amounts, but as a percentage of the total peptide content present in the hydrogel. It was also thought this information could be applied to optimize the MMP-2 triggered hydrogel drug delivery system to achieve the greatest percentage of specific release while minimizing the nonspecific release.

The third variable examined was the peptide sequence used. A number of MMP-2 cleavable sequences have been identified in the literature. Several general

characteristics exist in MMP-2 cleavable peptides. Defining a peptide sequence as P3, P2, P1, P1´, P2´, P3´ where the cleavage site is between P1 and P1´, P1´ tend to be hydrophobic, P2´ is hydrophobic or basic, and P3´ is an amino acid with a small residue (Turk, Huang, Hiro, & Cantley, 2001). However, not all MMP cleavable sequences have the same characteristics, and cleavage rates have been shown to vary among the different peptides. External factors can also affect the ability of MMP-2 to cleave a substrate peptide. Tauro found in previous work with this drug delivery system that peptide length increased the specificity for MMP-2 cleavage (Tauro, Lee, Lateef, & Gemeinhart, 2008). Hydrophilicity and ability to synthesize are two other factors that affect the ability to utilize MMP-2 cleavable peptides. The most thoroughly examined sequence was GPLGVRG. This peptide had been used by Vartak and had shown to be cleavable by MMP-2 (P1=glycine P1´=valine) in a study of interactions between MMP-2 and the integrin αvβ3. (Vartak, Lee, & Gemeinhart, 2009). This peptide sequence has also been used by Lee et. al. in a drug delivery system using micelles composed of PEGylated MMP sensitive peptides conjugated to doxorubicin (Lee, Park, Kim, & Byun, 2007).

Comparisons were made with two additional MMP cleavable peptide sequences. This was done to further confirm that the MMP-2 was responsible for the increased drug release in its presence. It was also done to demonstrate the drug delivery system could be used with multiple peptide sequences. There was also the possibility of further optimization, in that one peptide might show a greater efficiency in release than the other two. One of the chosen peptide sequences was PAGLLG, previously used by

Tauro in this drug delivery system (Tauro, Lee, Lateef, & Gemeinhart, 2008). The cleavage site is between the first glycine and the first leucine. The peptide was known to show specific release in the presence of MMP-2 with a k_{cat}/K_m ratio of $1.7x10^4 \pm 1x10^4$ M^{-1} s^{-1}. Also, comparisons between this work and previous work were considered helpful for optimizing the drug delivery system. The other peptide sequence selected was IPVSLRSG, where P1 is serine and P1´ is leucine. A study by Turk et. al. examined the hydrolysis of over 20 known MMP-2 sensitive peptides. Using this information, they created a "consensus peptide" sequence for MMP-2. This sequence was shown to have a k_{cat}/K_m ratio of $8.2x10^4 \pm 6x10^4$ M^{-1} s^{-1} and an increased cleavage rate (greater V_{max}/K_m) compared to know MMP-2 sensitive peptide sequences from FGFR-1 and MCP 3. However, a SPARC peptide was shown to have better cleavage rates than the optimized sequence (Turk, Huang, Hiro, & Cantley, 2001).

It is noted the three peptides selected not only differ in amino acid composition, but in length. This is a possible factor in the release rates as the cleaved fragment will be larger or smaller. However, all peptide sequences are much shorter than the hydrogel mesh, and the hydrogel-model drug complex in these studies occupied a fairly narrow range of molecular weight (1040-1340 Da). It was not expected that the peptide length by itself would be a factor in increased specificity for MMP-2 cleavage.

To further verify the TAMRA release was due to the cleaved peptide fragment, buffer from the release studies was examined using reverse phase high pressure liquid chromatography (HPLC). HPLC is a technique by which solution components are

separated from each other by degree of hydrophilicity (Fallon, Booth, & Bell, 1987). In reverse phase HPLC, the mobile phase is a somewhat polar liquid pumped through the hydrophobic stationary phase (column packing). The greater the hydrophobic surface area of the compound, the longer retention time in the column because the compound is has a greater affinity for the stationary phase. The elutent is detected by fluorescence, absorbance, or both. The anticipated cleaved peptide fragment TAMRA-GPLG has fewer hydrophobic residues and less hydrophobic surface area than the full peptide sequence TAMRA-GPLGVRGC. Therefore, it was expected that the elution time for the cleaved fragment would be shorter than for the uncut peptide. This shorter elution time would be present in chromatograms from the release buffer.

Further analysis of the released peptides was performed using matrix-assisted laser desorption/ionization/time of flight mass spectrometry (MALDI-TOF MS). Mass spectrometry is a technique for separating particles in a sample based on size and identifying their molecular weights with great accuracy. MALDI has been shown to be a useful technique to identify biomolecules. The sample is placed in a matrix, a solution of a crystalline substance that can easily transfer ions to the sample. The matrix-sample mixture is exposed to a laser. As the matrix and sample are vaporized, the matrix protects the sample from being destroyed by the energy source by absorbing the energy from the laser. The sample is also ionized in the process by the energy transfer from the matrix molecules to the sample species. The sample analysis is done by time of flight (TOF) technique. The ionized sample is deflected by an electric field that measures its velocity. The velocity of the ions is proportional to the inverse square root

of the mass charge ratio [$(m/z)^{-1/2}$] (Hillenkamp, Karas, Beavis, & Chait, 1991). The ions then drift into a field free region, where detection occurs. MALDI-TOF MS was used to find the molecular weights of species present in the samples, specifically in the elution peaks on the HPLC suspected to be the cleaved peptide.

3.2 Materials and Methods

3.2.1 Determining Excitation and Emission Wavelengths of TAMRA Conjugated Peptides.

TAMRA conjugated peptide was weighed and dissolved in tris buffered saline with zinc (TBS/Zn) for a composition of 32µg/mL. The buffer was composed of 50 mM Tris base, 200 mM sodium chloride (NaCl), 10mM calcium chloride dihydrate ($CaCl_2$-$2H_2O$), 0.5% Brij-35, and 50 µM zinc sulfate septahydrate ($ZnSO_4$-$7H_2O$) and adjusted to pH 7.4. Solution (100 µL) was pipetted into three wells of a 96 well plate (Corning Life Sciences, Corning, NY). The plate was placed in a Spectramax GeminiXS fluorescence plate reader (Molecular Devices Corporation, Sunnyvale, CA) and an emission spectrum protocol was run using an excitation wavelength of 540 nm, a range of 545 to 750nm. The wavelength for maximum fluorescence intensity was selected, and an excitation spectrum was performed from 350nm to just under the emission wavelength. This process was repeated until the maximum excitation and emission were found. The procedure was performed for TAMRA-PAGLLGC and TAMRA-IPVSLRSGC (Figures

3.1 and 3.2). The excitation and emission wavelengths for TAMRA-GPLGVRGC had previously been determined by another member of the group.

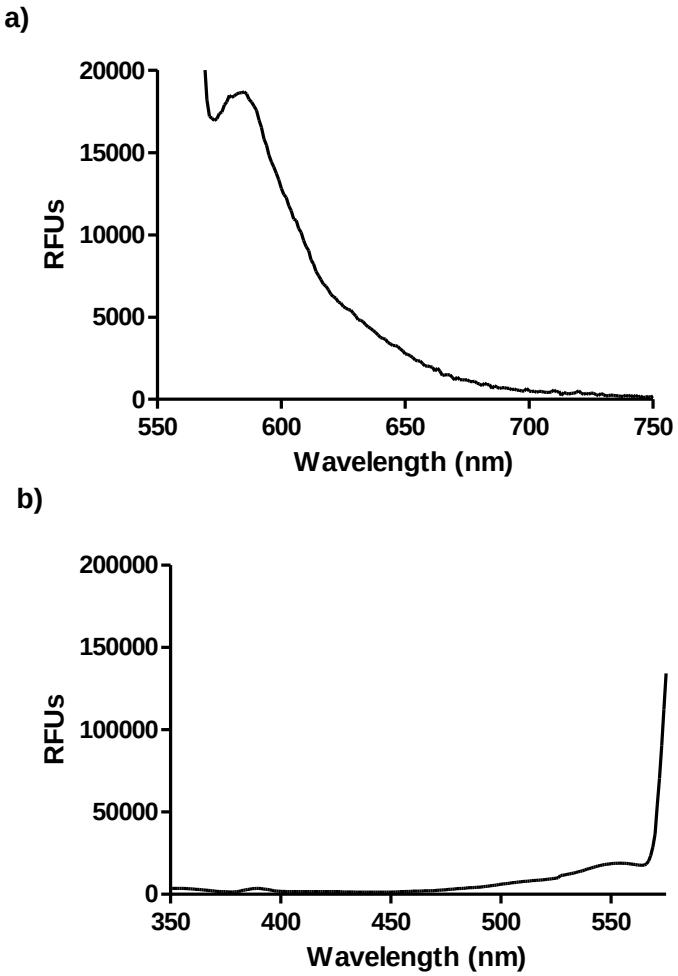

Figure 3.1 Emission (a) and excitation (b) spectra for TAMRA-PAGLLGC. Graphs representative of three samples.

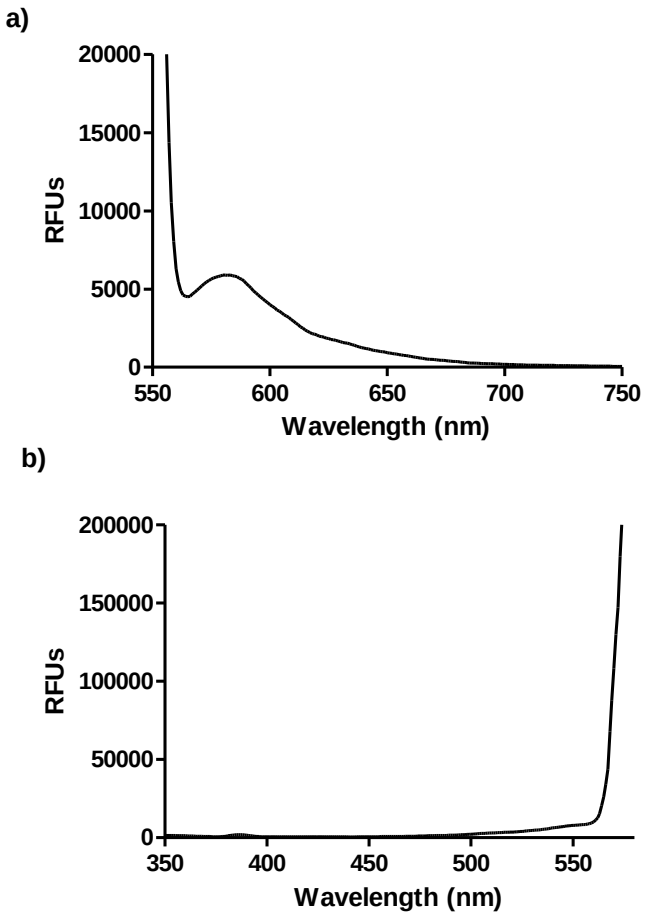

Figure 3.2 Emission (a) and excitation (b) spectra for TAMRA-PAGLLGC. Graphs representative of three samples.

When creating the standard curve for TAMRA-IPVSLRSGC, it was observed TBS/Zn without peptide had a high fluorescent signal at the maximum excitation and emission wavelengths for this peptide (560 nm and 580 nm, respectively). RFUs were in the range of 4000-5000. Out of concern that a high fluorescent signal would interfere with peptide release measurements, the excitation wavelength was altered to a wavelength near the maximum with less signal from TBS/Zn alone, while keeping

emission wavelength constant. At an excitation wavelength of 540 nm, the RFU values decreased less than 5 for TBS/Zn. An excitation wavelength of 540 nm and emission wavelength of 580 nm was used for all measurements with TAMRA-IPVSLRSGC (Table 3.2)

TABLE 3.1 EMISSION AND EXCITATION WAVELENGTHS FOR MMP CLEAVABLE PEPTIDES

Peptide	**Excitation Wavelength (nm)**	**Emission Wavelength (nm)**
TAMRA-GPLGVRGC	540	570
TAMRA-PAGLLGC	550	585
TAMRA-IPVSLRSGC	540	580

3.2.2 Standard Curve Creation.

The MMP cleavable peptide was dissolved in TBS/Zn. Peptide solution (200 μL) was pipetted into three wells of a 96 well plate (Corning Life Sciences, Corning, NY). Half the solution was transferred from each well into a new well. TBS/Zn was added to the new wells to dilute the solution. This process was repeated 5 to 7 times. Three wells were filled with TBS/Zn without peptide. The plate was read Spectramax GeminiXS fluorescence plate reader (Molecular Devices Corporation, Sunnyvale, CA) at the appropriate excitation and emission wavelengths. The standard curves were created to

translate a relative fluorescence unit (RFU) into an amount of peptide present. Two standard curves were created for TAMRA-GPLGVRGC (Figures 3.3 and 3.4). This was done because the experiments with low peptide loading (0.15 mM) were read at a different sensitivity on the flurorimeter than the experiments with medium and high peptide loading (0.5-1.75 mM). The PMT is a component of the fluorimeter that amplifies the fluorescent signal, and can be set at low, medium, or high sensitivity. Setting the PMT to low sensitivity will caused low fluorescence readings to be distorted or lost; at higher sensitivity caused saturation for highly concentrated samples. The standard curve for medium and high peptide loading release studies was created on low sensitivity, the standard curve for low peptide loading was created on medium sensitivity. Because the relative fluorescence unit (RFU) values in the release study for the low peptide loading were fairly small, there was a concern that low fluorimeter PMT sensitivity would not be able to distinguish between the absence and presence of fluorescence accurately. Therefore, a standard curve with the medium sensitivity was used. This standard curve could not be used for the other peptide loading concentrations, because at higher sensitivities, the fluorimeter saturates when reading higher RFU values.

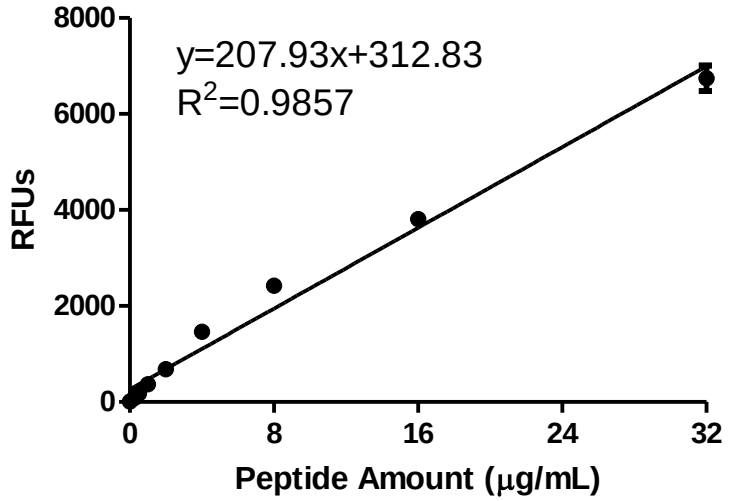

Figure 3.3 Standard Curve for TAMRA-GPLGVRGC at low PMT intensity. This curve was used for the medium and high loading conditions. Values are mean ± SD, n=3

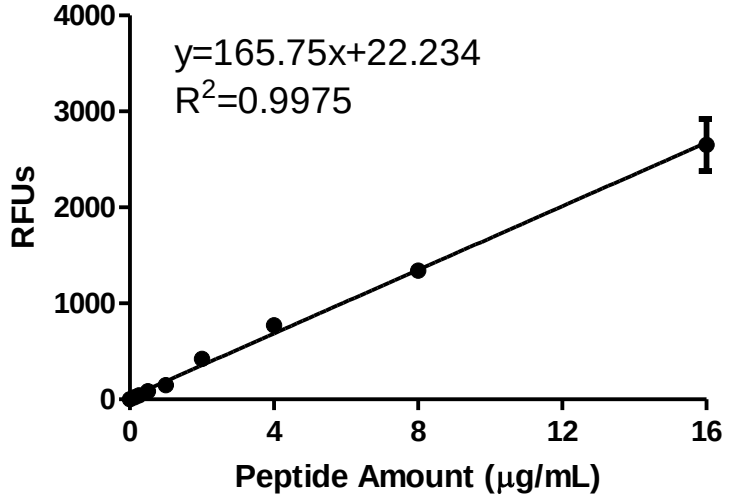

Figure 3.4 Standard Curve for TAMRA-GPLGVRGC at medium PMT intensity. This was used for the low peptide loading condition. Values are mean ± SD, n=3

Only one standard curve was created for TAMRA-PAGLLGC (Figure 3.5) and TAMRA-IPVSLRSGC (Figure 3.6). Had release experiments been conducted at low peptide loading for these peptides, a second standard curve would have likely been necessary.

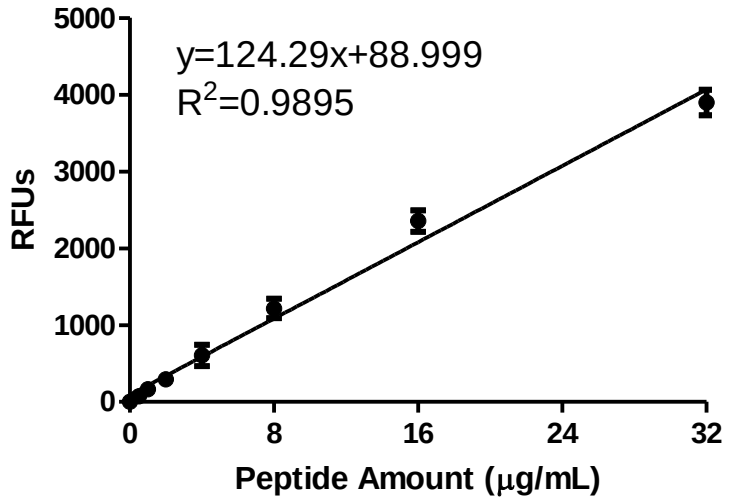

Figure 3.5 Standard curve for TAMRA-IPVSLRSGC. Values are mean ± SD, n=3

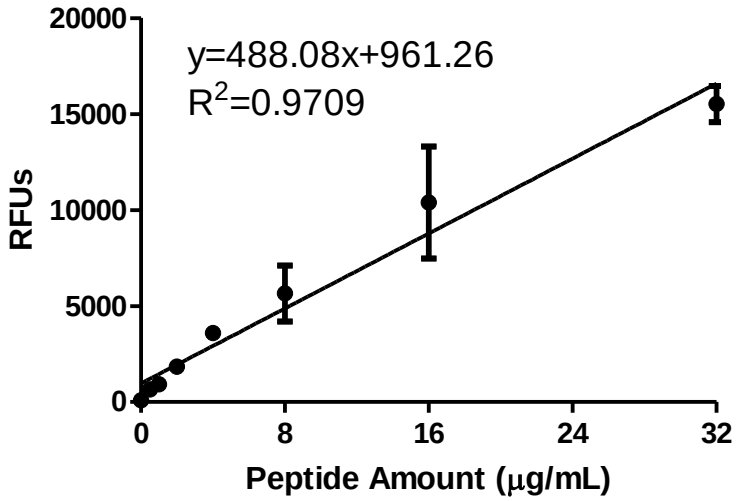

Figure 3.6 Standard curve for TAMRA-PAGLLGC. Values are mean ± SD, n=3

3.2.3 Peptide Release from Hydrogels.

Creation of hydrogels with conjugation of PEGDA to the MMP cleavable peptide.

The TAMRA conjugated peptide sequence (UIC Protein Research Laboratory) was attached to the PEGDA macromer at the appropriate concentration (Table 3.2). Hydrogels were polymerized using APS and TEMED, sheet casted, and incubated as described in section 2.2.2.

TABLE 3.2 COMPOSITION OF HYDROGELS WITH MMP CLEAVABLE PEPTIDE AT MULTIPLE CONCENTRATIONS

Intended Concentration (mM)	Initial Concentration (mM)	PEGDA Amount (mg)	Initial Volume (μL)	DDIW (μL)	APS (μL)	TEMED (μL)	Total Volume (μL)
0.15	0.30	150	500	420	35	45	1000
0.5	1.0	150	500	420	35	45	1000
1.0	2	150	500	420	35	45	1000
1.75*	3.5	150	500	420	35	45	1000

Hydrogel washing. After conjugation and polymerization, the hydrogel sheet was washed in TBS/Zn. The sheet was washed twice, allowing 3 to 4 hours for each wash. The sheet was then cut into 6mm discs using the biopsy punch. Each disc was placed in a 24 well plate with 1 mL TBS/Zn buffer. Hydrogels were then washed overnight. The buffer fluorescence was checked the next day by pipetting 100 μL from each well into a 96 well plate and reading the plate in a Spectramax GeminiXS fluorescence plate reader (Molecular Devices Corporation, Sunnyvale, CA) at the appropriate excitation and emission wavelengths (Table 3.2). Hydrogels continued to be washed in TBS/Zn buffer until buffer fluorescence was stable. Typically, this required a total of 4 to 5 washes.

Creation of hydrogels without peptide. Hydrogels were polymerized using APS and TEMED, sheet casted, and incubated as described in section 2.2.1. Hydrogels were

washed in TBS/Zn to swell and remove unreacted macromer and initiators. Once swollen, they were cut into 6mm discs using a biopsy punch.

Peptide release studies. Hydrogel discs with or without conjugated peptide were placed in a 96 well plate. The wells with hydrogels were filled with either TBS/Zn or TBS/Zn + 9 nM active MMP-2 (EMD/Calbiochem, Gibbstown, NJ). Hydrogels were incubated at 37°C. Buffer fluorescence was measured at 2, 4, 6, 8, 24, 48, 72, and 96 hours. At each time point, the buffer fluorescence was measured by removing 100µL of buffer from each well and placing in a black 96 well plate (Corning Life Sciences, Corning, NY). The remaining buffer was removed from the wells and replaced, and the MMP-2 was resupplemented. The black 96 well plate was read in a Spectramax GeminiXS fluorescence plate reader (Molecular Devices Corporation, Sunnyvale, CA) at the appropriate excitation and emission wavelengths.

Determination of total peptide content. Hydrogel discs washed but not used in the release study were hydrolyzed to calculate total peptide content. Hydrogel discs were placed in a 50 mL centrifuge tube (BD Biosciences, Franklin Lakes, NJ). One milliliter of 1N sodium hydroxide was added to the tube. The tube was heated in a water bath at 100 °C for fifteen minutes or until the hydrogel had been hydrolyzed. The tube was weighed. The pH of the hydrolyzed solution was measured using a Fisher Accumet pH meter (Thermo Fisher Scientific, Waltham, MA). For TAMRA-GPLGVRGC, the pH was adjusted to around 7.52, the pH value of the peptide in TBS/Zn. For TAMRA-PAGLLGC, this value was 7.53, and for TAMRA-IPVSLRSGC, this value was 7.55. The tube was

reweighed. The volume of added hydrocholoric acid was determined by subtracting the mass prior to pH adjustment from the mass after pH adjustment. The density of hydrochloric acid was approximated as 1 g/cm^3. Total volume was calculated by adding this amount to the 1mL of sodium hydroxide and the volume of the original hydrogel. Hydrolyzed solution (100 μL) was pipetted into three wells of a 96 well plate and read using a Spectramax GeminiXS fluorescence plate reader (Molecular Devices Corporation, Sunnyvale, CA) at the appropriate excitation and emission wavelengths (Table 3.2). The mean RFU value was used to determine the total RFU value. This value was put in the standard curve equation to determine the total mass of peptide in the hydrogel.

To confirm sodium hydroxide did not significantly alter fluorescence intensity compared to TBS/Zn, TAMRA-GPLGVRGC was weighed and dissolved in TBS/Zn at a composition of 64 μg/mL. The solution was diluted to 10μL/mL in either TBS/Zn or sodium hydroxide. Solutions (100 μL) was pipetted into a 96 well plate (Corning Life Sciences, Big Flats, NY) and read using a Spectramax GeminiXS fluorescence plate reader (Molecular Devices Corporation, Sunnyvale, CA) at λ_{ex}=540 nm and λ_{em}=570 nm.

Mean peptide content was used to determine the percentage release in the hydrogel. Ratio of peptide relased with MMP-2 to peptide relased in buffer (p_r) was calculated by dividing percentage released with MMP-2 over percentage released in

buffer. Standard deviation was calculated using propagation of error formula for division (Ku, 1966):

$$\frac{1}{\sqrt{n}}\frac{X}{Z}\sqrt{\frac{\sigma_X}{X^2}+\frac{\sigma_Z}{Z^2}-2\frac{\sigma_x\sigma_y}{XZ}\rho_{XZ}} \quad (3.1)$$

where n is the number of samples. X is the peptide release with MMP-2, Z is the peptide release in buffer only, σ_x and σ_z are the variance of X and Z, respectively and ρ_{XZ} is the covariance of X and Z. Because the measurements of peptide release were independent of each other, covariance was assumed to be 0.

3.2.4. Verification of Peptide Cleavage Using HPLC.

Buffer from release studies at either the 24 hour or 48 hour time point was examined using a Waters HPLC system (Waters Corportation, Milford MA). A 10μL sample was run through a Symmetry C18 column using a gradient mobile phase of acetonitrile (ACN) and filtered DDIW at a rate of 1 mL/minute for 60 minutes. The initial mobile phase composition was 20% ACN/80% DDIW and the final concentration was 80% ACN/20% DDIW. Samples were detected using a Waters fluorescence detector set to 540 nm excitation, 570 nm emission. To establish the elution time of the original peptide, TAMRA-GPLGVRGC was dissolved in TBS/Zn at a concentration of 25 μM. The solution was analyzed with HPLC under the same conditions.

3.2.5 MALDI-TOF MS of peptide cleavage from purified MMP-2

Hydrogel creation. The TAMRA and conjugated peptide sequence was conjugated to PEGDA 20,000. The hydrogel was polymerized with APS and TEMED as described in section 2.2.2, incubated, and washed.

Peptide release. Hydrogel discs were placed in a 96 well plate (Corning Life Sciences, Corning, NY) in SF EMEM with either 9 nM active MMP-2 (EMD/Calbiochem, Gibbstown, NJ) or 9nM MMP-2 and 2mM GM6001 (EMD/Calbiochem, Gibbstown, NJ). The hydrogels were incubated at 37°C for 24 hours. Media was analyzed using HPLC as described in section 3.2.4. Samples were fractionated by collecting the mobile phase elutent corresponding to chromatogram peaks as it exited the fluorescence detector. Fractions were analyzed using MALDI-TOF mass spectrometry. 1ul of sample were mixed with 1ul of a saturated matrix solution (a-cyano-4-hydroxycinnamic acid in 1: 1 acetonitrile and water) and 1 ul of this mixture was spotted onto a MALDI plate and analyzed using a Voyager-DE PRO high performance bench-top matrix-assisted laser desorption ionization/time-of-flight (MALDI/TOF) mass spectrometer (Applied Biosystems, Foster City, CA, USA) equipped with a 337 nm pulsed nitrogen laser. Mass spectra were acquired in a linear positive mode.

3.2.6 Statistics

Release studies and determination of peptide content were performed at least three times for verification. To determine significant differences, one way Analysis of Variance (ANOVA) was used. Post-hoc Student t-test was used to find statistically significant differences between groups. P-values less than 0.05 were considered to be statistically significant. HPLC samples were run once for each concentration and molecular weight combination for both the MMP group and the buffer group.

3.3 Results and Discussion

3.3.1 TAMRA Release from Hydrogels Using TAMRA-GPLGVRGC. Two variables, macromer molecular weight and peptide loading, were examined to determine the effect on release. Three values were selected for each variable. The PEGDA macromer molecular weights examined were PEGDA 3,400, PEGDA 10,000 and PEGDA 20,000. The three peptide loading concentrations were 0.15 mM, 0.5 mM, and 1.75 mM. There was an exception of PEGDA 3,400, in which the high loading concentration was 1.0 mM. Due to the comparatively small mesh size described in Chapter 2, there was concern that high loading would “clog” the hydrogel matrix and inhibit release. With each study, the increased peptide release was evident from an early time point. Hydrogels without conjugated peptide showed minimal RFU values that resulted in no release when measured by standard curve. The low peptide loading showed no significant difference at 96 hours with PEGDA 3,400 (Figure 3.7a), but a significant

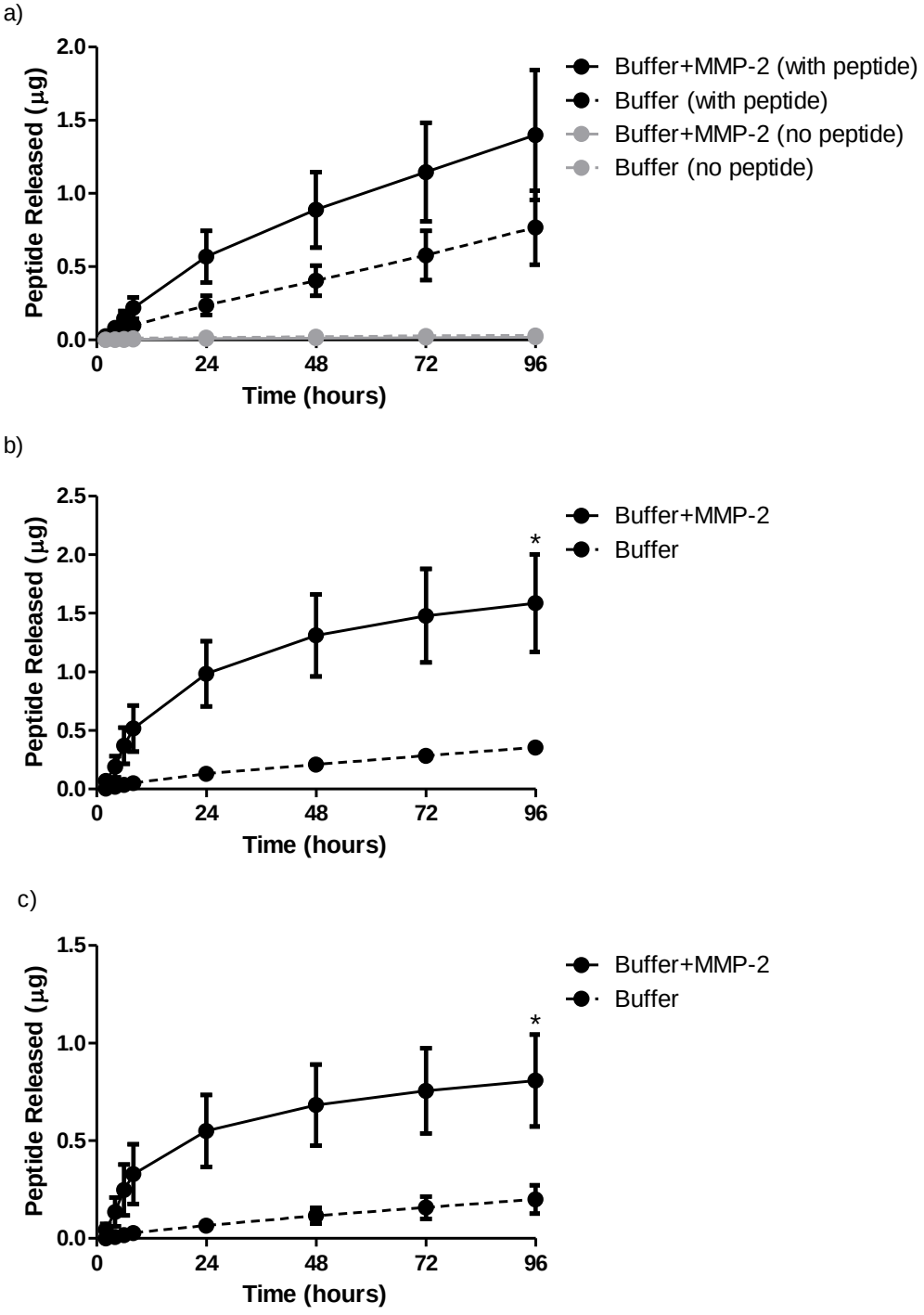

Figure 3.7 Release using active MMP-2 at a peptide concentration 0.15 mM in a) PEGDA 3,400, b) PEGDA 10,000, and c) PEGDA 20,000 hydrogels. Solid line is release with MMP-2, dashed line is release in buffer. Values are mean ± SD, n=3 *p<0.05

difference with PEGDA 10,000 (Figure 3.7b) ($p<0.05$) and PEGDA 20,000 (Figure 3.7c) ($p<0.05$). There was no significant difference in release amount with MMP-2 between the PEGDA 10,000 and PEGDA 20,000 ($p>0.05$). At medium peptide loading, all three weights-PEGDA 3,400-(3.8a), PEGDA 10,000 (3.8b), and PEGDA 20,000 (3.8c) showed a significantly greater peptide released with MMP-2 compared to buffer (p-values were $p<0.01$ for PEGDA 3,400 and $p<0.05$ for PEGDA 10,000 and PEGDA 20,000). There are no significant differences in amount released at the end of the study ($p>0.05$). In the high peptide loading condition, PEGDA 3,400 Hydrogels without conjugated peptide showed minimal RFU values that resulted in no release when

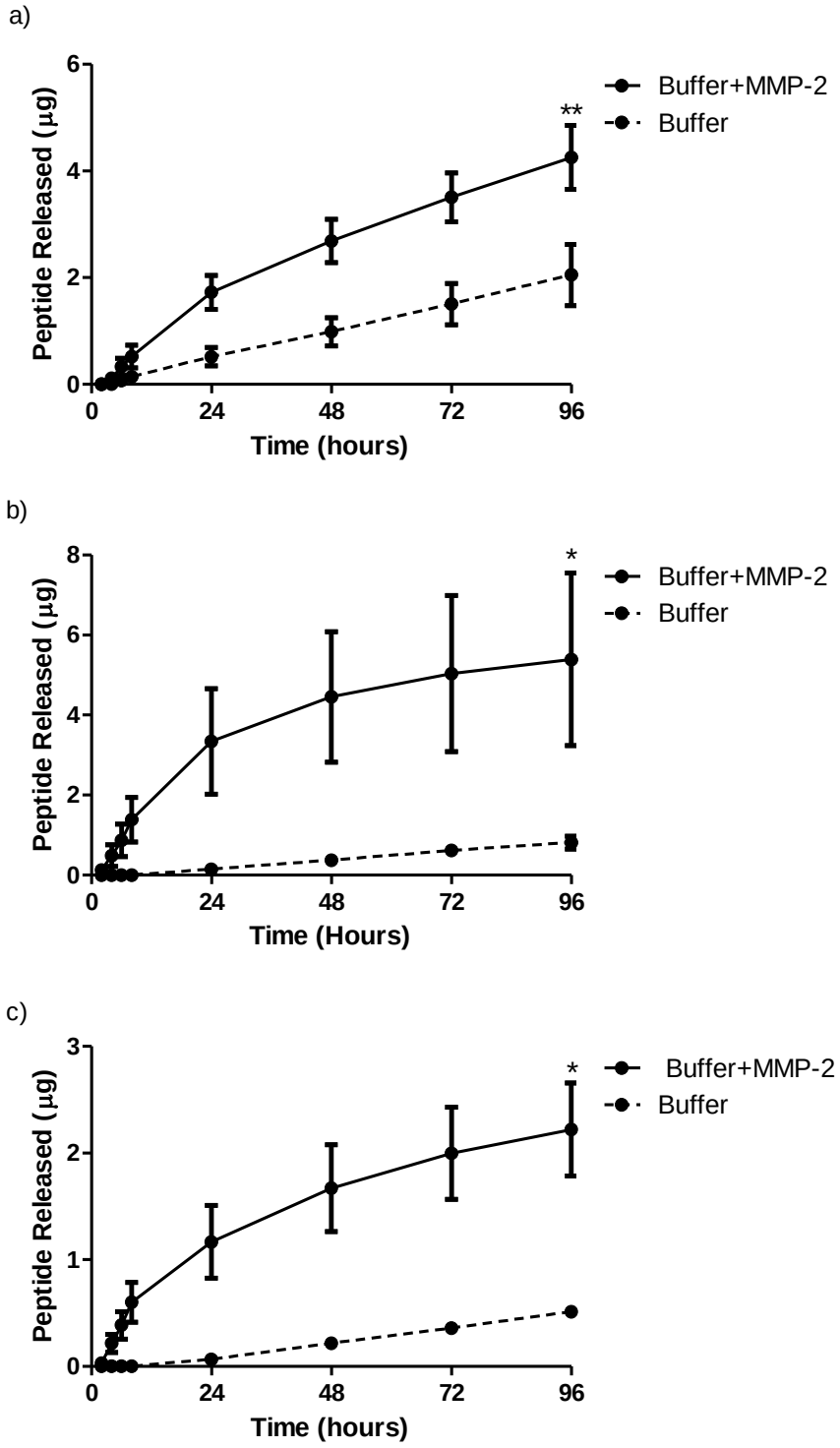

Figure 3.8 Release using active MMP-2 at a peptide concentration 0.5 mM in a) PEGDA 3,400, b) PEGDA 10,000, and c) PEGDA 20,000 hydrogels. Solid line is release with MMP-2, dashed line is release in buffer. Values are mean ± SD, n=3 *p<0.05 **p<0.01

significant difference at 96 hours compared to buffer (3.9a). The larger molecular weights-PEGDA 10,000 (3.9b) and PEGDA 20,000 (3.9c) showed a significant increase ($p<0.05$ and $p<0.01$, respectively). There was no significant difference in the amount released at 96 hours ($p>0.05$)

The determination of total peptide content by hydrogel hydrolysis made it possible to compare the different molecular weight and loading combinations to each other directly, and determine the presence or absence of differences in percentage of peptide released. In the hydrolysis reaction, the sodium hydroxide reacts with the ether bonds in the PEG. The polymer chains are broken and the hydrogel is transformed from a solid shape into a solution. Measuring the peptide amount by reading the hydrogels in the flurorimeter was attempted. Readings were done before and after MMP-2 mediated release studies. However, the results from this method were unreliable in that they did not match the measured release. It was concluded flurorimeter readings on solid hydrogels were not a valid measurement.

The hydrolysis method was validated by diluting peptide in both tris buffer and sodium hydroxide, to determine if the presence of sodium hydroxide interfered with the fluorescence. Comparison of the flurorimeter readings between the two groups showed no statistically significant difference. It was concluded from this that the presence of sodium hydroxide did not interfere with an accurate measurement of hydrogel peptide content.

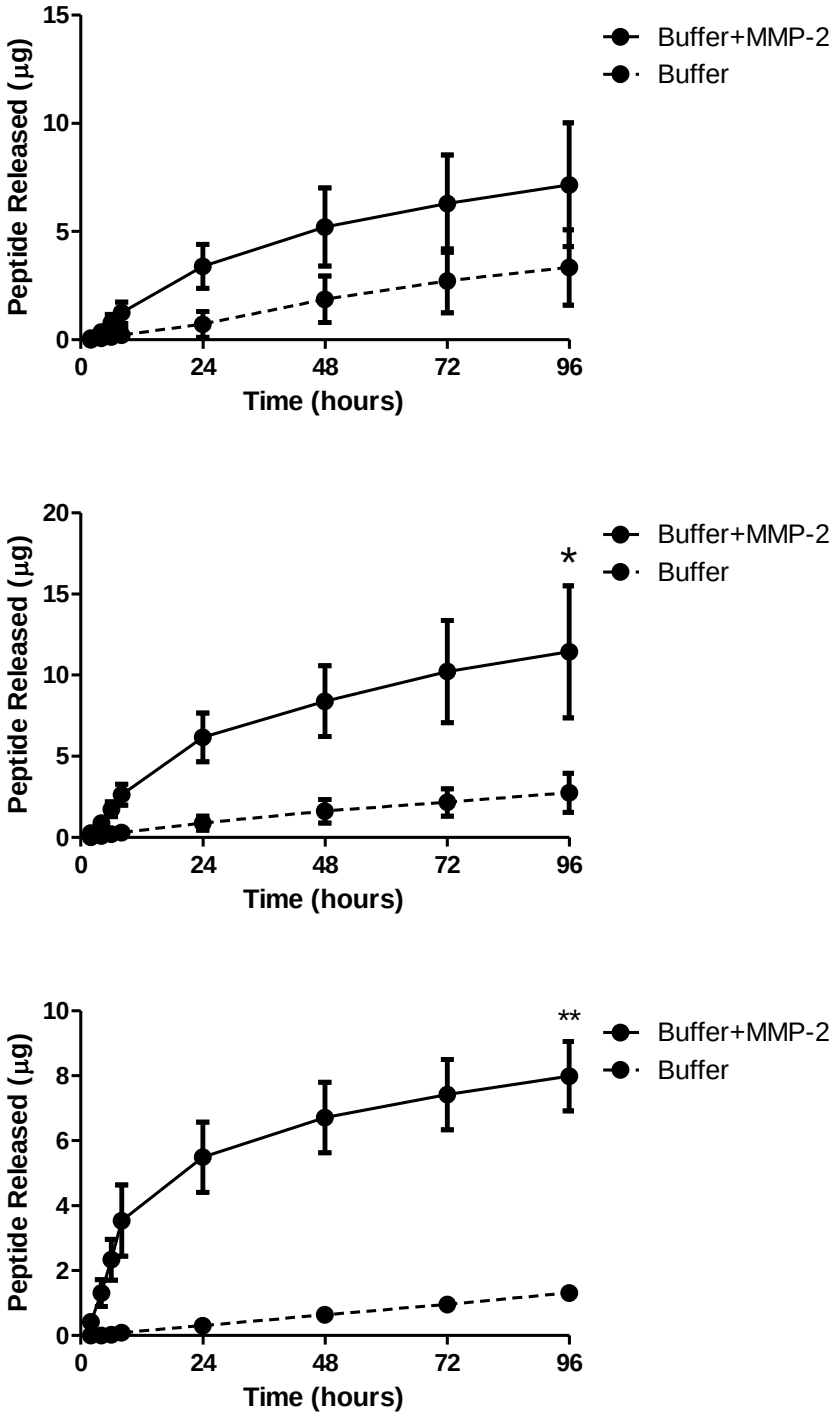

Figure 3.9 Release using active MMP-2 at a peptide concentration at 1.0 mM in a) PEGDA 3,400 and 1.75 mM in b) PEGDA 10,000, and c) PEGDA 20,000 hydrogels. Solid line is release with MMP-2, dashed line is release in buffer. Values are mean ± SD, n=3, *p<0.05 **p<0.01

There was no significant difference among the molecular weights at low peptide loading (Figure 3.10), medium peptide loading (Figure 3.11), or high peptide loading (Figure 3.12). Percent peptide released for each category was determined by dividing the peptide released at each time point by the total content. The results at the final time point (96 hours) were examined by peptide loading for each molecular weight ($p>0.05$ for all groups). There was also no significant difference in nonspecific release at any amount of peptide loading. Examination of the different molecular weights at each loading concentration at the final time point also showed no significant differences ($p>0.05$ for all groups).

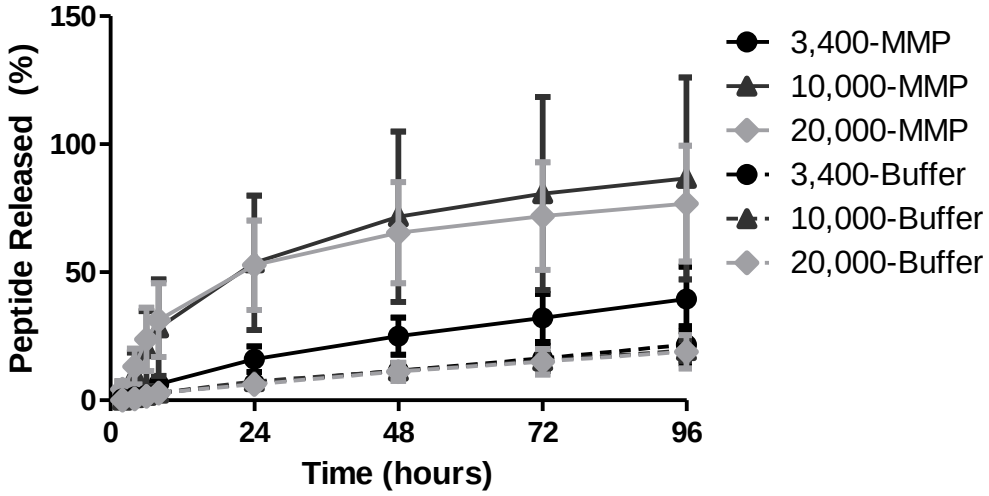

Figure 3.10 Percent release of the three molecular weights at low peptide loading (0.15 mM). Black is PEGDA 3,400, medium grey is PEGDA 10,000, and light grey is PEGDA 20,000. Solid lines are percent release with MMP-2, dashed lines are percent release in buffer. Values are mean ± SD, n=3.

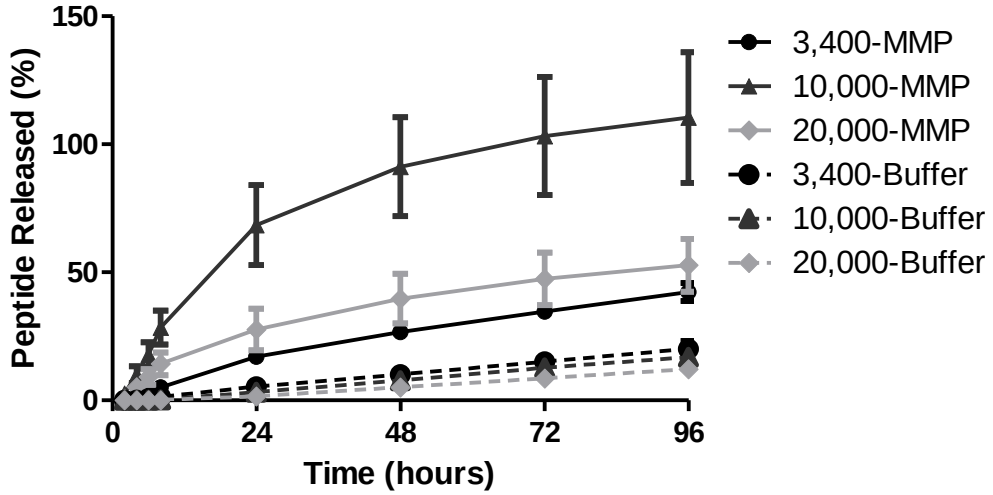

Figure 3.11 Percent release of the three molecular weights at medium peptide loading (0.5 mM). Black is PEGDA 3,400, medium grey is PEGDA 10,000, and light grey is PEGDA 20,000. Solid lines are percent release with MMP-2, dashed lines are percent release in buffer. Values are mean ± SD, n=3.

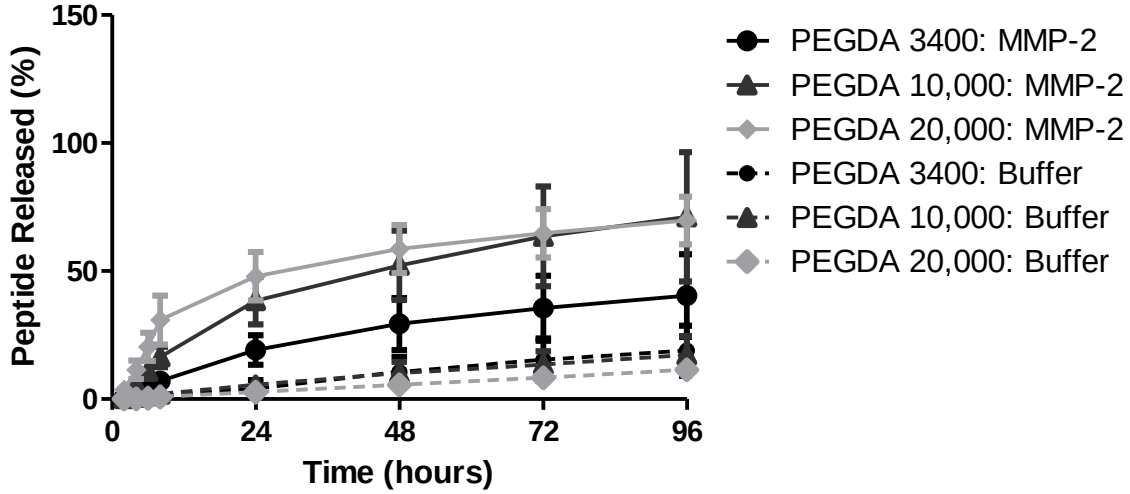

Figure 3.12 Percent release of the three molecular weights at medium peptide loading (1.0/1.75 mM). Black is PEGDA 3,400, medium grey is PEGDA 10,000, and light grey is PEGDA 20,000. Solid lines are percent release with MMP-2, dashed lines are percent release in buffer. Values are mean ± SD, n=3.

However, there was a larger difference between the peptide released in the presence of MMP-2 to the peptide released in buffer in the PEGDA 20,000 and PEGDA 10,000 than there was in the PEGDA 3,400 at 0.5 mM concentration. In the low and high loading conditions, the PEGDA 3,400 release in the presence of MMP-2 was not significantly higher at the final time point compared to release in buffer (Figures 3.7-3.9). It was significantly greater in the PEGDA 10,000 and PEGDA 20,000 groups at all concentrations.

Further analysis was done by taking the ratio of the peptide released in the presence of MMP-2 to the peptide released in buffer for each concentration (p_r). For the 0.15 mM concentration, p_r for PEGDA 10,000 and the PEGDA 20,000 was significantly higher than for PEGDA 3,400 ($p<.0.5$ for both) (Figure 3.13). The p_r for PEGDA 3,400 was around 2 (twice the release compared to buffer), while the p_r for PEGDA 10,000 and 20,000 was near 4-double the ratio of release compared to PEGDA 3,400.

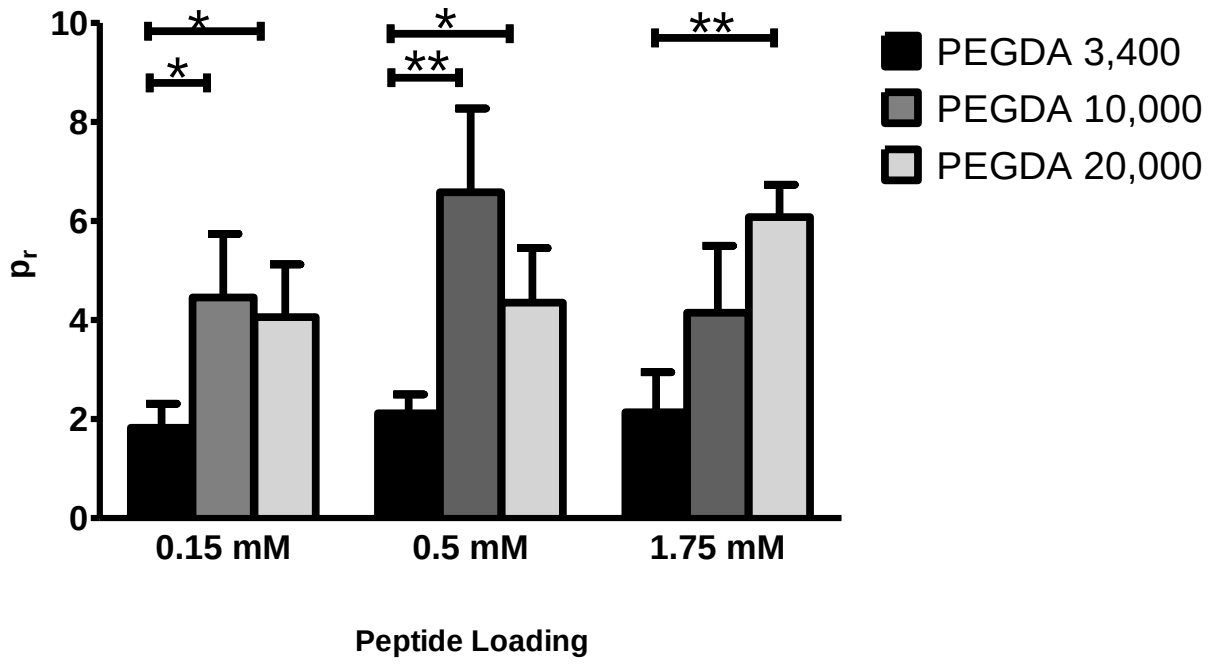

Figure 3.13 Ratio of peptide released in the presence of MMP-2 to the peptide released in buffer alone (p_r) Black is PEGDA 3,400, medium grey is PEGDA 10,000, and light grey is PEGDA 20,000. *p<0.05, **p<0.01.

For medium peptide loading, PEGDA 10,000 and PEGDA 20,000 also had a significantly higher p_r than PEGDA 3,400 ($p<0.01$ and $p<0.05$, respectively). The p_r was also near 2, while PEGDA 10,000 was three time greater (near 6) and PEGDA 20,000 had a p_r was twice as great. There was no significant difference between the PEGDA 10,000 and the PEGDA 20,000 in either group ($p>0.05$). For the high peptide loading, p_r for PEGDA 20,000 was significantly greater than the PEGDA 3,400 ($p<0.01$). There was no significant difference between the PEGDA 3,400 and the PEGDA 10,000, or the PEGDA 10,000 and PEGDA 20,000 ($p>0.05$). The p_r for PEGDA 3,400 was once again around 2, where PEGDA 20,000 was twice this amount. Because the PEGDA 3,400 has

a mesh size smaller than the dimensions of MMP-2, this suggests the increased p_r is due to MMP-2 entry.

Calculating the diffusion time for MMP-2 into the hydrogels provides further support for MMP-2 entry. Diffusion coefficient through the hydrogels was calculated by a simplified version of an equation developed by Peppas and Lustig:

$$\frac{D_e}{D_0} = 1 - \frac{r_s}{\xi} \quad (3.2)$$

where D_e is the effective diffusion coefficient, D_0 is the diffusion coefficient of the molecule in solvent, and r_s is the size of the solute molecule (Lustig & Peppas, 1988). D_o was calculated using the Stokes-Einstein equation :

$$D_0 = \frac{k_B T}{6\pi\eta\sigma} \quad (3.3)$$

where k_b is the Boltzmann constant ($1.380650 \times 10^{-23} \frac{m^2 \cdot kg}{s^2 \cdot K}$), T is temperature, η is solvent viscosity ($6.4 \times 10^{-4} \frac{kg}{s \cdot m}$ for water), and σ is molecule radius (Tabeting & Cheng, 2006). MMP-2 hydrodynamic radius (r_H) was found by treating MMP-2 as a prolate spheroid :

$$r_H = (ab)^{\frac{1}{3}} \frac{\beta^{\frac{1}{3}}\sqrt{\beta^2 - 1}}{\ln(\beta + \sqrt{\beta^2 - 1})} \quad (3.4)$$

Where a is the major radius of the ellipse, b is the minor radius, and β is the ratio of a to b (Hansen, 2004).

Diffusion time τ through the hydrogel was calculated by Equation 3.5:

$$\tau = \frac{L^2}{D_e}$$

where L is half the hydrogel thickness (Gemeinhart & Guo, 2004).

Diffusion time was calculated for all three hydrogels at 15% w/v (Table 3.3) at physiological temperature (310.15 K). To calculate r_H, half the length of MMP-2 was used for a (4.82 nm) and half the breadth was used for b (3.38 nm) and calculated to be 4.88 nm. Hydrodynamic radius was also used for solute size in equation 3.2. D_0 was 6.74 x 10^{-7} $\frac{cm^2}{s}$.

TABLE 3.3 MMP-2 DIFFUSION TIME THROUGH HYDROGELS

PEGDA Molecular Weight (g/mol)	**Mesh size (nm)**	**D_e ($\frac{cm^2}{s}$)**	**L (cm)**	**τ (hrs)**
3,400	4.19	N/A	0.075	N/A
10,000	9.11	3.13×10^{-7}	0.09	7.19
20,000	16.71	4.77×10^{-7}	0.1	5.82

τ was about 7 hours for PEGDA 10,000, almost 6 hours for PEGDA 20,000, and nonapplicable for PEGDA 3,400 since D_e/D_0 was negative. The validity of this calculation is limited by several factors. Structural irregularities in the hydrogel discussed in Chapter 2 will affect MMP-2 diffusion. MMP-2 position in relation to the mesh will vary and consequently affect diffusion. The contributions to release from surface peptide cleavage also contribute to the release of MMP-2 Equations 3.4 is acknowledged to have criticisms; further work has been done to develop equations of diffusion through hydrogels (Gemeinhart & Guo, 2004). However, this first order

approximation demonstrates MMP-2 diffusion time into the hydrogel is achieved within the time frame of the release studies.

3.3.3 Peptide Release Using TAMRA-PAGLLGC and TAMRA-IPVSLRSGC. Release for the two alternate peptides used PEGDA 10,000 and a concentration of 0.5 mM. These parameters were selected as the midpoint values for each variable examined, and because PEGDA 10,000 showed significantly greater release than the PEGDA 3,400 with MMP-2 compared to buffer (Figure 3.13). Both peptides showed greater release in the presence of MMP-2 than in buffer (Figure 3.14 and Figure 3.15) ($p<0.001$ for both peptides).

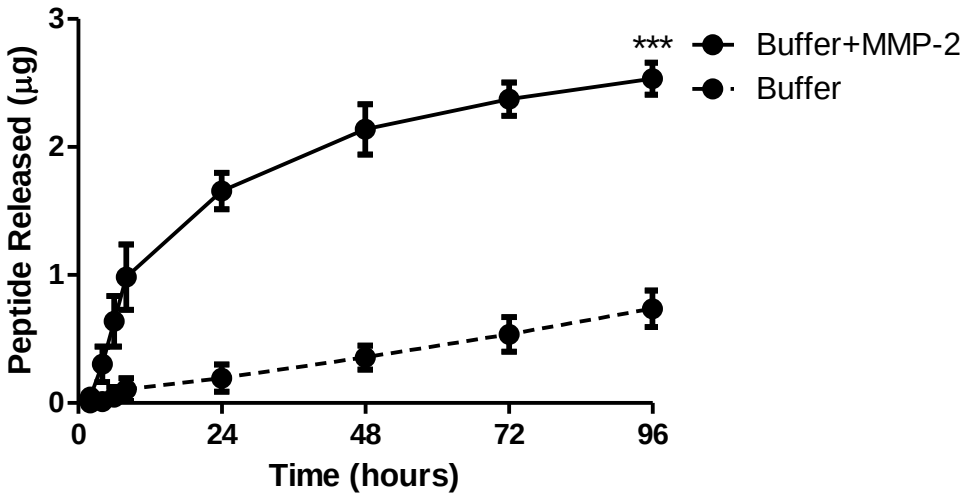

Figure 3.14 Release using active MMP-2 in PEGDA 10,000 hydrogels using TAMRA-PAGLLGC (0.5 mM). Solid line is release with MMP-2, dashed line is release in buffer. Values are mean ± SD, n=3 ***p<0.001.

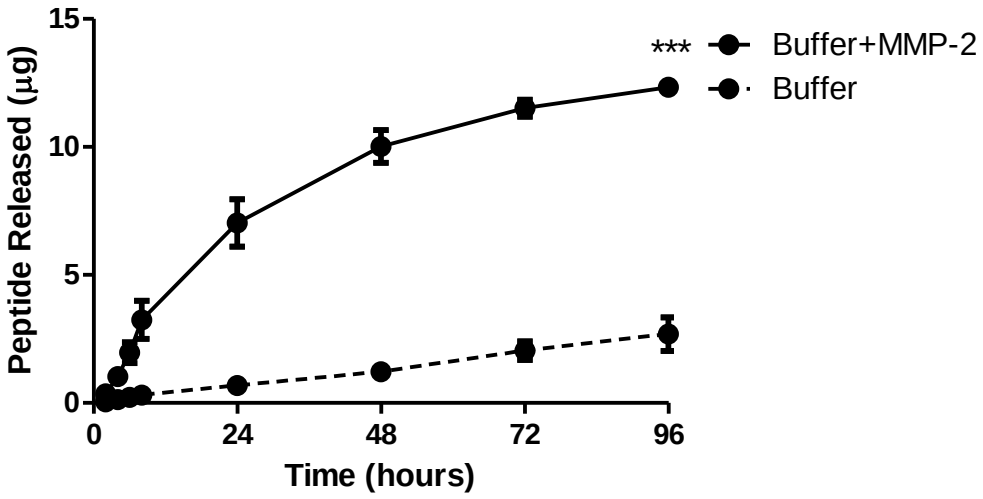

Figure 3.15 Release using active MMP-2 in PEGDA 10,000 hydrogels using TAMRA-IPVSLRSGC (0.5 mM). Solid line is release with MMP-2, dashed line is release in buffer. Values are mean ± SD, n=3 *** $p<0.001$.

It was also noted that the standard deviations for the three independent experiments were smaller compared to the release experiments with TAMRA-GPLGVRGC. Comparing percent released to that of PEGDA 10K with 0.5 mM TAMRA-GPLGVRGC, no significant difference was seen (Figure 3.16).

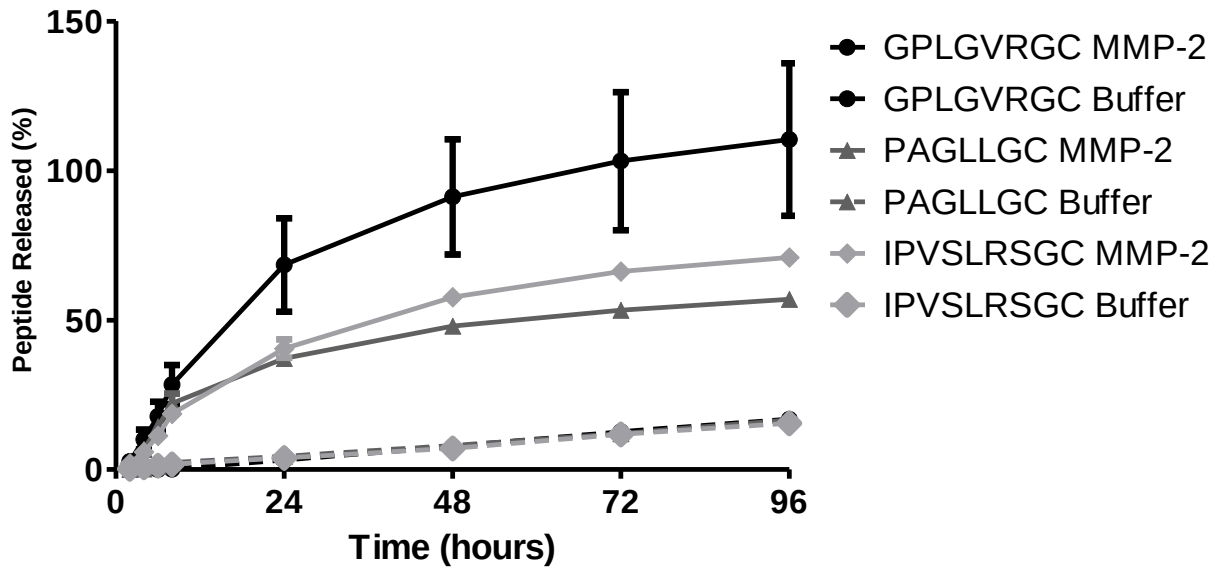

Figure 3.16 Percent release of three peptides in PEGDA 10,000 hydrogels at 0.5 mM peptide concentration. Black is GPLGVRGC, medium grey is PAGLLGC, and light grey is IPVSLRSGC. Solid lines are percent release with MMP-2, dashed lines are percent release in buffer. Values are mean ± SD, n=3.

However, when comparing p_r, the TAMRA-GPLGVRGC and TAMRA-IPVSLRSGC were significantly greater than the TAMRA-PAGLLGC (Figure 3.17). TAMRA-IPVSLRSGC also had higher loading and greater absolute amount released compared to the other two peptides. The amount released in the TAMRA-IPVSLRSGC hydrogels with MMP-2 was 12.33 ± 0.27 μg, significantly greater than 2.53 ±0.13 μg for TAMRA-PAGLLGC ($p<0.00001$) and 5.39 ±2.16 μg for TAMRA-GPLGVRGC ($p<0.005$).

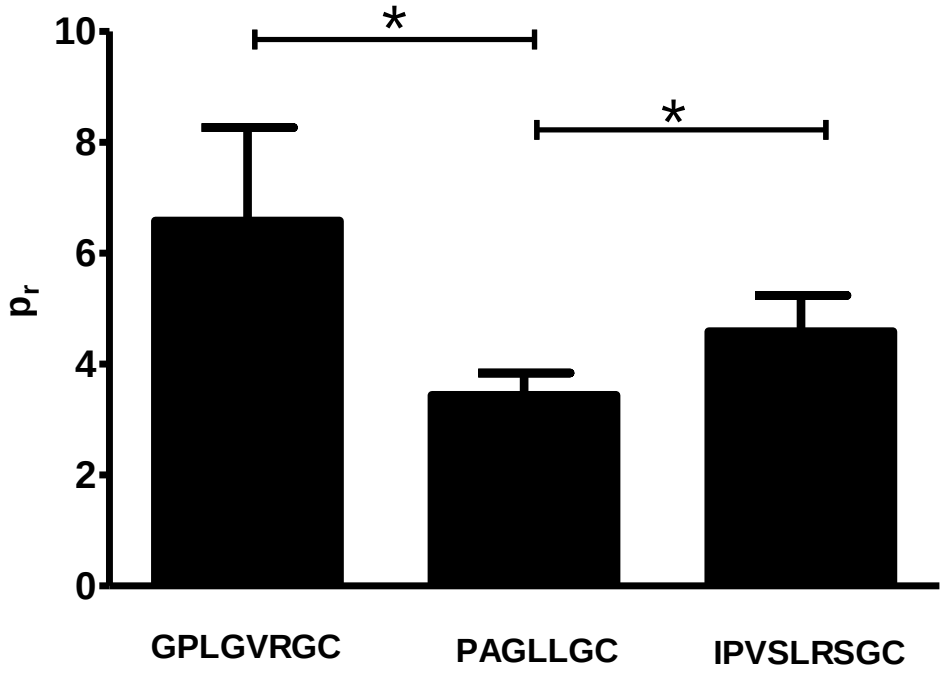

Figure 3.17 Ratio of peptide released in the presence of MMP-2 to the peptide released in buffer alone. Values are (mean ± SD/ mean ± SD) using the propagation of error formula to determine SD. *p<0.05.

The reason for the greater consistency of TAMRA-PAGLLGC and TAMRA-IPVSLRSGC compared to TAMRA-GPLGVRGC is unclear. If the greater consistency was due to greater affinity of MMP-2 for the peptide, it would have been reflected in the percentage released. TAMRA-GPLGVRGC may undergo conformational changes that inhibit MMP-2 from cleaving the peptide. Decreased cleavage efficiency could play a role in the the lower ratio of release with MMP-2 compared to buffer at 96 hours for TAMRA-PAGLLGC compared to the other two peptides. The k_{cat}/K_m ratio for GPLGVRG has not been reported, but the k_{cat}/K_m ratio was much higher for IPVSLRSG than for PAGLLG (Section 3.1).

Hydrophobicity may also be a contributing factor. Average hydrophobicity of each peptide was calculated by averaging the hydrophobicity values of its component amino acids using the hydrophobicity scale developed by Hopp and Woods (Hopp & Woods, 1981). The hydrophobicity of PAGLLGC is -0.7, while the hydrophobicity of GPLGVRGC is -0.2, and IPVSLRSGC is -0.3. It is possible that MMP-2 has a greater affinity for hydrophilic peptides. Another potential factor is peptide charge. GPLGVRGC and IPVSLRSGC both have a positively charged arginine residue, while PAGLLGC has no charged side chains. Chau et. al. experimented with altering the amount of charged groups on the dextran portion of their dextran-peptide-methotrexate MMP-2 and MMP-9 triggered drug delivery system by reacting carboxymethyl with ethanolamine. The neutral (least negative) peptide had the greatest K_{cat}/K_m ratio, indicating the most efficient cleavage (Chau, Tan, & Langer, 2004). They did not look at the effect of positive charges on the dextran or a combination of positive and negative charges, so a definitive comparison cannot be made between the dextran-peptide conjugate and the PEGDA-peptide hydrogel conjugate in this study. Although the TAMRA-peptide complexes studied were actually zwitterionic (since the TAMRA has carboxyl groups), TAMRA-PAGLLGC is the most negative of the three. Repeating this study with a neutral fluorophore would determine if the presence of charges in the peptide contributed to the percentage released. Another possibility is that the initial conjugation rates of the peptide to the PEGDA macromer varied among the peptides. This is being investigated by another researcher. Further studies will be needed to determine other reasons why

PAGLLGC was a less efficient MMP-2 cleavable peptide than the other two examined in this study.

3.3.4 Verification of Peptide Cleavage Using HPLC. The full TAMRA-GPLGVRGC peptide was found to have an elution peak of about 15 minutes (Figure 3.18). Two large peaks were seen in the chromatogram. There is also a small peak seen around two minutes, but it is much smaller compared to the later elution peaks. Had a smaller concentration been used for the sample, the peaks at 2-3 minutes would not have been detected. It was expected that samples exposed to MMP-2 would have a peak present at a shorter elution time than the full peptide because the cleaved peptide fragment has less hydrophobic surface area than the full peptide and therefore would have less affinity for the column. This peak would not be present in the samples incubated in buffer only, because no cleavage should be occurring in the absence of MMP-2.

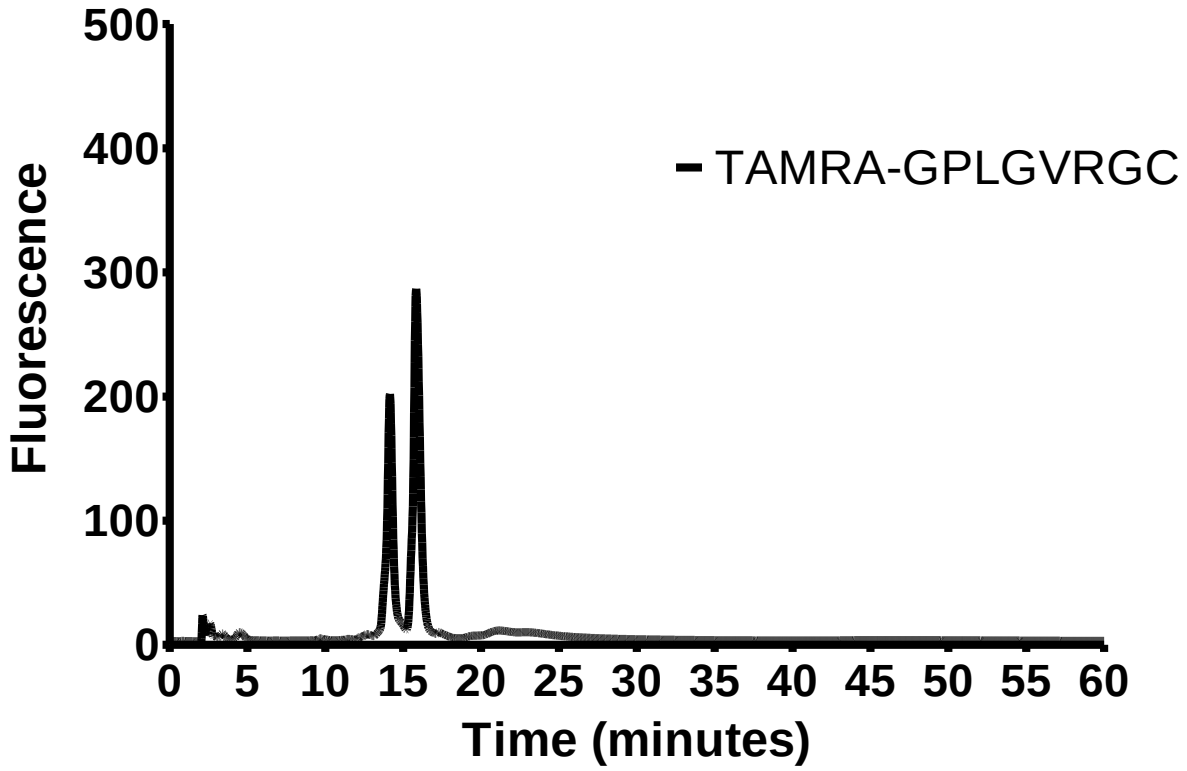

Figure 3.18 HPLC fluorescence chromatogram of TAMRA-GPLGVRGC (25 μM) in TBS/Zn.

Samples of release buffer incubated in MMP-2 show an elution peak of about 2.5-3 minutes for PEGDA 3,400 at all the concentrations (Figure 3.19). The fluorescence intensity was greatest for the high loading condition and markedly decreased for the low and medium loading conditions. There is a peak in this range with buffer alone, but it is markedly smaller than the peaks from the MMP groups. The fluorescence intensity is around 10, where the peak fluorescence intensity is about 20 for the low loading, 60 for the medium loading, and over 250 for the high loading conditions.

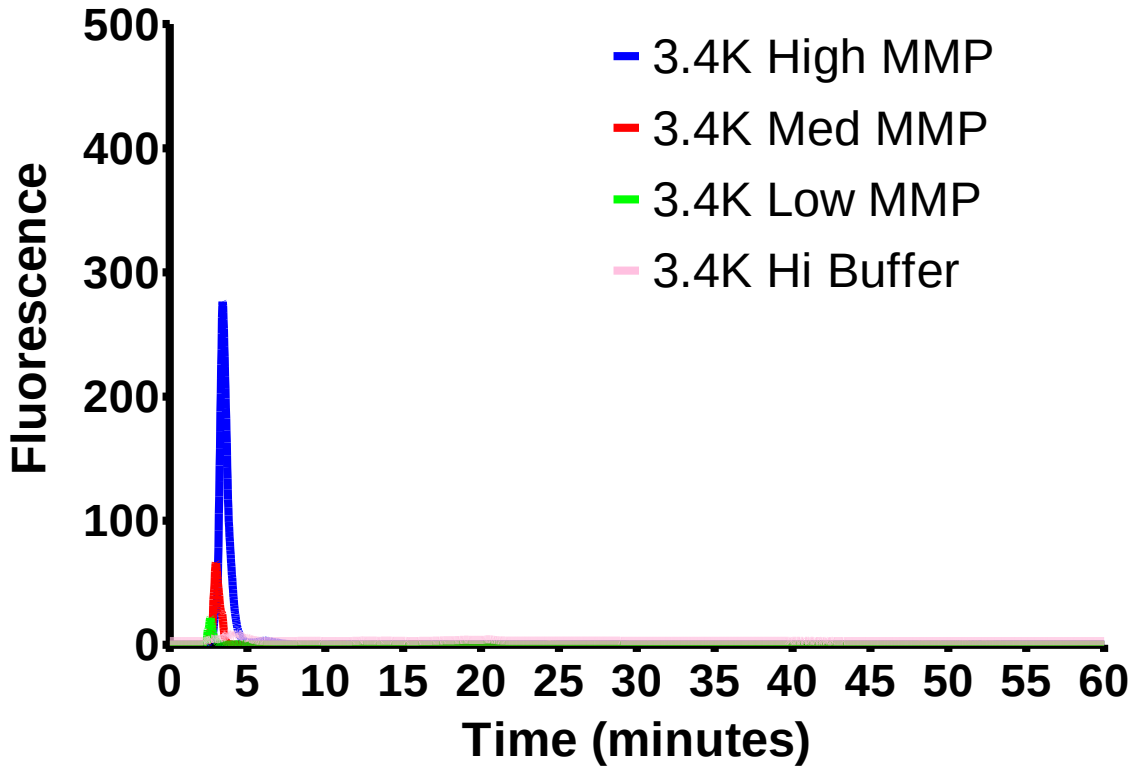

Figure 3.19 HPLC fluorescence chromatogram from release studies using PEGDA 3,400. Blue=1.0 mM loading, red=0.5 mM loading, green=0.15 mM loading, pink=buffer only.

The PEGDA 10,000 chromatograms show peaks at the same elution time (2.5-3 minutes) (Figure 3.20). A higher peak intensity for the medium loading (over 400) than the high loading (approximately 180). This may have been due to an unusually high release for the particular time point for the PEGDA 10,000 medium loading (approximately 60). The peak for low loading is smaller than both, and a peak for buffer alone is nonexistent.

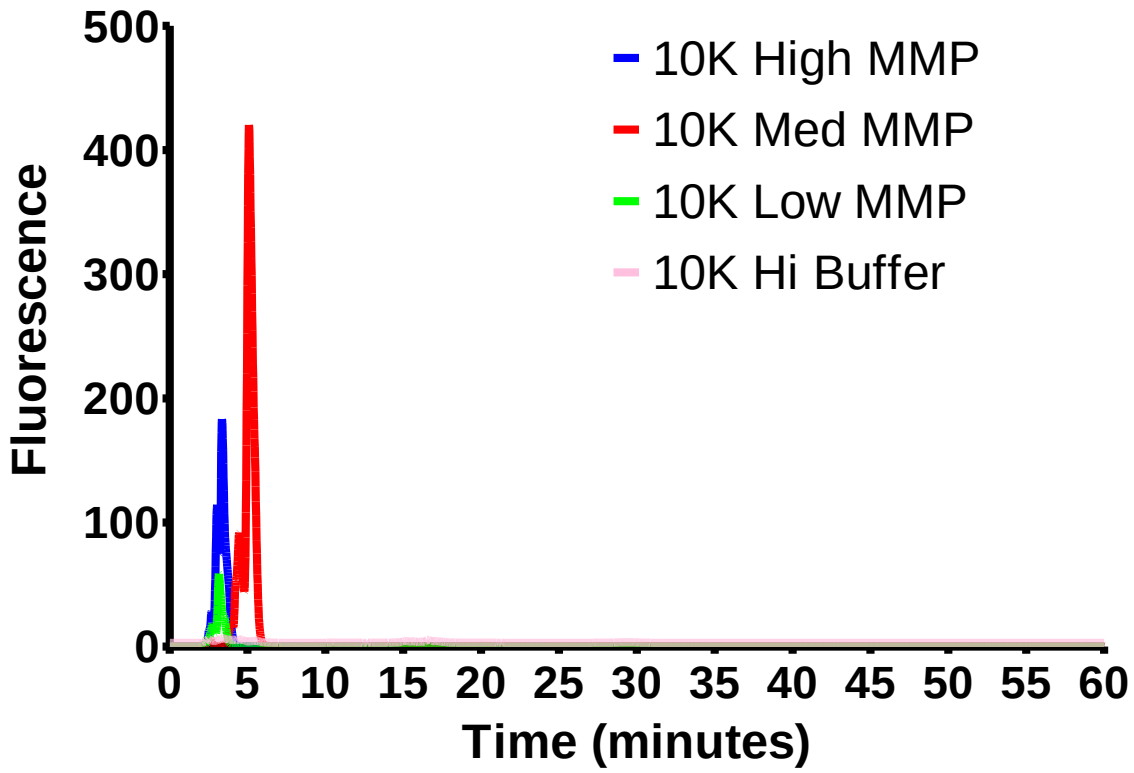

Figure 3.20 HPLC fluorescence chromatogram from release studies using PEGDA 10,000 Blue=1.75 mM loading, red=0.5 mM loading, green=0.15 mM loading,pink= buffer only.

For PEGDA 20,000, peaks are again present in the 2.5-3 minute range (Figure 3.21). The high peptide loading had the highest peak intensity (approximately 350), with a much lower intensity for the medium loading (approximately 50) (Figure 3.21a) or low loading (near 5) (Figure 3.21b). There was no peak seen in the buffer only sample. The shorter elution time for the peptide indicates that the release is a result of MMP-2 cleavage of the TAMRA-conjugated peptide.

a)

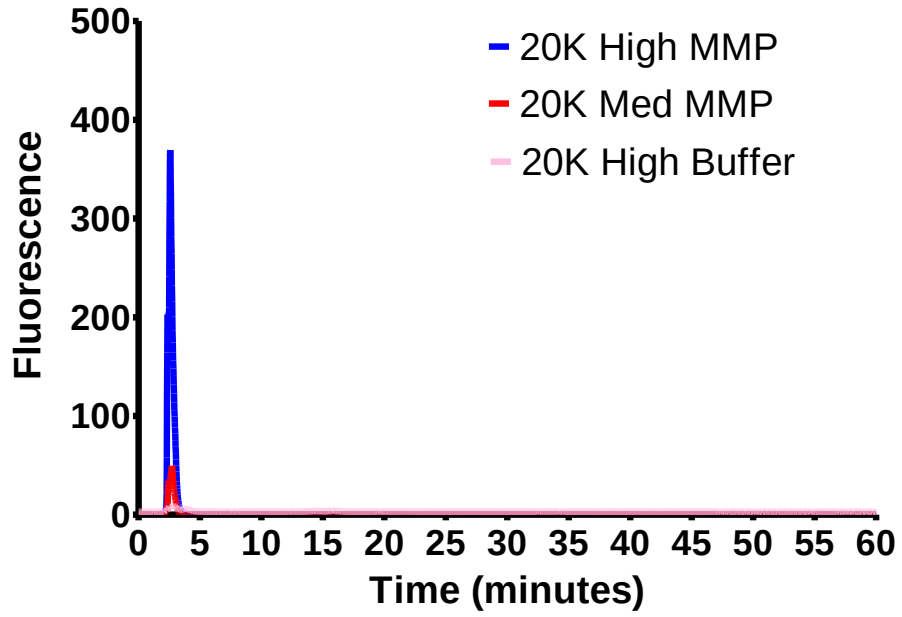

b)

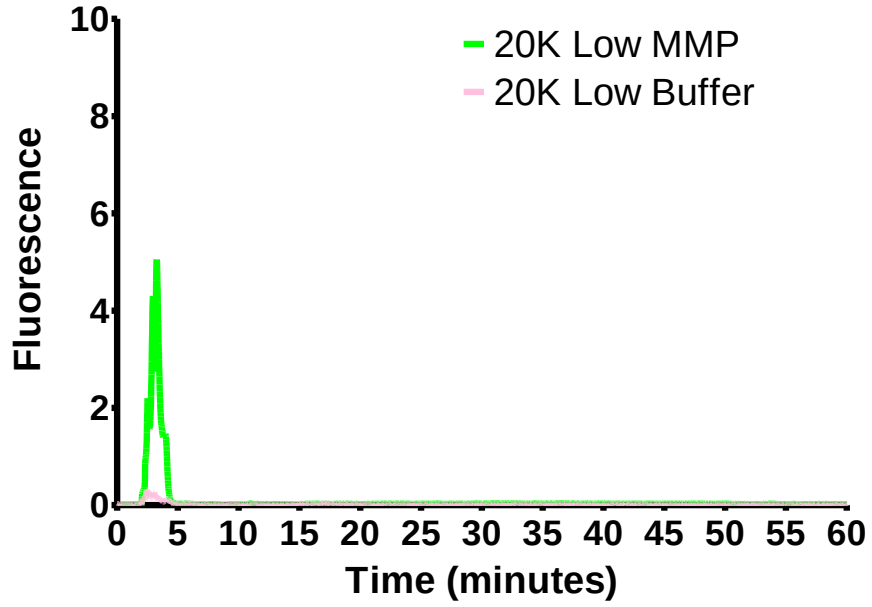

Figure 3.21 HPLC fluorescence chromatogram from release studies using PEGDA 20,000 a) Blue=1.75 mM loading, red=0.5 mM loading,pink = buffer only (from high loading) b) Green= 0.15 mM loading and pink=buffer only (from low loading). Low loading shown on a separate graph to accommodate difference in scale.

Although the presence of an earlier peak in the fluorescence chromatogram is indicative of an alteration in the peptide, this is not conclusive evidence of peptide cleavage. It also does not indicate the site of cleavage within the peptide. It is possible the peak is not between the glycine and valine as anticipated, or that there are multiple cleavage sites within the same peak. Therefore further analysis was done on the eluted peak using MS.

3.3.5 MALDI-TOF MS of peptide cleavage from purified MMP-2

The sample with MMP-2 and GM6001 did not any peaks analyzed by mass spectrometry because the peaks intensities were too low in intensity for an effective mass spectrometry analysis (Figure 3.22). Since GM6001 is an MMP-2 inhibitor and there are no other proteases present, the low peak intensity in the sample with MMP-2

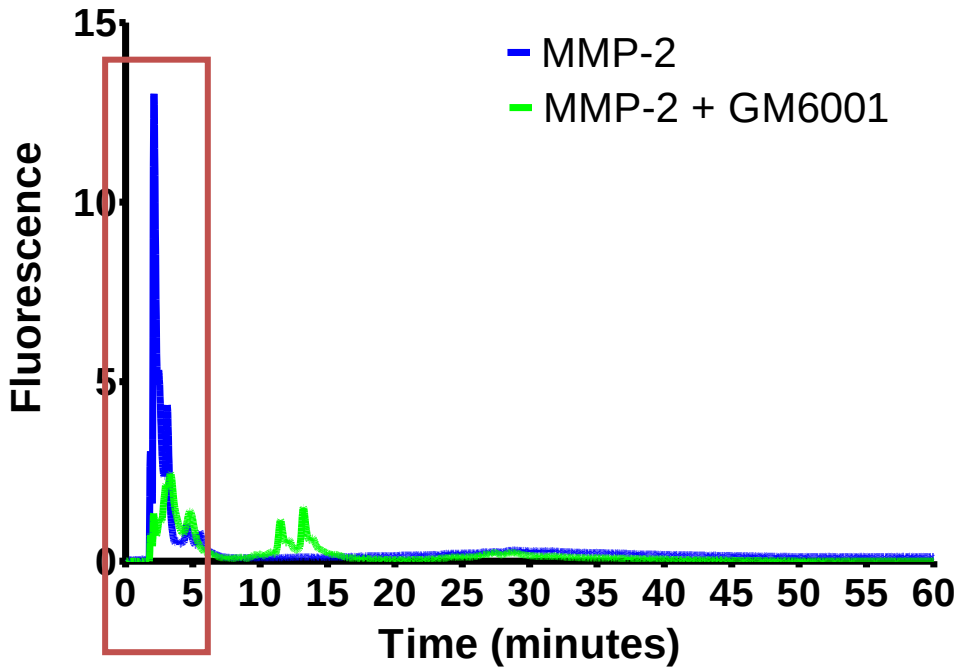

Figure 3.22 HPLC fluorescence chromatogram of release from hydrogels with TAMRA-GPLGVRGC for 24 hours. The black peak at 2.5 minutes (in the red box) was collected and analyzed by MALDI-TOF MS. Blue= MMP-2 and green= incubation with MMP-2 and GM6001.

and GM6001 is consistent with MMP-2 inhibition. MS showed the highest intensity peak at 441.0004 m/z, corresponding to the molecular weight TAMRA alone (Figure 3.23).

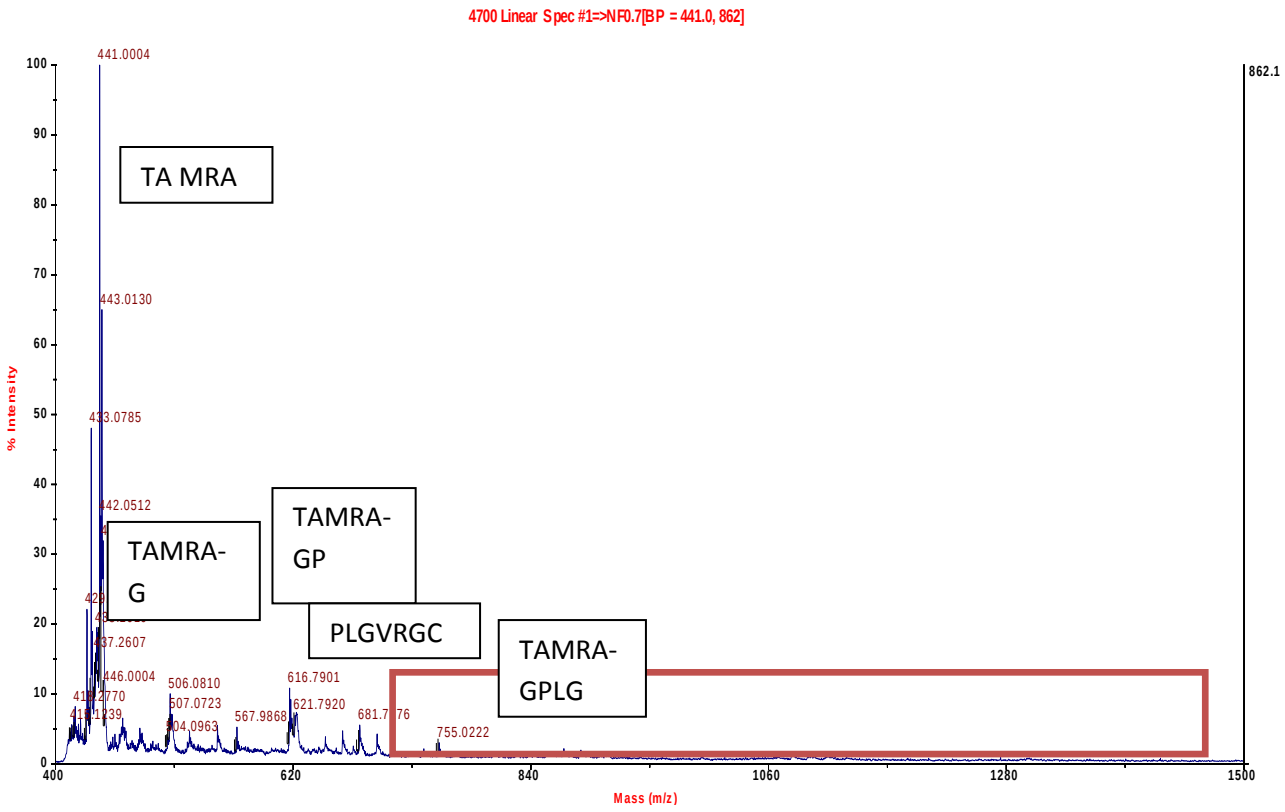

Figure 3.23 MALDI-TOF MS of peak collected from release with MMP-2 (2.5 minute elution time). Red box marks area shown in detail in Figure 3.24. Peaks are labeled with corresponding peptide sequences.

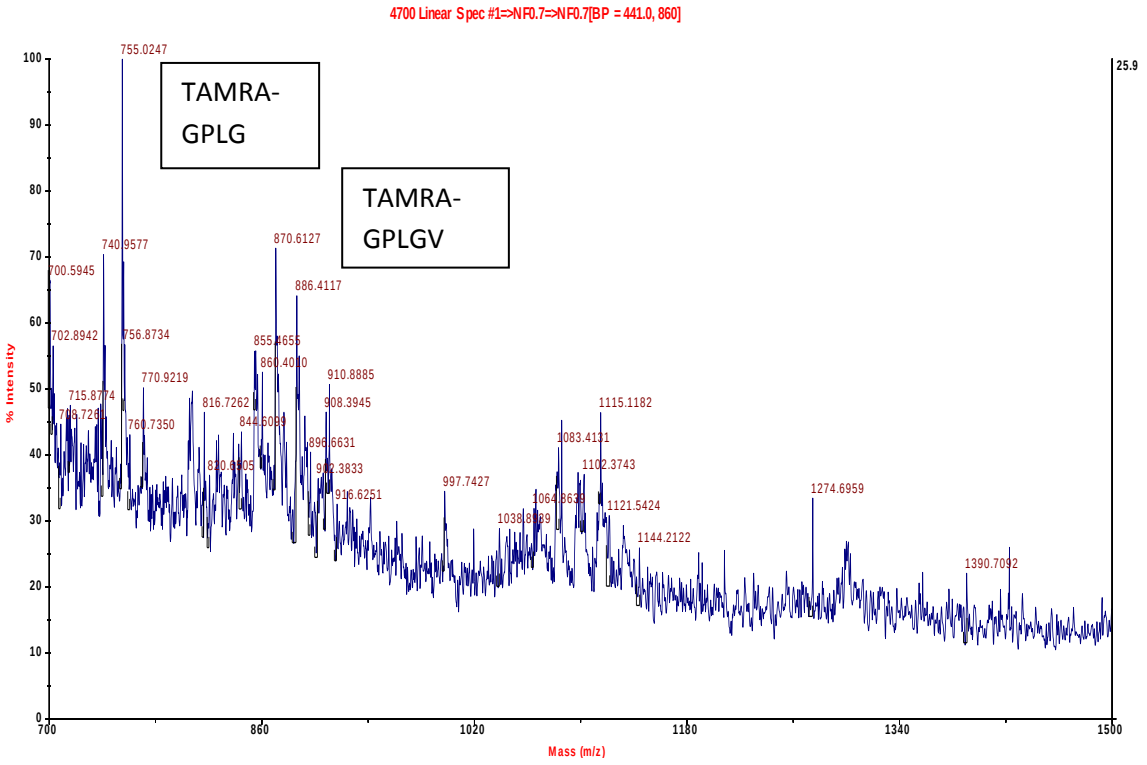

Figure 3.24 MALDI-TOF MS for peak collected from release with purified MMP-2 (enlarged area of Figure 3.23).

Smaller peaks were at 506.0810, 616.7901, 681.7176, and 755.0222 m/z. The 755.0222 peak corresponds to TAMRA-GPLG, the expected cleavage site of MMP-2. The 506.0810 peak corresponds to TAMRA-G, the 616.7901 corresponds to TAMRA-GP, and 681.7176 corresponds to PLGVRGC. An enlarged version of the spectrum (Figure 3.24) shows the 755 m/z peak is the largest in range. There are numerous smaller peaks, most notably at 740.9577 m/z and 870.6127 m/z. No molecular weight in the peptide sequence corresponds to the 740.9577 peak, but the 870.6127 peak is close to TAMRA-GPLGV.

The presence of many multiple peaks was an unexpected finding in this experiment. A potential explanation is that the MMP-2 is able to cleave at multiple sites, though the secondary site cleavage is slower than the primary site. It is also possible in the case of TAMRA, TAMRA-G and TAMRA-GP that a secondary cleavage occurs from the cleaved fragment TAMRA-GPLG. Nonetheless, it can be confirmed that the peaks present in the MS results are not solely due to the presence of collagen fragments. MMP-2 is responsible for the cleavage of the TAMRA-conjugated peptide. Further MS analysis in the presence of MMP-2 secreting cells will be discussed in Chapter 4.

3.4 Conclusions

It has been shown that active MMP-2 can cleave an MMP-2 sensitive peptide conjugated throughout a hydrogel matrix. This was demonstrated over multiple molecular weights and multiple concentrations. The two higher molecular weights of PEGDA showed a greater ratio of release from MMP-2 compared to buffer compared to PEGDA 3,400. As seen in Chapter 2, the mesh size of PEGDA 3,400 is 4.19±0.01 nm, smaller than the dimensions of active MMP-2, while the PEGDA 10,000 and PEGDA 20,000 mesh sizes are large enough to accommodate the enzyme. This suggests that the greater ratio of release of peptide in the two higher molecular weights is due to the entry of MMP-2 into the hydrogel. Some optimization was indicated not only by using the larger molecular weight, but in the selection of MMP-2 cleavable peptides. Cleavage of the peptide was successfully confirmed by HPLC for all molecular weights and

concentrations examined. The use of alternate known MMP-2 sensitive peptides further confirms MMP-2 mediated cleavage and release from the hydrogel.

4. *In vitro* MMP-2 Mediated Peptide Release From Hydrogels

4.1 Background

In order to advance the MMP-2 triggered hydrogel-based drug delivery system, it must be demonstrated that active MMP-2 from living cells can cleave the target peptide and release the API. One of the challenges of *in vitro* experiments is to define the conditions for optimal active MMP-2 expression. Although there are many commercially available cancer cell lines, most do not express MMP-2 in its active form. The intercellular and matrix signaling present in a multicellular organism is may be different in a cell line, or be absent altogether. Additionally, cancer cell lines are prone to mutations, which may alter the expression of active MMP-2, either by increasing or inhibiting the expression. Matters are complicated by the fact that MMP-2, like all MMPs, is expressed in an inactive form (known as proMMP-2) that requires activation by other factors, including cell-ECM interactions. The MMP may be expressed by the cell, but the cells or environment may lack the ability to activate MMPs (Vartak & Gemeinhart, 2007).

Several cell lines have been identified that can produce and activate MMP-2. The human fibrosarcoma line HT-1080 has been shown to produce and activate MMP-2 without the addition of any growth factors or other chemicals. As described in Chapter 1, HT-1080 cells are frequently used in experiments involving MMP-2, including MMP-2 triggered drug delivery experiments.

The human glioblastoma cell line U-87 MG has also been utilized in MMP-2 *in vitro* experiments. U-87 MG cells do not activate MMP-2 when cultured on a two dimensional surface, i.e., at the bottom of a tissue culture plate in typical culture conditions. U-87 MG cells can be stimulated to activate MMP-2 in 2-D cell culture by adding additional substances. Concanavalin A (ConA) is a lectin isolated from the jack bean (Saleemuddin & Hussain, 1991). It has been shown that ConA induces the expression of membrane type MMP 1 (MT1-MMP), a known cellular activator of MMP-2. It has also been shown that MMP-2 is activated in the presence of breast cancer cells treated with ConA (Yu, et al., 1997). U-87 MG cells can also activate MMP-2 when in contact with collagen I. Azzam et. al. found that that multiple breast cancer cell lines grown in collagen I gels had significant activation of MMP-2, but those grown on Matrigel, plastic, or thin layers of collagen showed very little activation (Azzam, Arand, Lippman, & Thompson, 1993).

Numerous release experiments were attempted using HT-1080 or U-87 MG cells by growing the cells on a two dimensional surface, i.e., at the bottom of a well plate. All experiments failed to show a significant increase in peptide release compared to a control group without cells. Initially, experiments were done with HT-1080 cells in fully supplemented EMEM. Different cell densities were attempted. A search of the literature noted that other researchers working with MMP cleavable peptides were conducting their *in vitro* studies in serum free media. One of the principal components of fetal bovine serum is α-2 macroglobulin, a known inhibitor of MMPs. One group observed *in vitro* peptide cleavage with HT-1080 cells in the presence of serum free media, but

peptide cleavage in the presence of serum supplemented media (Chau, Tan, & Langer, 2004). Experiments were conducted with HT-1080 cells in serum-free media, but no increase in peptide release compared to controls was seen. It was hypothesized that the cysteine residues in the peptide were forming disulfide bonds, and the dimerized peptide had an altered fluorescence intensity. Tris-2-carboxyethylphosphine (TCEP), a known reducer of disulfide bonds, was added to the peptide-PEGDA solution prior to stirring. The addition of TCEP had no effect. Lim et. al successfully MMP-2 sensitive peptide cleavage and subsequent drug release by using conditioned serum free media from U-87 MG cells (Lim, et al., 2010). This was attempted using conditioned media from HT-1080 cells, but failed to show a significant increase in peptide release compared to a control of non-conditioned serum free media.

Experiments were also attempted using U-87 MG cells in 2-D. These experiments were performed using 10 μg/mL ConA. High doses of ConA can be toxic to cells, but it had been shown previously that 10 μg/mL did not significantly impact cell viability (Vartak, 2009). However, experiments in the U-87 MG cells in two dimensions did not show a significantly greater increase in the presence of cells compared to controls.

Gelatin zymography was performed on HT-1080 cells and U-87 MG cells stimulated with ConA to verify the presence of active MMP-2. The presence of active MMP-2 from HT-1080 and U-87 MG cells was verified by gelatin zymography. Zymography is a polyacrylamide electrophoresis technique designed to detect enzymes. A substrate (i.e., gelatin) is present throughout the polyacrylamide gel. If

enzyme is present, it will digest the substrate in the band area. When the gel is stained, the bands where the enzyme is present will be clear since the protein substrate is degraded. The rest of the gel, still containing protein, will be blue. Zymography is a highly sensitive technique, detecting enzyme amounts from nanograms to picograms (Lantz & Ciborowski, 1994).

A release experiment was performed that used U-87 MG cells in a three-dimensional collagen matrix (Figure 4.1). Hydrogel rods were inserted into the collagen gels, and the released measured by the presence and intensity of elution peaks on HPLC. As a comparison, release in the presence of purified MMP-2 was also examined. This study also looked at the effect of a broad-spectrum MMP inhibitor on peptide release from hydrogels. Gelatin zymography was also performed on the U-87 cells grown in collagen gels to verify the presence of active MMP-2. MS was used to further analyze eluted peaks from samples in the presence of cells and cells with GM6001.

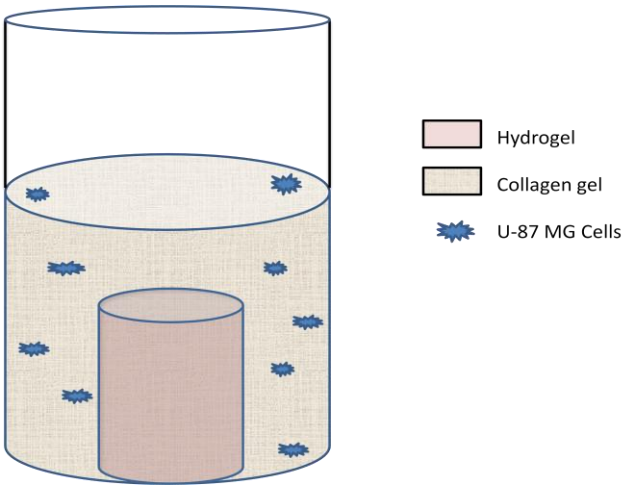

Figure 4.1 Schematic of sample in the U-87 MG 3-D study (one well in a 96 well plate). Cells are dispersed throughout the collagen gel. MMP-2 diffuses through the collagen to cleave the peptide, resulting in TAMRA release.

It was believed that the contact with collagen I would stimulate the cells to activate MMP-2 secreted by U-87 MG cells, which would in turn cleave the peptide sequence and release TAMRA into the media. The presence of active MMP-2 would be present as a band at the level of an active MMP-2 control on the gelatin zymography. This release experiment also served as a model for eventual *in vivo* hydrogel implantation in an animal model. The collagen matrix resembled brain tissue in both sample size and tissue consistency. MALDI-TOF MS was expected to a show a molecular weight corresponding to TAMRA-GPLG in the presence of U-87 MG cells. This peak was expected to be absent in the presence of an MMP inhibitor.

4.2 Materials and Methods

4.2.1 Verification of MMP-2 Activation

Cell culture. The human fibrosarcoma cell line HT-1080 (ATCC, Manassas, VA) was maintained in Eagle's minimum essential medium (Mediatech, Manassas, VA) supplemented with 10% fetal bovine serum (Gemini), 1% penicillin/streptomycin (Mediatech), 200 mM l-glutamine, 110 mg/ML sodium pyruvate, and non-essential amino acids. Cells were cultured in T150 tissue culture flasks (BD, Bedford, MA). Cells were harvested by trypsinizing (Mediatech) and passaged every 4-7 days at 1:20 to 1:50.

The human glioma cell line U-87 MG (ATCC, Manassas, VA) was maintained in supplemented EMEM. Cells were cultured in T150 tissue culture flasks (BD, Bedford, MA). Cells were harvested by trypsinizing (Mediatech) and passaged every 7 days at 1:10 to1:20.

Conditioned media collection-HT-1080 cells. HT-1080 cells (ATCC, Manassas, VA) were removed from a T150 tissue culture flask by removing the media from the flask and adding 1.5 mL Trypsin/EDTA (0.05%). The trypsin was neutralized by supplemented EMEM. The cells were centrifuged at 1,000 rpm for five minutes. The cells were resuspended in EMEM and counted using a Coulter Counter (Beckman Coulter, Brea, CA). The cell-media solution was diluted to obtain the desired cell density. The cells were placed in 48 well plates (Corning Life Sciences, Corning, NY) and incubated overnight. The following day, the media was changed to serum-free

supplemented EMEM. Media was collected from the wells at 24 and 48 hours. The removed media was centrifuged at 10,000 rpm for three minutes at 4 °C. The media was stored at -80 °C for further use.

Conditioned media collection-U-87 MG cells (2-D). U-87 MG cells (ATCC, Manassas, VA) U-87 MG cells were harvested from a tissue culture flask, centrifuged, resuspsended in EMEM, and counted. The cell-media solution was diluted to obtain the desired cell density. The cells were placed in 48 well plates (Corning Life Sciences, Corning, NY) and incubated overnight. The following day, the media was changed to serum-free supplemented EMEM and 10 μg/mL ConA (Sigma-Aldrich, St. Louis, MO). Media was collected from the wells at 24 and 48 hours. The removed media was centrifuged at 10,000 rpm for three minutes at 4 °C. The media was stored at -80 °C for further use.

Gelatin zymography. Gelatin zymography was performed using a MiniPROTEAN II Multi Casting Chamber electrophoresis cell on Ready Gel® precast gels (Bio-Rad, Hercules, CA). Samples were diluted 1:2 in a sample buffer consisting of 62.5 mM Tris-HCl, 4% sodium dodecyl sulfate (SDS), 25% glycerol, and 0.01% bromophenol blue. Active MMP-2 was used as a control by diluting in 0.5 M Tris-HCl to a concentration of 9 nM. The gel was run in a buffer consisting of 25 mM Tris, 192 mM glycine and 0.1% SDS. The gel was run at a voltage of 100 V for 60 to 70 minutes. After removing from the cell, the gel was washed in a renaturing solution of 2.5% Triton X-100 for 30 minutes. The gel was then washed in a development solution of 50 mM Tris base, 200

mM NaCl, 5 mM $CaCl_2$-$5H_2O$, and 0.02% Brij-35 for five minutes and incubated in development solution overnight. The gel was stained with a solution of 10% acetic acid, 40% methanol, 50% DDIW, and 0.5% R-2 50 Brilliant Blue (Coomassie) for one hour. The gel was destained with a solution of 10% acetic acid, 40% methanol and 50% DDIW until bands appeared, changing the destaining solution as needed. The gel was destained until the stacking gel portion was clear. The gel was photographed on a light box.

4.2.2 *In vitro* peptide release study using U-87 MG cells

Creation of hydrogels with conjugation of PEGDA to the MMP cleavable peptide. TAMRA-GPLGVRGC (UIC Protein Research Laboratory) was conjugated to PEGDA20,000 (Laysan Bio, Arab, AL). A cylindrical mold was created by wrapping wax paper into a small tube. The wax paper was wrapped around a thin metal rod to ensure consistency of tube diameter between batches. The bottom of the tube was covered in Parafilm to prevent leakage. Hydrogels were polymerized using APS and TEMED as described in section 2.2.2. The hydrogel was injected into the cylindrical mold and incubated.

Hydrogel washing. After conjugation and polymerization, the rods were washed in a solution of Dulbecco's phosphate buffered saline (DPBS) without calcium and magnesium (Mediatech, Manassas, VA). The rods were washed twice, allowing 3 to 4 hours for each wash. The rod was then cut into approximately 2.5 mm long segments

using a razor. Electronic calipers were used to measure length. Each disc was placed in a 24 well plate with 1 mL DPBS and washed until buffer fluorescence was stable.

Creation of hydrogel rods without peptide. PEGDA 20,000 hydrogels were polymerized using APS and TEMED as described in section 2.2.1, polymerized in a cylindrical mold, and incubated. Hydrogels were washed in DPBS at least twice to remove unreacted monomer and initiators. Hydrogels were cut into 2.5 mm sections.

As an MMP-2 inhibitor, a solution of GM6001 was prepared by dissolving powereded GM6001 (EMD/Calbiochem, Gibbstown, NJ) in dimethyl sulfoxide (DMSO) at a concentration of 2.5 mM.

Peptide release in the presence of collagen embedded U-87 MG cells. U-87 MG cells were harvested from a T150 flask, centrifuged, resuspended in DPBS, and counted. The cells were diluted to a density of $2x10^6$ cells/mL. The cells were embedded in a collagen gel to create a 3 dimensional tumorlike environment. A solution was created of collagen I (BD Biosciences, Franklin Lakes, NJ), sodium hydroxide, cell suspension, and DPBS such that the final concentration of collagen I was 2.5 mg/mL and the final cell density was 1.0×10^6 cells/mL. Collagen gels without cells were made in the same manner, with additional DPBS replacing the cell suspension. Each collagen gel had a volume of 100 μL. The collagen gels were incubated at 37 °C for thirty minutes. Gels were removed from the incubator and a total of 50μL solution was added in the form of SF EMEM, MMP-2, GM6001, and/or DMSO

(Table 4). The gels were incubated at 37°C. After an additional two hours, the collagen gels were removed from incubation, and hydrogel rods with or without peptide were added (Table 4). Additional MMP-2, GM6001, or DMSO was added to the appropriate wells. The hydrogels in collagen were incubated at 37°C. Two time points were examined, 8 hours and 24 hours. Samples were collected by removing the hydrogel from the well and centrifuging all contents at room temperature at 10,000 rpm for ten minutes. The supernatant was filtered through a 0.45 μm syringe filter (Millipore, Billerica, MA) and stored at -20 °C All samples were analyzed using HPLC as described in section 3.2.4.

Conditioned media collection of U-87 MG cells (3-D). U-87 MG cells (ATCC, Manassas, VA) were removed from a harvested from a T150 tissue culture flask, centrifuged, resuspended in DPBS, and counted. The cells were embedded in collagen gels. The plate was incubated at 37 °C for 30 minutes. Collagen gels were removed from incubation and 50 μl SF EMEM was added. An additional 50 μl SF EMEM was added was added two hours later. Supernatant was collected at 8 and 24 hours and stored at -80 °C. Gelatin zymography was performed on samples at both time points.

TABLE 4 EXPERIMENTAL SETUP FOR 3-D IN VITRO RELEASE STUDY

Sample	Hydrogel with Peptide	Hydrogel WIthout Peptide	Cells	MMP (9 nM)	DMSO (10 µL/mL)	GM6001 (25 µM)
1	-	+	-	-	-	-
2	-	+	+	-	-	-
3	+	-	+	-	-	-
4	+	-	-	-	-	-
5	+	-	+	-	+	-
6	+	-	-	-	+	-
7	+	-	+	-	-	+
8	+	-	-	-	-	+
9	+	-	-	+	-	-
10	-	+	-	+	-	-
11	+	-	-	+	-	+
12	-	-	-	-	-	-

4.2.3 Identification of *in vitro* peptide cleavage by MALDI-TOF MS

MALDI-TOF MS of selected *in vitro* xamples. Several HPLC samples from the *in vitro* study in 4.2.2 were fractionated by collecting the mobile phase elutent corresponding to chromatogram peaks as it exited the fluorescence detector. Fractions were anazylzed using MALDI-TOF MS as described in section 3.2.5.

Gelatin zymography and *in vitro* release study were performed three times for verification. Figures shown are representative of three experiments. MALD-TOF MS was performed once for each sample category.

4.3 Results and Discussion

4.3.1 Verification of MMP-2 activation. For HT-1080 cells, the cell densities examined were 1 $x10^6$, $5x10^5$, and $1x10^5$ cells/mL. Bands were seen in the gelatin zymography for HT-1080 cells at both 24 and 48 hours for all cell densities corresponding to the molecular weight of active MMP-2 (Figure 4.2).

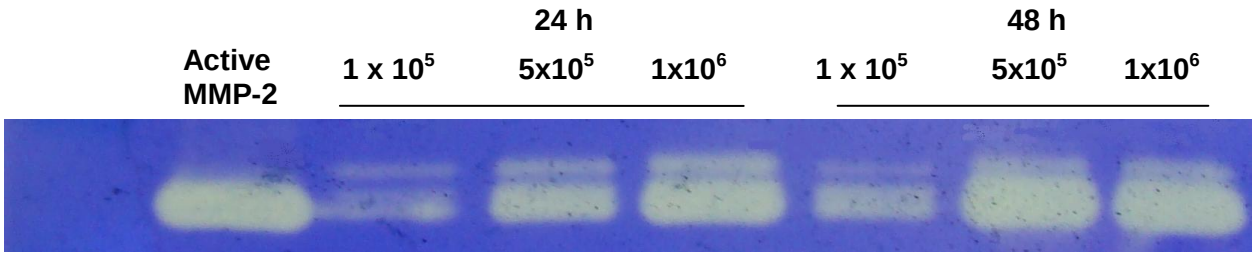

Figure 4.2 Gelatin zymography of HT-1080 cells

Several lanes had a set of two bands. The top band is most likely proMMP-2, as it has a slightly greater molecular weight (72 kDa) than the active form (62 kDa). Multiple papers have shown gelatin zymographies with both proMMP-2 and active MMP-2 run as controls, and have shown the pro-MMP-2 to appear directly above the active MMP-2 (Vartak, Lee, & Gemeinhart, 2009) (Pavlaki, Hymowitz, Chen, Bahou, & Zucker, 2002). Greater band intensity was seen with an increase in cell density. Greater band intensity was also seen at the 48 hour point at compared to the 24 hour point. The U-87 MG cells were examined in 2-D 1 x 10^6, 5x 10^5, 1x10^5, and 5x10^4 cells/mL. Bands were present at all times and cell densities (Figure 4.3). Increased band intensity was seen with increasing cell density and at 48 hours compared to 24 hours. Bands believed to be proMMP-2 were also seen.

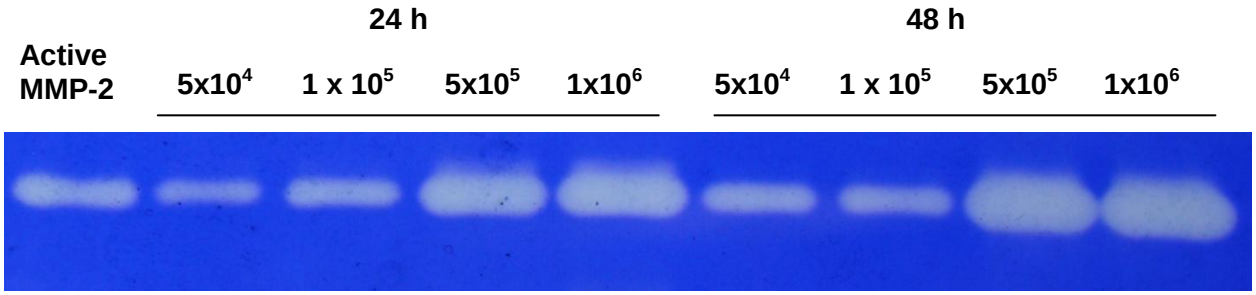

Figure 4.3 Gelatin zymography of ConA stimulated U-87 MG cells in 2-D

Although zymography can indicate the presence of enzyme and its molecular weight, it cannot be used to determine the quantity of active MMP-2 present in the sample. The band intensity cannot be used to infer relative amounts of MMP-2 present, as the relationship between band intensity and active MMP-2 is nonlinear. Brighter intensity of bands is suggestive of greater MMP-2 present, but exact comparisons between amounts cannot be determined by this technique. Nonetheless, band intensity for the HT-1080 cells at 1 x 10^6 at 24 hours and both 5 x 10^5 and 1 x 10^6 at 48 hours is similar in intensity to the control. For the U-87 MG cells in 2-D, 1 x 10^5 at both time points is similar in band intensity to the control, and 5x10^5 and 1x10^6 have intensities greater than control at both time points. Protein detection techniques such as Western Blot or ELISA can be utilized for MMP-2, but the antibodies available are not specific to the active form of the enzyme. Any measurement of MMP-2 content would include both the inactive and active forms of the enzyme. Since the determination of active MMP-2 presence was essential to the study, Western Blot and ELISA were not utilized.

Another limitation of the gelatin zymography study was that this technique does not show the activity of the MMP-2 present. The failure of the peptide release studies in 2-D may be explained by the fact that while the MMP-2 was being expressed and activated, it was not able to cleave peptide. There are a few explanations for this. As described in Chapter 1, proMMP-2 is activated by cleaving the propeptide domain, reducing the molecule size from 74kDa to 64 kDa. The 64 kDa form undergoes a second activation by another MMP-2 molecule which brings molecular weight to 62kDa. It is possible this final autoactivation is not occurring. The difference between a 62 kDa and 64kDa band would not be visible on the polyacrylamide gels used for zymography. A possibility explored was that SF EMEM had a component that was inhibiting MMP-2 activity, or that the absence of zinc in SF EMEM prevented MMP-2 from cleaving peptide. Purified activated MMP-2 was incubated with hydrogels in SF EMEM with and without zinc, in a manner similar to the release experiments described in part 3. Peptide release was demonstrated in EMEM, and the presence of zinc had no effect on release. A third, untested possibility is that the microenvironment of the plated cells expressed proteins that inhibited the activity of MMP-2.

4.3.2 *In vitro* peptide release study using U-87 MG cells. To examine peptide release from MMP-2 activating cells, supernatant from hydrogels incubated with cells was analyzed using HPLC. In the presence of cells, a peak was eluted at about 2.5 minutes, identical to the elution time seen with the samples from the MMP-2 release studies. This peak was higher in intensity at 24 hours than at 8 hours. The sample with hydrogel and without cells had a very small peak at this elution time (Figure 4.4).

a)

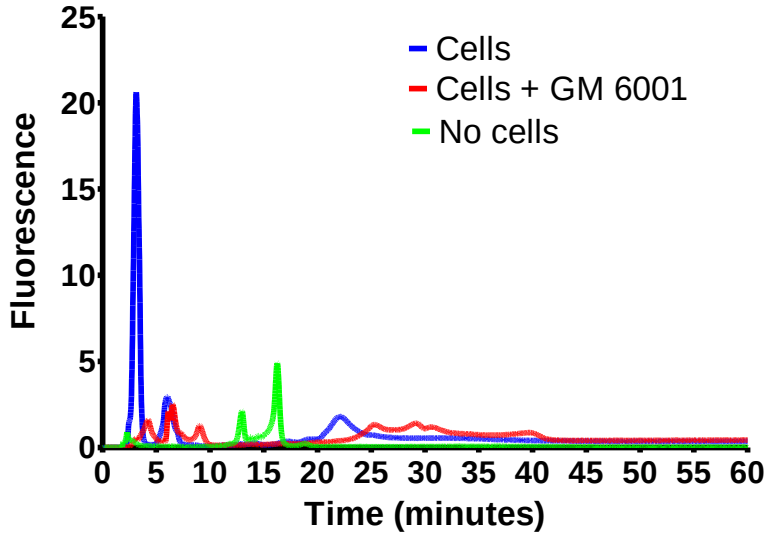

b)

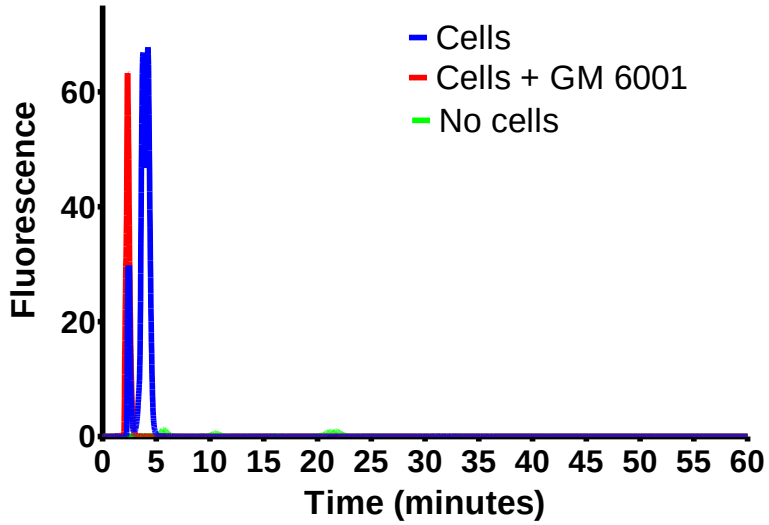

Figure 4.4 HPLC chromatogram from U-87 MG *in vitro* study, at a) 8 hours and b) 24 hours. Blue=hydrogel with cells, red=hydrogel with cells and GM6001, green=hydrogel with no cells. Figures repsresentative of three experiments.

GM6001 was used to inhibit the effects of MMP-2, and it was expected that no peak would be seen at 2.5 minutes. A peak was present in the sample with cells and GM6001, but it was lower in intensity than the sample with cells alone for two of the three samples run. Hydrogels were also incubated with DMSO as a vehicle control for the GM6001. It was necessary to determine if inhibition of peptide release was due to the GM6001 itself, or the toxicity of DMSO to the cells (Figure 4.5). Release was also examined without cells in the presence of GM6001 and DMSO. The peak with cells and DMSO was much greater in intensity than with GM6001, indicating the decrease in peak intensity is due to GM6001 and not due to an adverse effect of the DMSO on the cells.

a)

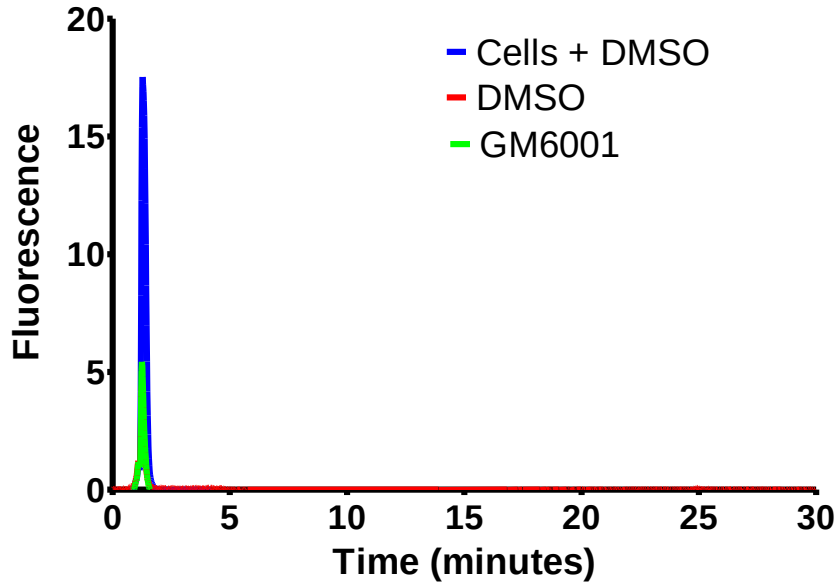

b)

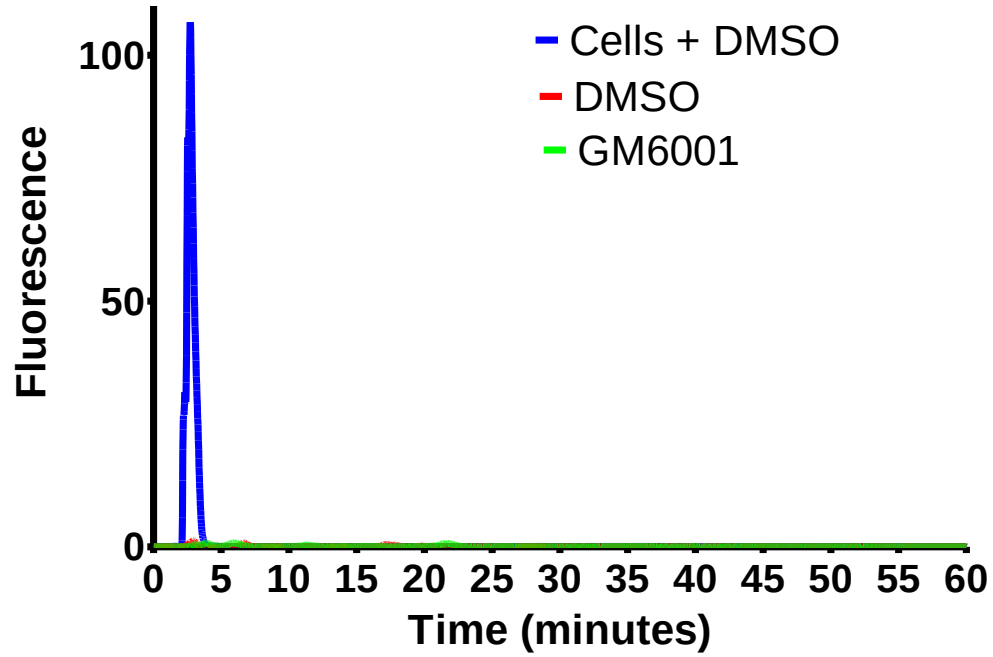

Figure 4.5 HPLC chromatogram from U-87 MG *in vitro* study at a) 8 hours and b) 24 hours. Blue=hydrogel with cells and DMSO, red=hydrogel with DMSO, green=hydrogel and GM6001.Figures representative of three experiments.

Sample with active MMP-2 showed a peak detected at 2.5 minutes, the same time as the peak seen in the presence of cells. GM6001 was also used in conjunction with purified MMP-2 and showed a decreased peak intensity (Figure 4.6).

a)

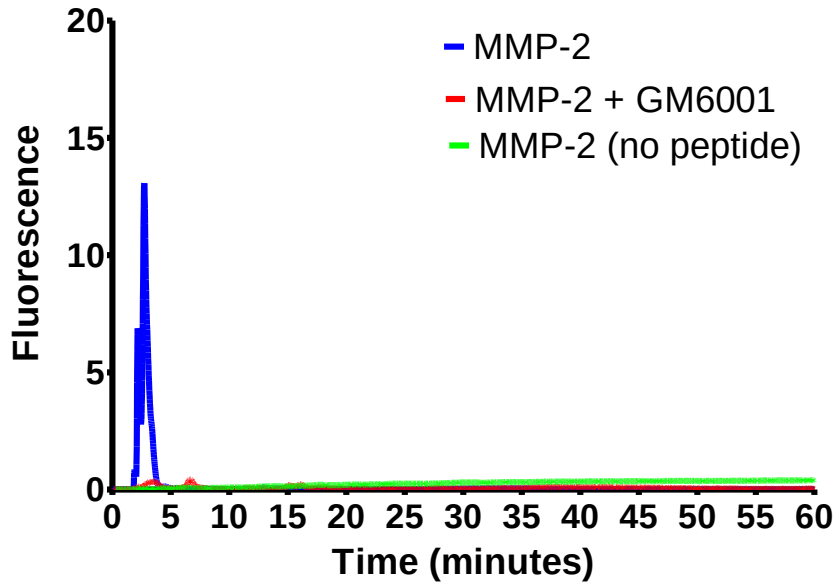

b)

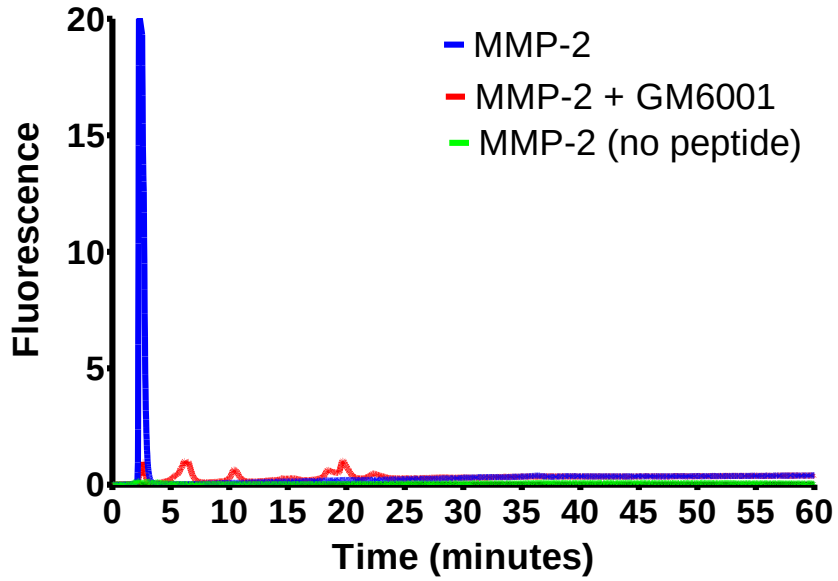

Figure 4.6 HPLC chromatogram from U-87 MG *in vitro* study at a) 8 hours and b) 24 hours.Blue=Hydrogel with active MMP-2, red=hydrogel without peptide and active MMP-2, and green=hydrogel with MMP-2 and GM6001. Figures representative of three experiments.

Controls were also done with hydrogels without peptide with cells, without cells and with MMP-2, and of collagen only. These samples showed no fluorescence peaks at either time point. (Figure 4.7).

a)

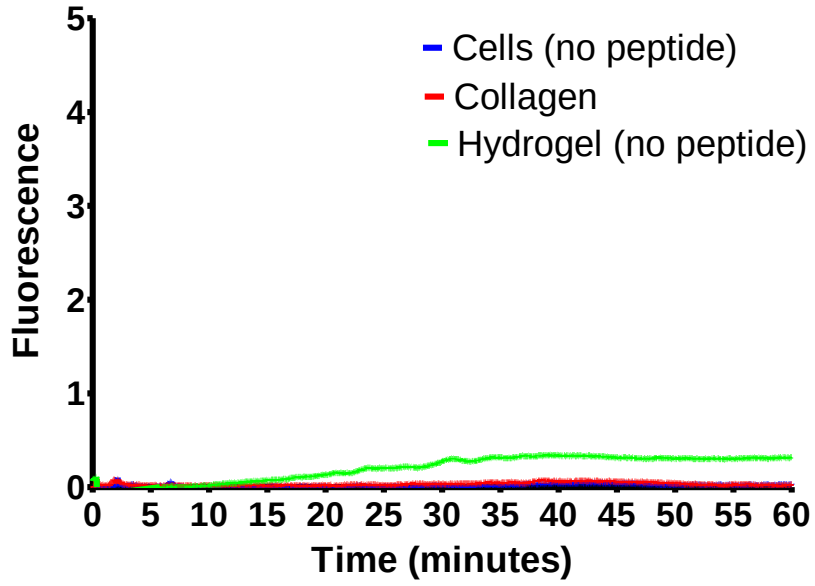

b)

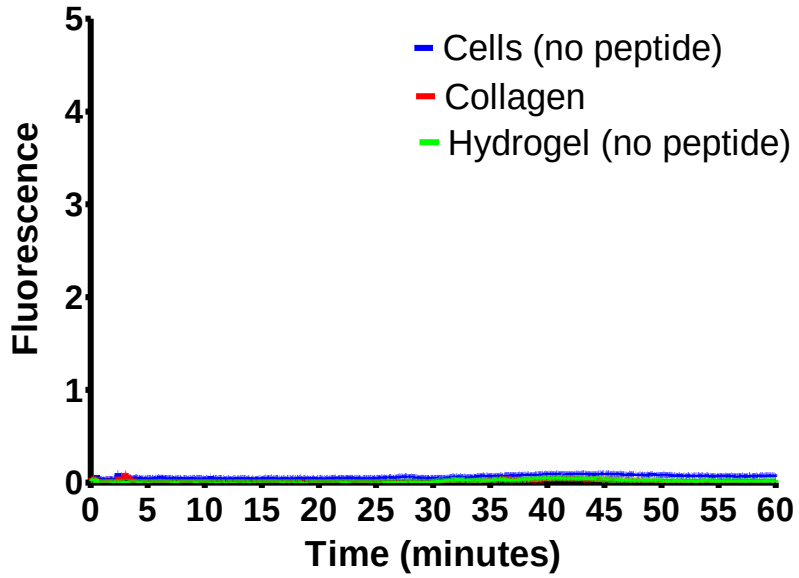

Figure 4.7 HPLC chromatogram from U-87 MG *in vitro* study at a) 8 hours and b) 24 hours. Blue=cells with hydrogel (no peptide), red=collagen only, green=hydrogel without peptide. Figures representative of three experiments.

Gelatin zymography of U-87 MG cells under the conditions of this study confirmed the presence of active MMP-2 at both timepoints (Figure 4.8). An unexpected band was seen towards the bottom of the gel. This band was not seen in the HT-1080 zymography or the U-87 MG 2-D zymography. Because this enzyme can degrade gelatin, it may be contributing to peptide cleavage and TAMRA release. According to work published by Snoek Van Beurden and Von de Hoff, other MMPs are able to degrade the gelatin in zymography, including MMP-1, MMP-8 and MMP-13. However, it is unlikely this lower band is one of the MMPs in question because the bands would be

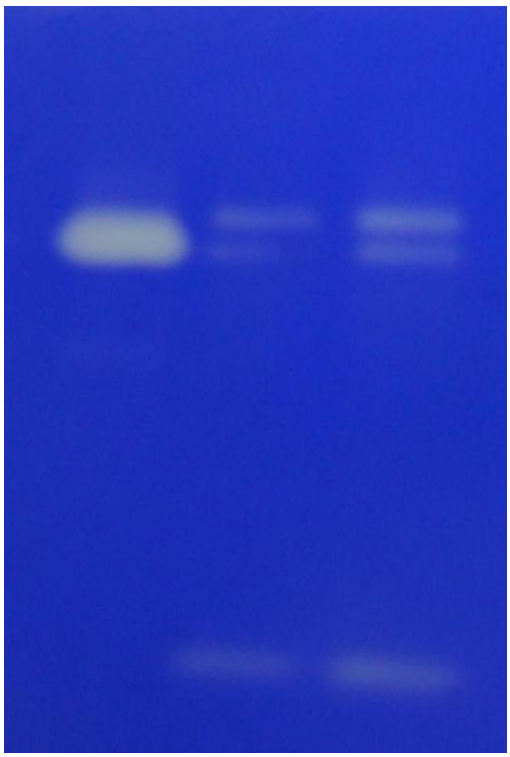

Figure 4.8 Gelatin zymography of U-87 MG cells incubated in a 3-D collagen gel.

much fainter than the MMP-2 bands (Snoek-van Beurden & Von den Hoff, 2005). Another possibility for the unknown enzyme is MMP-7, which has demonstrated gelatinolytic activity and has been reported to be expressed in brain tumors (Woessner & Taplin, 1988, Rome, Arsaut, Taris, Couillard, & Louisseau, 2007) The absence of molecular weight markers prevents estimates of the unknown enzyme's molecular weight. Molecular weight markers are difficult to detect on zymography gels as the staining limits the band visibility. The only definitive statement that can be made is that the unknown enzyme is smaller than 62 kDa, the molecular weight of active MMP-2. MMP-1, MMP-8, and MMP-13 all have latent and active forms that are smaller 62 kDa. ProMMP-1 has a minor 57 kDa form and major 52 kDa form, which are respectively cleaved to 47 kDa and 42 kDa active forms (Goldberg, Wilhelm, Kronberger, Bauer, Grant, & Eisen, 1986). MMP-8 has a 75 kDa latent form and active forms ranging in size from 22-57 kDa (Hasty, Hibbs, Kang, & Mainardi, 1986). MMP-13 has a latent form of 60 kDa, an intermediate form of 50 kDa, and a final active form of 48 kDa (Knauper, Lopez-Otin, Smith, Knight, & Murphy, 1996). MMP-7 has a molecular weight of 28 kDa for the latent form and 19 kDa for the active form (Woessner & Taplin, 1988). Further identification of this low molecular weight enzyme will be necessary for the full understanding of *in vitro* release in this drug delivery system.

4.3.3 Identification of i*n vitro* peptide cleavage by MALDI-TOF MS. Three peaks seen on HPLC were collected and analyzed using MS. From the sample with cells, the peaks at 2.5 minutes (Peak A) and 5 minutes (Peak B) at 24 hours. The third peak was from the sample with cells and GM600, at 2.5 minutes (Peak C) . For Peak A (Figure

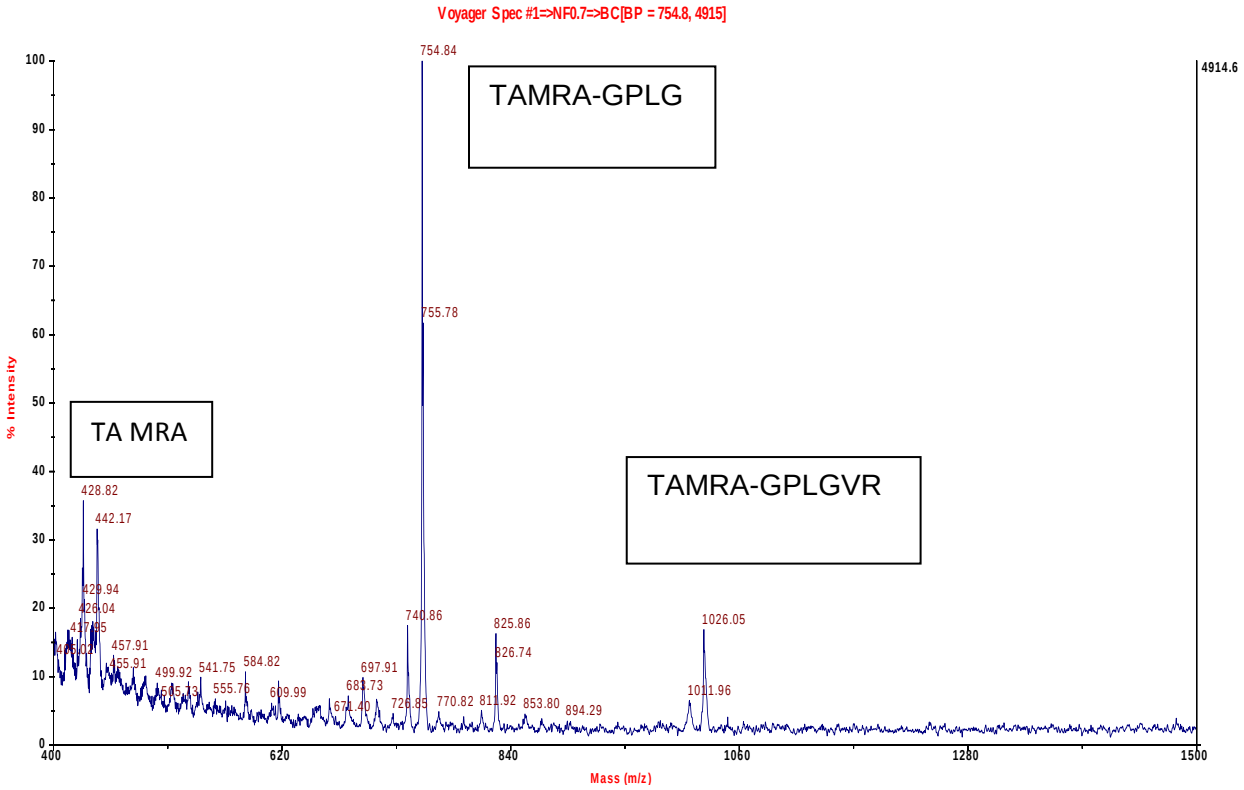

Figure 4.9 MALDI-TOF MS for Peak A (release in the presence of cells, 2.5 minute elution time). Peaks labeled with corresponding peptide fragments.

4.9), the highest intensity peak was at 754.84 mass charge ratio (m/z). This molecular weight corresponded to TAMRA-GPLG, the expected cleavage site of MMP-2. Peaks of much less intensity were at 428.42 and 442.17 m/z. The peak values were close to the molecular weight of TAMRA. Another peak is at 1011.96 m/z, which corresponded to the molecular weight of TAMRA-GPLGVR. Numerous other small peaks were seen that did not correspond to any molecular weight in the peptide sequence.

The second peak examined was Peak B (Figure 4.10). The TAMRA and TAMRA-GPLGVR peaks were at 435.84 and 1009.95 m/z respectively. A somewhat prominent peak is seen at 667.45 m/z. The peptide fragment that corresponded to this molecular weight was GPLGVRG.

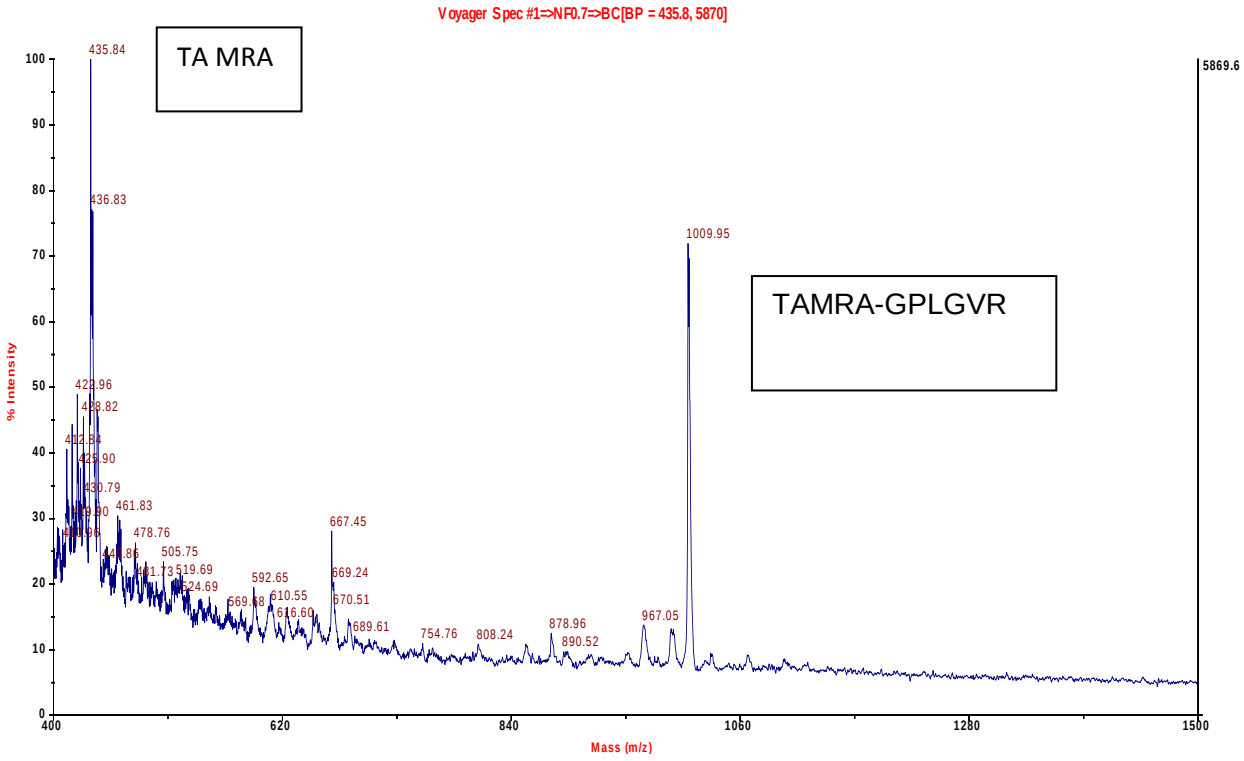

Figure 4.10 MALDI-TOF mass spectrometry for PeakB (release in the presence of cells, 5 minute elution time). Peaks labeled with corresponding peptide fragments.

The third peak was examined was Peak C (Figure 4.11). The TAMRA and TAMRA-GPLGVR peaks were once again at 435.80 and 1010.52 m/z, respectively. The

possible GPLGVRG peak was also at 667.55 m/z. Two additional peaks were present: a high intensity peak at 574.87 m/z and a much lower intensity peak at 878.28 m/z. The molecular weights corresponded to TAMRA-GP and TAMRA-GPLGV, respectively.

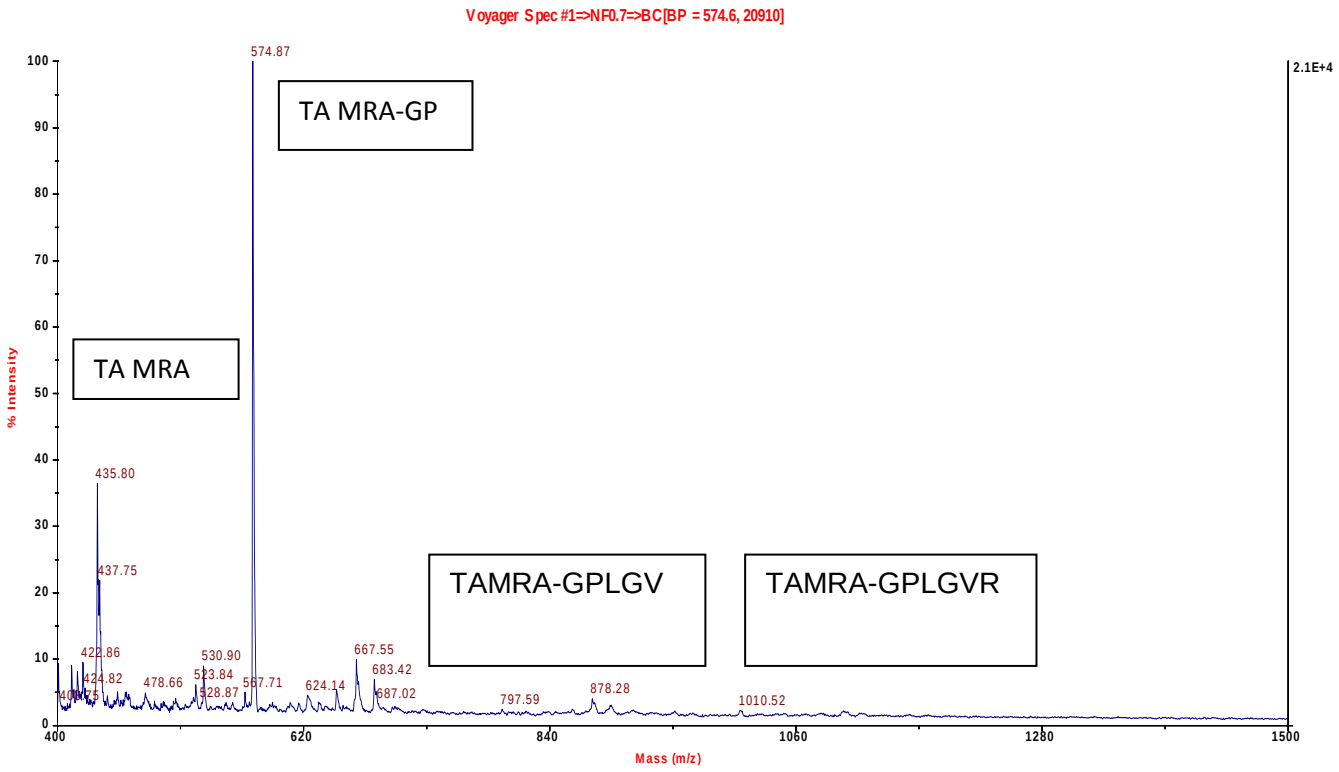

Figure 4.11 MALDI-TOF MS for Peak 3 (release in the presence of cells and GM6001, 2.5 minute elution time). Peaks labeled with corresponding peptide fragments.

The presence of the TAMRA-GPLG molecular weight from the sample taken with cells confirms that the MMP-2 is cleaving and releasing the peptide, as MMP-2 has been confirmed to be expressed by the cells and activated as shown on gelatin zymography.

TAMRA-GPLG is the expected cleavage site for MMP-2. Also, nothing was detected at this m/z in the presence of cells and GM6001, indicating the MMP-2 was inhibited from cleaving the peptide. Although the m/z range tested was up to 1500, nothing was detected at or near 1170, the mass of the full TAMRA-GPLGVRGC peptide. This provides further confirmation that the full peptide does not elute at 2.5 minutes and the fluorescence peak seen at the elution time is a cleaved product.

Other peptide fragments were seen in all three samples-namely, the TAMRA and the TAMRA-GPLGVR. These may be due to other proteases expressed by the U-87 MG cells. It is also possible that a cleaved fragment, e.g., TAMRA-GPLG, experienced a secondary cleavage either by MMP-2 one or more additional proteases expressed by the cells. In the sample with cells and GM6001, the additional fragments TAMRA-GP and TAMRA-GPLGV were detected that were not seen in the peaks with cells without GM6001. A possible explanation is that these fragments were cleaved by proteases that have less affinity for the GPLGVRG and are slower to act. The MMP-2 would cleave the peptide faster than the other proteases, leaving no substrate for it to act upon. In the absence of MMP-2, the other proteases had substrate available and cleaved the peptide (Figure 4.12).

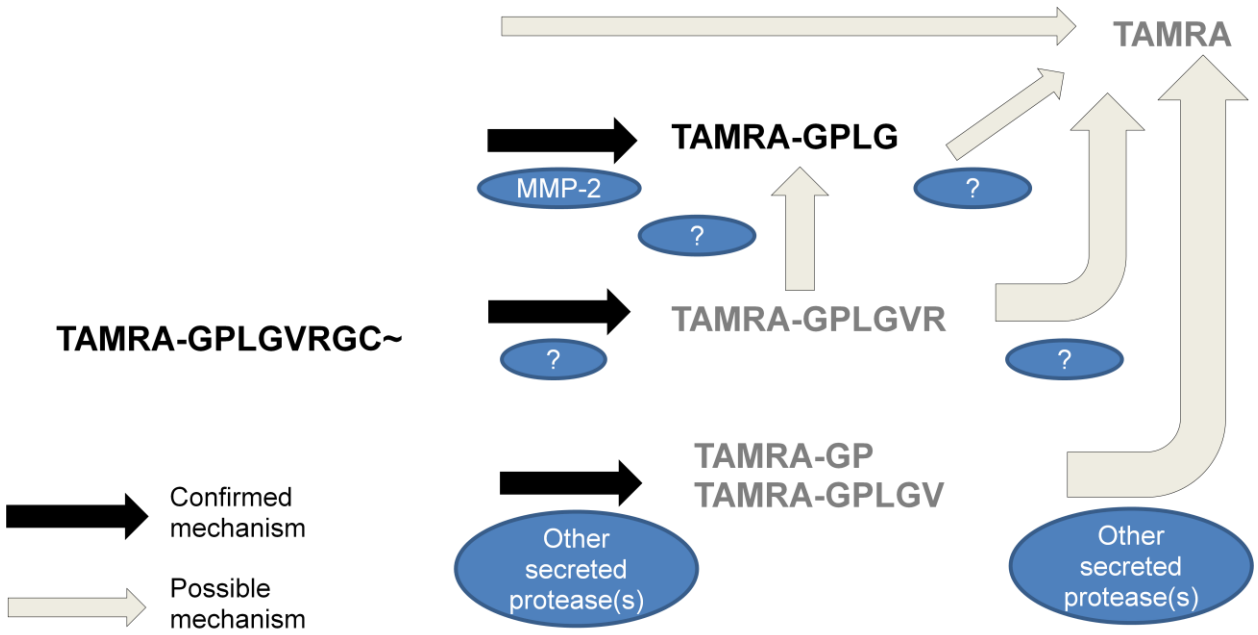

Figure 4.12 Schematic of proposed peptide cleavage. Active MMP-2 cleaves TAMRA-GPLGVRG from the hydrogel between the glycine and valine. TAMRA-GPLGVR may be formed by MMP-2 or another protease, and it is possible TAMRA-GPLG is a secondary product of TAMRA-GPLGVR. When MMP-2 is inhibited by GM6001, other protease(s) cleave the peptide to TAMRA-GP and TAMRA-GPLGV. TAMRA may possibly be a secondary cleavage product of TAMRA-GPLG, TAMRA-GPLGVR, TAMRA-GP, or TAMRA-GPLGV. TAMRA may also be cleaved directly from the conjugated peptide.

There are several limitations to the interpretation of any MS data. One is the assumption that ionization does not fragment any species present in the sample. This is an uncommon occurrence with soft ionization techniques. The fact that specific peptides are observed confirms that sample fragmentation due to ionization is minimal.

Also, it is unlikely that fragmentation would produce definitive high intensity peaks. Another limitation is that is it assumed each species is only ionized by one charge. Since the measurement made is mass to charge ratio, a species with two charges would be detected at half its molecular weight. The consistent presence of peaks corresponding to molecular weights of the peptide sequence makes this unlikely.

4.4 Conclusions

The verification of expression and activation of MMP-2 in multiple cell lines and cellular condtions was achieved using gelatin zymography. In HT-1080 cells and in U-87 MG cells, active MMP-2 presence increased with time and with increasing cell density. Despite the presence of active MMP-2, release studies using cells failed to show an increase in release with cells compared to hydrogels incubated without cells.

The 3-D U-87 MG study confirmed the cleavage of peptide and release from the hydrogel by MMP-2. The peak elution time at 2.5 minutes in the presence of cells is an indication that MMP-2 is being expressed and activated by the U-87 MG cells, and this MMP-2 is cleaving the peptide. This is further supported by the reduction in peak intensity in the presence of GM6001. The reduction or absence of a peak at 2.5 minutes in samples without MMP-2 or cells also supports the notion of MMP-2 mediated peptide cleavage and release.

Mass spectrometry confirmed the TAMRA-GPLG cleavage site in the presence of cells. The spectrometry data also showed peptide cleavage at other sites, possibly due to one or more proteases secreted by the cells. GM6001 blocked MMP-2 peptide cleavage between the glycine and valine residues.

5. Conclusions and Future Work

5.1 Conclusions

In this work, it has been shown that PEGDA hydrogels can be created with a controllable mesh size. PEGDA 3,400 hydrogels were shown to have a mesh size too small for MMP-2 entry. PEGDA 10,000 hydrogels were fabricated to have a large enough mesh for MMP-2 entry, and PEGDA 20,000 hydrogels had a larger mesh than the PEGDA 10,000. A PEGDA composition of 15% w/v was chosen to maximize mesh size while maintaining durability at all molecular weights. Mesh size verification using tensile testing to find molecular weight between crosslinks showed slightly smaller mesh sizes than measured with swelling. However, the PEGDA 10,000 and PEGDA 20,000 still had mesh sizes large enough for MMP-2 entry both with and without the incorporation of peptide.

MMP-2 released the model API in the presence of MMP-2 in nine of the eleven conditions tested. API release was seen at all three concentrations tested with the PEGDA 10,000 and 20,000. In looking at percent release, the nonspecific release (buffer only) was roughly 10% at 96 hours at all molecular weights, peptide concentrations, and peptide sequences. Although a greater percent release was not seen at larger molecular weight PEGDA, the ratio of amount released with MMP-2 to amount released in buffer was greater for the PEGDA 20,000 compared to PEGDA 3,400 at all three concentrations tested. PEGDA 10,000 was greater than PEGDA 3,400

at the low and medium peptide concentrations. Because the mesh size of PEGDA 3,400 is smaller than the dimensions of MMP-2, this suggests the increased release is due to MMP-2 entry into the hydrogel. Comparison between the different loading amounts at each molecular weight showed no significant differences either in the MMP-2 mediated release or in the nonspecific release. Peptide cleavage for all molecular weights and concentrations was confirmed by HPLC. Release studies using alternate MMP cleavable peptide sequences supported MMP-2 mediated peptide cleavage and suggested optimization improvements for this drug delivery system. The alternate peptides showed greater consistency in release than GPLGVRG, which could have potential uses for further optimization.

Experiments with U-87 MGs in 3-D culture demonstrated MMP-2 secreted from cells could also cleave the peptide and release the model API. This experiment also provided a model for hydrogel insertion in an *in vivo* environment. Mass spectrometry confirmed the expected cleavage site of TAMRA-GPLG for MMP-2, and identified multiple secondary cleavage sites. Gelatin zymography confirmed the presence of active MMP-2 produced in this release study, as well as in HT-1080 cells and U-87 MG cells in 2-D when stimulated with ConA.

In summary, active MMP-2, whether directly or secreted by cells and activated, is able to cleave the peptide conjugated to the hydrogel matrix and release the API, and there is an indication that the MMP-2 is able to enter the hydrogel if the mesh size is greater than the dimensions of the enzyme. Further optimization can be achieved by

using one of the two higher molecular weights (PEGDA 10,000 or 20,000) and the peptide sequence IPVSLRSG. This information could be used to inform research using hydrogels for MMP-triggered drug delivery or other drug delivery applications. A potential application would be to create MMP-triggered pH sensitive hydrogels in which the mesh expands at a specific pH, allowing MMP entry.

5.2 Future Work

The majority of future experiments involve further release studies. Release should be examined using the IPVSLRSG peptide at different molecular weights and concentrations as performed with the GPLGVRG peptide. Because the IPVSLRSG peptide showed greater consistency in release, further optimization may be ascertained with the two variables examined. The kinetics of the IPVSLRSG peptide should also be measured and compared to the amount determined by Turk (Turk, Huang, Hiro, & Cantley, 2001).

The release experiments were normalized by PEGDA composition, all using at 15% w/v. As mentioned in Chapter 3, this resulted in vast differences in loading among the different molecular weights, since there were large differences in the amount of available acrylate groups. A set of experiments should be done to normalize the different molecular weight PEGDA macromers by concentration of acrylate groups. Mesh size, loading, and percentage release would be measured. It may be possible to combine loading with a higher percentage of release. Solubility issues may prevent all

three molecular weight macromers from being examined in this fashion, particularly with the PEGDA 20,000.

Tensile testing of the hydrogels should be continued, beginning with independent replication of the samples tested. In addition, the samples should be tested at three different frequencies, as strain rate is known to affect the elastic modulus of polymers. As the strain rate increases, the elastic modulus of the material increases. The strain rate has less of an effect than adjusting testing temperature from below to above the glass transition temperature (Fried, 2008). Nonetheless, different strain rates should be examined to determine an average modulus for each molecular weight.

The next experiment to be conducted with the *in vitro* portion of this work is to quantify the amount of peptide being cleaved for both with MMP-2 from cells and with purified MMP-2. This can be done by calculating the area under the peak curve and comparing it to a standard curve of TAMRA-GPLG peaks at known concentrations. This amount should be compared to the release studies in Chapter 3 to examine the effect of other solid matter (i.e., collagen) on the diffusion of MMP-2 and resultant peptide cleavage. Comparisons with the PEGDA 10,000 and PEGDA 3,400 would also be valuable in verifying the data from Chapter 3. The low molecular weight gelatin degrading enzyme should be identified. A potential approach is to review the literature for other proteases expressed by U-87 MG cells. The enzyme could be extracted from the gel, followed by mass spectrometry to confirm the molecular weight. The absence of peptide cleavage in the 2-D *in vitro* experiments should also be investigated. The initial

experiment would be to test MMP-2 activity under the experimental conditions using a commercial MMP-2 substrate. This would confirm if the MMP-2 is reaching its active state, and quantify the activity present.

An effort should be made to reduce the nonspecific release of the drug delivery system. Alternate attachment chemistries should be explored that may be more stable than the cysteine-acrylate bond. One possibility is to attach the peptide via a lysine residue using EDC/sulfyl-NHS chemistry. Another approach is to synthesize acrylate-PEG-peptide chains and incorporate them in PEGDA at the time of polymerization. This approach was used with the cellular adhesion motif RGDS and successfully demonstrated peptide presence throughout the hydrogel (Stephens-Altus, Sundelacruz, Rowland, & West, 2011).

Finally, efficacy experiments using an actual drug should be conducted with the fully optimized drug delivery system to determine cytotoxicity of MMP-2 secreting cells. These should be followed by animal experiments to measure reduction in tumor volume, toxicity, disease free survival, and rate of recurrence. If animal studies demonstrate the MMP-2 triggered hydrogel drug delivery system as an effective treatment, an important step will be taken in the treatment of glioblastoma.

Works Cited

Albright, C. F., Graciani, N. H., Yue, E., Stein, R., Lai, Z., Diamond, M., et al. (2005). Matrix metalloprotease-activated doxorubicin prodrugs inhibit HT1080 xenograft growth better than doxorubicin with less toxicity. *Molecular Cancer Therapeutics* (4), 751-760.

Anseth, K., Bowman, C. N., & Brannon-Peppas, L. (1996). Mechanical properties of hydrogels and their experimental determination. *Biomaterials , 17* (17), 1647-1657.

Attenello, F., Mukherjee, D., Datoo, G., McGirt, M. J., Bohan, E., Weingart, J. D., et al. (2008). Use of Gliadel (BCNU) wafer in the surgical treatment of malignant glioma: a 10 year institutional experience. *Annals of Surgical Oncology , 15* (10), 2887-2893.

Azzam, H. S., Arand, G., Lippman, M., & Thompson, E. W. (1993). Association of MMP-2 activation potential with metastatic progression in human breast cancer cell lines independent of MMP-2 production. *Journal of the National Cancer Institute* (85), 1758-1764.

Bae, M., Cho, S., Song, J., Lee, G., Kim, K., Yang, J., et al. (2003). Metalloprotease specific poly(ethylene glycol) methyl ether-peptide-doxorubicin conjugate for targeting anticancer drug delivery based on angiogenesis. *Drugs Experimental Clinical Research , 20* (1), 15-23.

Ballabh, P., Braun, A., & Nedergaard, M. (2004). The blood brain barrier: an overview. Structure, regulation, and clinical implications. *Neurobiology of Disease , 16*, 1-14.

Bhattarai, N., Gunn, J., & Zhang, M. (2010). Chitosan-based hydrogels for controlled, localized drug delivery. *Advanced Drug Delivery Reviews , 62* (1), 83-99.

Bjugstad, K., Lampe, K., Kern, D., & Mahoney, M. (2010). Biocompatibility of poly(ethylene glycol)-based hydrogels: an analysis of the glial response over space and time. *Journal of Biomedical Materials Research Part A , 95A* (1), 79-91.

Bock, H. C., Puchner, M. J., Lohman, F., Schutze, M., Koll, S., Ketter, R., et al. (2010). First-line treatment of malignant glioma with carmustine implants followed by concomitant radiochemotherapy: a multicenter experience. *Neurosurgery Reveiw , 33*, 441-449.

Bode, W., & Maskos, K. (2003). Structural basis of the matrix metalloproteinases and their physiological inhibitors, the tissue inhibitors of metalloproteinases. *Biological Chemistry , 384* (6), 863-872.

Brannon-Peppas, L., & Peppas, N. (1990). Equilibrium Swelling Behavior of pH Sensitive Hydrogels. *Clinical Engineering Science , 46* (3), 715-722.

Brinckerhoff, C. E., & Martrisian, L. M. (2002). Matrix metalloproteinases: a tail of a frog that became a prince. *Nature Reviews. Molecular Cell Biology , 3* (3), 207-214.

Butler, G. S., Butler, M. J., Atkinson, S., Will, H., Tamura, T., Schade van Westrum, S., et al. (1998). The TIMP2 membrane type I metalloproteinase "receptor" regulates the concentration and efficient activation of progelatinase A. *Journal of Biological Chemistry* (273), 871-880.

Callister, W. D. (2007). *Materials Science and Engineering: An Introduction.* New York: John Wiley and Sons.

Central Brain Tumor Registry of the United States. (2007-2008). *Primary Brain Tumors in the United States.* Hinsdale, IL: Central Brain Tumor Registry of the United States.

Chakraborti, S., Mandal, M., Das, S., Mandal, A., & Charkraborti, T. (2003). Regulation of matrix metalloproteinases: an overview. *Molecular and Cellular Biochemistry , 253* (1-2), 269-285.

Chao, P.-H. G., Yodmuang, S., Wang, X., Sun, L. K., & Vunjak-Novakovic, G. (2010). Silk hydrogel for cartilage tissue engineering. *Journal of Biomedical Materials Research , 95B* (1), 84-90.

Chau, Y., Tan, F., & Langer, R. (2004). Syntehsis and characterization of dextra-peptide-methotrexate conjugates for tumor targeting by matrix metalloproteinase II and matrix metalloproteinase IX. *Bioconjugate Chemistry , 15* (4), 931-941.

Coviello, T., Matricardi, P., Marianecci, C., & Alhaique, F. (2007). Polysaccharide hydrogels for modified release formulations. *Journal of Controlled Release , 119* (1), 5-24.

Cowie, J., & Arrighi, V. (2008). *Polymers: Chemistry and Physics of Modern Materials.* Boca Raton: CRC Press.

Demeule, M., Regina, A., Jodoin, J., Laplante, A., Dagenais, C., Berthelet, F., et al. (2002). Drug transport to the brain: key roles for the efflux pump p-glycoprotein in the blood-brain barrier. *Vascular Pharmacology , 38* (6), 339-348.

Deryugina, E. I., & Quigley, J. P. (2006). Matrix metalloproteinases and tumor metastasis. *Cancer Metastasis Reviews , 25* (1), 9-34.

Drury, J., & Mooney, D. (2003). Hydrogels for tissue engineering: scaffold design variables and applications. *Biomaterials , 24* (24), 4337-4351.

Fallon, A., Booth, R., & Bell, L. (1987). *Laboratory Techniques in Biochemstry and Molecular Biology: applications of HPLC in biochemistry.* New York, NY: Elsevier Science Publishing Company.

Flory, P. J. (1953). *Principles of Polymer Chemistry.* London: Cornell Press.

Flory, P., & Rehner, R. (1943). Statistical mechanics of crosslinked polymer networks. I. Rubberlike elasticity. *Journal of Chem. Phys. , 11*, 521.

Foda, H. D., & Zucker, S. (2001). Matrix metalloproteinases in cancer invasion, metastasis, and angiogenesis. *Drug Discovery Today , 6* (9), 478-482.

Fridman, R. (2003). Surface Assocation of Secreted Matrix Metalloproteinases. *Current Topics in Developmental Biology , 54*, 75-99.

Fried, J. (2008). *Polymer Science and Technology.* Westford, MA: Prentice Hall Professional and Technical Reference.

Garripelli, V. K., Kim, J.-K., Son, S., Kim, W. J., Repka, M. A., & Jo, S. (2011). Matrix metalloproteinase-sensitive thermogelling polymer for bioresponsive local drug delivery. *Acta Biomaterialia* (7), 1984-1992.

Gemeinhart, R., & Guo, C. (2004). Fast Swelling Hydrogel Systems. In N. Yui, R. Mrsny, & K. Park, *Reflexive Polymers and Hydrogels: Understanding and Designing Fast Responsive Polymeric Systems* (pp. 247-248). Boca Raton, FL: CRC Press.

Goldberg, G., Wilhelm, S., Kronberger, A., Bauer, E., Grant, G., & Eisen, A. (1986). Human fibroblast collagenase: Complete structure and homology to a oncogene transformation-induced rat protein. *Journal of Biological Chemistry , 261* (14), 6600-6605.

Guo, X., Liao, J., Park, H., Raphael, R., Tabata, Y., Kasper, F., et al. (2010). Effects of TGF-B3 and preculture period of osteogenic cells on the chondrogenic differentiation of rabbit marrow mesenchymal stem cells encapsulated in a bilayered hydrogel composite. *Acta Biomaterialia , 6* (8), 2920-2931.

Gupta, N. V., & Shivakumar, H. (2009). Preparation and characterization of superporous hydrogels in a pH sensitive drug delivery system for pantoprazole sodium. *Current Drug Delivery , 6*, 505-510.

Gupta, P., Vermani, K., & Garg, S. (2002). Hydrogels: from controlled release to pH-responsive drug delivery. *Drug Discovery Today , 7* (10), 569-579.

Haas, T., & Madri, J. (1999). Extracellular Matrix-Driven Matrix Metalloproteinase Production in Endothelial Cells: Implications for Angiogenesis. *Trends in Cardiovascular Medicine , 9* (3-4), 70-77.

Hamidi, M., Azadi, A., & Rafiei, P. (2008). Hydrogel nanoparticles in drug delivery. *Advanced Drug Delivery Reviews , 60* (15), 1638-1649.

Hansen, S. (2004). Translational friction coefficient for cylinders of arbitrary axial ratios estimated by Monte Carlo simulation. *Journal of Chemical Physics , 121* (18), 9111-9115.

Hasty, K., Hibbs, M., Kang, A., & Mainardi, C. (1986). Secreted forms of human neutrophil collagenase. *Journal of Biological Chemistry , 261* (12), 5645-5650.

Hatakeyama, H., Akita, H., Kogure, K., Oishi, M., Nagasaki, Y., Kihira, Y., et al. (2007). Development of a novel systemic gene delivery system for cancer therapy with a tumor specific cleavable PEG-lipid. *Gene Therapy* (14), 68-77.

Hesse, E., Hefferan, T. E., Tarara, J. E., Haasper, C., Mueller, R., Krettek, C., et al. (2009). Collagen type I hydrogels allows migration, proliferation, and osteogenic differentiation of rat bone marrow cells. *Journal of Biomedical Materials Research Part A , 94* (2), 442-449.

Hillenkamp, F., Karas, M., Beavis, R. C., & Chait, B. T. (1991). Matrix assisted laser desorption/ionization of mass spectrometry of biopolymers. *Analytical Chemistry , 63* (24), 1193-1203.

Hopp, T. P., & Woods, K. R. (1981). Prediction of protein antigenic determinants based on amino acid sequences. *Proceedings of the National Academy of Sciences , 78* (6), 3824-3828.

Huynh, D., Im, G., Chae, S., Lee, K., & Lee, D. (2009). Controlled release of insulin from pH/temeprature-sensitive injectable pentablock copolymer hydrogel. *Journal of Controlled Release , 37* (1), 20-24.

Josef, E., Zilberman, M., & Bianco-Peled, H. (2010). Composite algniate hydrogels: An innovative approach for the controlled release of drugs. *Acta Biomaterialia , 6*, 4642-4649.

Kim, H. S., & Yoo, H. S. (2010). MMPs-responsive release from electrospun nanofibrous matrix for local gene therapy: in vitro and in vivo evaluation. *Journal of Controlled Release , 145*, 264-271.

Kim, J., Hefferan, T. E., & Lu, L. (2000). Potential of hydrogels based on poly(ethylene glycol) and secbacic acid as orthopedic tissue engineering scaffolds. *Tissue Engineering: Part A , 15* (8), 2299-2307.

Kim, J.-K., Anderson, J., Jun, H.-W., Repka, M. A., & Jo, S. (2009). Self-Assembling Peptide Amphiphille-Based Nanofiber Gel for Bioresponsive Cisplatin Delivery. *Molecular Pharmaceutics , 6* (3), 978-985.

Kim, S. W., Bae, Y. H., & Okano, T. (1992). Hydrogels: swelling, drug loading, and release. *Pharmaceutical Research , 9* (3), 283-290.

Klouda, L., & Mikos, A. (2008). Thermoresponsive hydrogels in biomedical applications. *European Journal of Pharmaceutics and Biopharmaceutics , 68* (1), 34-45.

Knauper, V., Lopez-Otin, C., Smith, B., Knight, G., & Murphy, G. (1996). Biochemical characterization of human collagenase-3. *Journal of Biological Chemistry , 271* (3), 1544-1550.

Kopecek, J. (2009). Hydrogels: From Soft Contact Lenses and Implants to Self-Assembled Nanomaterials. *Journal of Polymer Science: Part A Polymer Chemistry , 47* (22), 5929-5246.

Kratz, F., Drevs, J., Bing, G., Stockmar, C., Scheuermann, K., Lazar, P., et al. (2001). Development and in vitro efficacy of novel MMP-2 and MMP-9 specific doxorobubicin albumin conjugates. *Bioorganic and Medicinal Chemistry* (11), 2001-2006.

Ku, H. (1966). Notes on the use of propogation of error formuals. *Journal of Research on the National Bureau of Standards-C. Engineering and Instrumentation , 70C* (4), 263-273.

Lantz, M. S., & Ciborowski, P. (1994). Zymographic techniques for the detection and characterization of microbial proteases. *Methods of Enzymology* (235), 563-594.

Lee, G. Y., Park, K., Kim, S. Y., & Byun, Y. (2007). MMPs-specific PEGylated peptide-DOX conjugate micelles that can contain free doxorubicin. *European Journal of Pharmaceutics and Biopharmaceutics , 67*, 646-654.

Lee, K., Cussler E.L., M. M., & McHugh, M. (1990). Pressure-dependent phase transitions in hydrogels. *Chemical Engineering Science* (45), 766-767.

Lee, S.-W., Kim, W. J., Park, J. A., Choi, Y. K., Kwon, Y.-W., & Kim, K.-W. (2006). Blood brain barrier interfaces and brain tumors. *Archives of Pharmaceutical Research , 29* (4), 265-275.

Lei, Y., & Segura, T. (2009). DNA delivery from matrix metalloproteinase degradable poly(ethylene glycol) hydrogels to mouse cloned mesenchymal stem cells. *Biomaterials* (30), 254-265.

Lim, S.-H., Jeong, Y.-I., Moon, K.-S., Ryu, H.-H., Jin, Y.-H., Jin, S.-G., et al. (2010). Anticancer activity of PEGylated matrix metalloproteinase cleavable peptide-conjugated adriamycin against malignant glioma cells. *International Journal olf Pharmaceutics , 387*, 209-214.

Lin, C.-C., & Anseth, K. (2009). PEG hydrogels for the controlled release of biomolecules in regenerative medicine. *Pharmaceutical Research , 26* (3), 631-643.

Lin, C.-C., & Metters, A. T. (2006). Hydrogels in controlled release formulations: Network design and mathetmatical modeling. *Advanced Drug Delivery Reviews , 58* (12-13), 1379-1408.

Lu, M.-K., Chen, P.-H., Shih, Y.-W., Cheng, Y.-T., Huang, E.-T., Liu, C.-R., et al. (2010). (Alpha)-Chaconine Inhibits Angiogenesis in vitro by reducing matrix metalloproteinase-2. *Biological and Pharmaceutical Bulletin , 33* (4), 622-630.

Lustig, S., & Peppas, N. (1988). Solute diffusion in swollen membranes. IX. Scaling laws for solute diffusion in gels. *Journal of Applied Polymer Science , 36* (4), 735-747.

Mamada, A., Tanaka, T., Kungwatchakun, D., & Irie, M. (1990). Photoinduced phase transition of gels. *Macromolecules* (23), 1517-1519.

Mann, B. K. (2003). Biologic Gels in Tissue Engineering. *Clinics in Plastic Surgery , 30* (4), 601-609.

Mannello, F., Tonti, G., & Papa, S. (2005). Matrix metalloproteinase inhibitors as anticancer therapeutics. *Current Cancer Drug Targets , 5* (4), 285-298.

Mansour, A. M., Drevis, J., Esser, N., Hamada, F. M., Badary, O. A., Unger, C., et al. (2003). A new approach for the treatment of malignant melanoma: enhanced antitumor efficacy of an albumin bindng doxorubicin prodrug that is cleaved by matrix metalloproteinase-2. *Cancer Research* (63), 4062-4066.

Martin, M. D., & Matrisian, L. M. (2007). The other side of MMP: Protective roles in tumor progression. *Cancer Metastasis Reviews , 26* (3-4), 717-724.

Matsumura, Y., & Maeda, H. (1986). A new concept for macromolecular therapeutics in cancer chemotherapy: mechanism of tumoritropic accumulation of proteins and the antitumor agent smancs. *Cancer Research , 46* (12 (Part 1)), 6387-6392.

McCawley, L. J., & Matrisian, L. M. (2000). Matrix metallloproteinases: multifunctional contributors to tumor progression. *Molecular Medicine Today , 6* (4), 149-156.

Miyata, T., Asami, N., & Uragami, T. (1999). A reversibly antigen-responsive hydrogel. *Nature* (399), 766-769.

Morgunova, E., Tuutila, A., Bergmann, U., Isupov, M., Lindqvist, Y., Schneider, G., et al. (1999). Structure of human pro matrix metalloproteinase-2: activation mechanism revealed. *Science , 284*, 1667-1670.

Nelson, A. R., Fingleton, B., Rothenberg, M., & Martrisian, L. M. (2000). Matrix Metalloproteinases: Biologic Activity and Clinical Implications. *Journal of Clinical Oncology , 18* (5), 1135-1149.

Ogawa, T., Akazawa, T., & Tabata, Y. (2010). In vitro proliferation and chondrogenic differentiation of rat bone marrow stem cells for TGF-B1 release. *Journal of Biomaterials Science, Polymer Edition , 21* (5), 609-621.

O'Reilly, M. S., Wiederschain, D., Stetler-Stevenson, W. G., Folkman, J., & Moses, M. A. (1999). Regulation of Angiostatin Production by Matrix Metalloproteinase-2 in a Model of Concomitant Resistance. *Journal of Biological Chemistry* , 29568-29571.

Pavlaki, M. C., Hymowitz, M., Chen, W.-T., Bahou, W., & Zucker, S. (2002). A conserved sequence within the propeptide domain type 1 matrix metalloprotease is critical for function as an intramolecular chaperone. *Journal of Biological Chemistry , 277* (4), 2740-2749.

Peppas, N. A. (1986). *Hydrogels in Medicine and Pharmacy* (Vol. 1). Boca Raton: CRC Press.

Peppas, N., Bures, P., Leonbandung, W., & Ichikawa, H. (2000). Hydrogels in Pharmaceutical Formulations. *European Journal of Pharmaceutics and Biopharmaceutics , 50* (1), 27-46.

Peppas, N., Huang, Y., Torres-Lugo, M., Ward, J., & Zhang, J. (2000). Physicochemical foundations and structural design of hydrogels in medicine and biology. *Annual Review of Biomedical Engineering , 2*, 9-29.

Qiu, Y., & Park, K. (2001). Environment-sensitive hydrogels for drug delivery. *Advanced Drug Delivery Reviews , 53* (3), 321-329.

Rahman, M. (2010). Evaluation of Biomedical Hydrogel Parameters for Biomolecular Diffusion in Controlled Drug Delivery. Chicago: University Of Illinois at Chicago.

Randolph, M., Anseth, K., & Yaremchuk, M. (2003). Tissue engineering of cartilage. *Clinics in Plastic Surgery , 30* (4), 519-537.

Rao, J., Yamamoto, M., Mohaman, S., Gokaslan, Z., Fuller, G., Stetler-Stevenson, W., et al. (1996). Expression and localization of 92 kDa type IV collagenase/gelatinase B (MMP-9) in human gliomas. *Clinical and Experimental Metastasis , 14* (1), 8-12.

Rome, C., Arsaut, J., Taris, C., Couillaud, F., & Louiseau, H. (2007). MMP-7 (Matrilysin) expression in human brain tumors. *Molecular Carcinogenesis , 46*, 446-452.

Saleemuddin, M., & Hussain, Q. (1991). Concanavalin A: A useful ligand for glycoenzyme immobilization: a reveiw. *Enzyme Microbiology Technology , 13*, 290-295.

Salinas, C., & Anseth, K. (2009). Mesenchymal stem cells for craniofacial tissue regeneration: designing hydrogel delivery vehicles. *Journal of Dental Research , 88* (8), 681-692.

Sawaya, R. E., Masaaki, Gokaslan, Z. L., Wang, S. W., Mohanam, S., Fuller, G. N., et al. (1996). Expression and Localization of 72 kDa Type IV collagenase (MMP-2) in human malignant gliomas in vivo. *Clinical and Experimental Metastasis* , 35-42.

Shu, X. Z., Ghosh, K., Liu, Y.-C., Palumbo, F. S., Luo, Y., Clark, R. A., et al. (2003). Attachment and spreading of fibroblasts on an RGD peptide modified injectable hyaluronan hydrogel. *Journal of Biomedical Materials Research, Part A , 68* (2), 365-375.

Siegel, R., Ward, E., Brawley, O., & Jamal, A. (2011). Cancer statistics, 2011: the impact of eliminiating socioeconomic and racial disparities on premature cancer deaths. *CA: A Cancer Journal for Physicians* (61), 212-236.

Snoek-van Beurden, P. A., & Von den Hoff, J. M. (2005). Zymographic techniques for the analysis of matrix metalloproteases and their inhibitors. *Biotechniques* (38), 73-83.

Stephens-Altus, J., Sundelacruz, P., Rowland, M., & West, J. (2011). Development of bioactive photocrosslinkable fibrous hydrogels. *Journal of Biomaterials Research Part A , 98A* (2), 167-176.

Tabeting, P., & Cheng, S. (2006). *Introduction to Microfluidics.* Oxford: Oxford University Press.

Tauro, J. (2006). Matrix Metalloprotease Sensitive Hydrogels For Delivery of Platinates. *Biopharmaceutical Sciences* . Chicago, IL: University of Illinois at Chicago.

Tauro, J., & Gemeinhart, R. A. (2005). Matrix Metalloprotease triggered delivery of cancer chemotherapeutics from hydrogel matrices. *Bioconjugate Chemistry , 16*, 1133-1139.

Tauro, J., Lee, B.-S., Lateef, S. S., & Gemeinhart, R. A. (2008). Matrix metalloprotease selective peptide substrates cleavage within hydrogel matrices for cancer chemotherapy activation. *Peptides , 29* (11), 1965-1973.

Terada, T., Iwai, M., Kawakami, S., Yamashita, F., & Hashita, M. (2006). Novel matrix metalloproteinase-2 cleavable peptide-lipid containing galactosylated liposomes for hepatocellular carcinoma selective targeting. *Journal of Controlled Release* (111), 333-342.

Turk, B. E., Huang, L. L., Hiro, E. T., & Cantley, L. (2001). Determination of protease cleavage site motifs using mixture based oriented peptide libraries. *Nature Biotechnology , 19*, 661-667.

Ulijn, R. V. (2006). Enzyme responsive materials: a new class of smart biomaterials. *Journal of Materials Chemistry , 16* (23), 2217-2225.

Valtonen, S., Timonen, U., Toivanen, P., Kalimo, H., Kivipelto, L., Heiskanen, O., et al. (1997). Interstitial Chemotherapy with carmustine-loaded polymers for high-grade gliomas: a Randomized Double-Blind Study. *Neurosurgery , 41* (1), 44-49.

Vartak, D. (2009). Investigation of Integrin av-B3-Matrix Metalloprotease-2 Functional Association as Molecular Targets. Chicago, IL: University of Illinois at Chicago.

Vartak, D., & Gemeinhart, R. A. (2007). Matrix metalloproteases: underutlizized targets for drug delivery. *Journal of Drug Targeting , 15* (1), 1-20.

Vartak, D., Lee, B.-S., & Gemeinhart, R. A. (2009). In-vitro interaction of functional interaction between integrin avB3 and matrix metalloprotease-2. *Molecular Pharmaceutics , 6* (6), 1856-1867.

Wen, P. Y., & Kesari, S. (2008). Malignant Gliomas in Adults. *New England Journal of Medicine , 359*, 492-507.

Westphal, M., Hilt, D. C., Bortey, E., Delavault, P., Olivares, R., Wakme, P. C., et al. (2003). A phase 3 trial of local chemotherapy with biodegradable carmustine (BCNU) wafers (Gliadel wafers) in patients with primary malignant glioma. *Neuro-Oncology , 5* (2), 79-88.

Woessner, J., & Taplin, C. (1988). Purification and properties of a small matrix metallloproteinase of the rat uterus. *Journal of Biological Chemistry , 263* (34), 16918-16925.

Yu, M., Bowden, E., Sitlani, J., Sato, H., Seiki, M., Mueller, S., et al. (1997). Tyrosine phosphorylation mediates ConA induced membrane type 1 matrix metalloproteinase expression and matrix metalloproteinase-2 activation in MDA-MB-231 human breast carcinoma cells. *Cancer Research* (57), 5028-5032.

Zucker, S., Pei, D., Cao, J., & Lopez-Otin, C. (2003). Membrane Type-Matrix Metalloproteinases (MT-MMP). *Developmental Biology* , 1-74.

Vita

Amy Elizabeth Ross

Education

- M.S. in Bioengineering, University of Illinois at Chicago, 2011
- B.A. in Psychology, DePaul University, 1998

Experience

- Research Assistant, Biomedical Polymer Science Lab, 2010-2011

Publications

1. Desai ES, Tang MY, Ross A, Gemeinhart RA. Macroporous Hydrogel Scaffolds: A Platform for Cell Encapsulation, *Submitted for publication.*

Poster Presentations

- A. Ross and R.A. Gemeinhart "Evaluation of Parameters of Poly(ethylene glycol) Diacrylate Hydrogel Penetration by Matrix Metalloproteinase-2" UIC College of Pharmacy Research Day, February 2011
- A. Ross, M. Tang, B.S. Lee, and R. A. Gemeinhart "Matrix Metalloproteinaise-2-Mediated Drug Release from Poly(ethylene glycol) Diacrylate Hydrogels" Midwest Bioengineering Career Conference, April 2011. **Received 2nd prize.**
- A. Ross, M. Tang, B.S. Lee, and R. A. Gemeinhart "Matrix Metalloproteinaise-2-Mediated Drug Release from Poly(ethylene glycol) Diacrylate Hydrogels" UIC Student Research Forum, April 2011
- A. Ross and R.A. Gemeinhart "Evaluation of Parameters of Poly(ethylene glycol) Diacrylate Hydrogel Penetration by Matrix Metalloproteinase-2" American Association of Pharmaceutical Sciences National Biotechnology Conference, May 2011
- A. Ross and R.A. Gemeinhart "Evaluation of Parameters of Poly(ethylene glycol) Diacrylate Hydrogel Penetration by Matrix Metalloproteinase-2" Pharmaceutics Graduate Student Research Meeting, June 2011
- M. Tang, A. Ross, B.S. Lee, and R.A. Gemeinhart "Tumoroid Model for Degradation Stimulated Drug Release "Pharmaceutics Graduate Student Research Meeting, June 2011

Leadership

- Events Coordinator, Controlled Release Society Student Chapter, 2010-2011

Professional Memberships

- American Association of Pharmaceutical Sciences